Title	Response of Soil-Structure Interaction System Considering the Nonlinearity of Soil during Earthquake and Tsunami Disaster
Author(s)	PROK, Narith
Citation	高知工科大学，博士論文
Date of issue	2016-09
URL	http://hdl.handle.net/10173/1421
Rights	
Text version	ETD

Response of Soil-Structure Interaction System Considering the Nonlinearity of Soil during Earthquake and Tsunami Disaster

PROK Narith

DISSERTATION

Submitted in partial fulfillment of the requirements for the degree of
Doctor of Engineering in the Graduate School of Systems Engineering of
Kochi University of Technology
Kochi, Japan

Review Committees:

Professor KAI Yoshiro, Advisor
Professor TAKAGI Masataka, Co-Advisor
Professor NAKAI Shoichi, Co-Advisor
Professor SHIMA Hiroshi, Member
Professor OKA Koichi, Member

September 2016

ACKNOWLEDGEMENTS

Firstly, I would like to express my sincere gratitude to my advisor Prof. Yoshiro Kai for his kindness, motivation, and immense advice to support my research work. In addition, I am greatly indebted to him that cannot be described in words for his patience and encouragement throughout my study. Without his valuable assistance, this research work would not have been completed and succeeded.

My sincerely thanks also go to all my thesis committee members: Prof. Masataka Takagi, Prof. Nakai Shoichi, Prof. Hiroshi Shima, and Prof. Koichi Oka for their insightful comments and questions in order to qualify and enhance the scope of my research. Furthermore, I would like to thank to all professors and staffs in the department of systems engineering for their kindness and encouragements.

Besides this, I would like to express my appreciation to Kochi University of Technology (KUT) for providing me SSP scholarship and all members of International Relations Center (IRC) for their cooperation of administrative works, especially Director Sakikawa Shinichiro, during my study course.

My Special thanks go to Dr. Ros Soty for his valuable effort and encouragement for the opportunity to pursue my study at Kochi University of Technology and Ms. Rath Sovannsathya for her encouragement and support during this period. My gratitude also extends to all members of infrastructure system lab (Kai's lab) for their kindness and helpfulness.

Finally, I would like to express another special thanks my family and relatives for their unconditional love, support, and encouragement throughout all the difficulties during my study in Japan.

ABSTRACT

The 2011 Great East Earthquake and Tsunami in Japan have left unexpected remains of the devastation of many buildings and casualties. According to seismologists' estimation, the great future earthquake will hit Japan again along the Nankai Trough and can trigger another subsequent powerful tsunami disaster. These disasters can cause more devastations and casualties than the 2011 Great East Earthquake and Tsunami. Thus, many efforts have been made to mitigate the devastation of these inevitable disasters.

The structural damage experienced from the 2011 Great East Earthquake and Tsunami disaster is important for future structural design guidelines. According to the field survey report, the structural response resulting from the interaction of nonlinear response of soil medium was assigned as a crucial effect under earthquake and subsequent tsunami disaster. This interaction can cause serious damage to structure during earthquake and overturning during tsunami disaster.

Therefore, the objective of this thesis is to propose analytical models considering nonlinear soil-structure interaction (SSI) using substructure approach during earthquake disaster and the nonlinear effect of near-field soil on the response of structure during tsunami disaster. However, in order to obtain these targets, the nonlinear response of soil material and motion in each time step was significant. Thus, another analytical model is proposed to consider nonlinear response of soil material and motion.

In this paper, the analytical model considering nonlinear response of soil material and motion was presented. The target motion and soil material at surface layer was achieved. This nonlinear response motion showed a good agreement with linear response for a few seconds from starting point and with equivalent-linear response for the last several seconds. This agreement confirmed about the validation of proposed analytical model considering nonlinear response of soil material and motion.

Furthermore, the seismic response of structure under SSI effect using substructure approach was conducted under existing and proposed analytical model considering nonlinear response of soil material and motion. The comparison results of structural response under both analytical model showed that the responses under existing analytical model were larger than the proposed analytical model. These discrepancies showed the overestimated results of using existing analytical under substructure approach compared to actual response of structure under earthquake disaster. Thus, the nonlinear SSI effect on the response of structure should be considered and taken into account. This analytical model also showed about the adequateness of using

substructure approach.

Beside this, the analytical model considering the nonlinear effect of near-field soil on the response of structure under tsunami force was presented. This proposed analytical model was included boundary and segment division of near-field soil column. In addition, the effect of earthquake and tsunami force on the near-field soil column was also presented. The effect of near-field soil on structural response was considered under two significant effects: tsunami and earthquake-tsunami effect. In case of tsunami effect, the responses of fixed-base structure were larger than the responses considering near-field soil effect. This result showed the overestimated result of using fixed-base structure without considering the effect of near-field soil, especially the nonlinear response of near-field soil. In case of earthquake-tsunami effect, the responses of structure considering near-field soil effect under tsunami force were larger than the responses under earthquake-tsunami relationship. This result showed the effect of earthquake on the near-field soil and the responses of structure during tsunami disaster. Thus, the effect of earthquake-tsunami relationship on the response of structure should be considered and taken into account, especially for clayey soil condition that needs long time to recover after earthquake disaster.

In conclusion, the effect of nonlinear response of soil medium was absolutely significant on the response of structure during earthquake and tsunami disaster. Thus, this effect should be considered and taken into account based on the proposed analytical models.

TABLE OF CONTENTS

LIST OF FIGURES

LIST OF TABLES

CHAPTER I. INTRODUCTION

I.1. BACKGROUND

The tragedy of the 2011 Great East Earthquake and Tsunami in Japan has left unexpected remains of the devastation of many buildings and casualties. This experience brings to a serious concern for the great future earthquake that can occur any time along the Nankai Trough in the near future and can trigger a subsequent powerful tsunami disaster, as shown in Fig. 1.1.

The structural damage experienced from these mega disasters is very important and necessary for the future structural design guidelines under earthquake and tsunami force. According to the field reports, many RC buildings were damaged and overturned under earthquake and tsunami disaster.

From these structural damage, it can be categorized into two types of RC building damage: partially damage and overturning of structure.

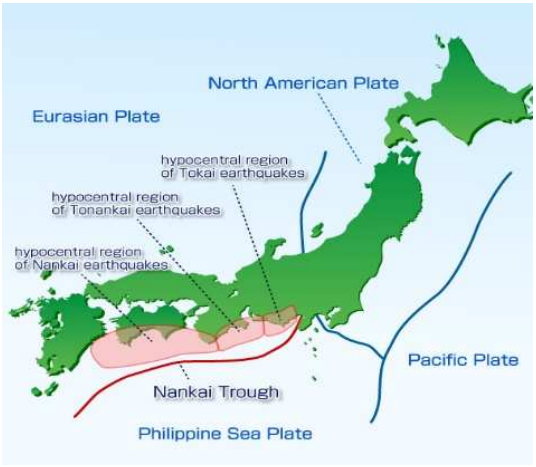

Figure I.1 Future earthquake zones along Nankai Trough [1]

I.1.1. Partially Damage of Structure

The effect of earthquake and tsunami force has damaged many structural elements such as pile foundation, column, and RC wall as shown in Fig. 1.2. Among of many recommendations for future structural design, the effect of nonlinearity of soil medium and ground motion amplification is important factors that need to consider [2]. The effect of SSI was regarded as a significant factor that causes serious damage of

structural element, especially for soft soil condition that is commonly located along the coastal area.

Thus, the interaction of nonlinear response of soil medium is a potential effect that needs to consider on the structural damage response.

(a) Damage of pile head [3]

(b) Damage of column [2]

(c) Damage of RC wall [4]

(d) Damage of RC building [2]

Figure I.2 Partially damage of RC building

I.1.2. Overturning of Structure

The overturning of RC building in Onagawa town, as shown in Fig. 1.3, is another impressive issue for the damage of RC buildings under tsunami force. The overturning-moment response of structure is regarded as a significant factor to control the stability of structure during tsunami disaster. Hydrostatic and buoyant force were regarded as the main effects on the overturning of structure while the contribution of soil medium was considered only for pile foundation friction.

Regarding the contribution of soil medium on the overturning-moment of structure, the soil condition was performed a significant role. During earthquake disaster, soil condition has been deformed or changed the state condition from hard to soft soil. This

situation causes seriously response of structure under subsequent tsunami disaster such as overturning of structure.

Figure I.3 Overturned buildings in Onagawa town [5]

I.2. STATEMENT OF PROBLEMS

Based on the recommendation from field reports, the effect of nonlinear SSI was recommended for future design of structure [2]. However, substructure approach, a frequently used method in SSI problem, is unable to perform a fully nonlinear response analysis yet which is taken into account the nonlinearity of soil material.

Besides this, the nonlinear effect of near-field soil on the response of structure, such as overturning-moment, under tsunami disaster has not been considered or studied yet.

The description of each problem was presented in the following sections.

I.2.1. Existing Analytical Model Considering SSI Effect under Earthquake Disaster

In order to perform SSI analysis, various methods and analytical models have been proposed such as Finite Element Method (FEM), Boundary Element Method (BEM), the coupling of Finite-Boundary Element Method (FEM-BEM), Discrete Element Method (DEM), etc. These methods can be categorized as direct and substructure (indirect) approach [6]. Due to the simplicity and time consumption, substructure

approach is frequently used in practical work and research field. In this approach, the analysis procedure is distinguished into three steps: foundation input motion (FIM), dynamic impedance, and the seismic response of structure.

However, this approach can be performed only with equivalent-linear SSI effect, which corresponds to the equivalent-linear response of soil material and FFGM in FD. Thus, this restriction was regarded as a state of problem for substructure approach and need for further improvement.

I.2.2. Existing Analytical Model for Response of Structure under Tsunami Disaster

During tsunami disaster, the overturning-moment response of structure was regarded as a significant factor controlling the stability of structure. Many analytical studies and guidelines have proposed various relative parameters considering the effect of tsunami forces on the response of structure such as lateral force [7] and buoyant force [4].

However, the nonlinear effect near-field soil on the response of structure was another important parameter that needs to consider. This consideration would contribute on the response of structure such as overturning-moment.

I.3. OBJECTIVE OF RESEARCH

I.3.1. Originality and Contribution of Research

The nonlinear effect of near-field soil on the structural response under tsunami disaster was the originality of this thesis. Commonly, the interaction effect between soil and structure was considered and studied only under earthquake force while the consequence of this interaction effect under subsequent tsunami force has not been studied yet. This study would bring for further consideration and comprehension of interaction effect between soil and structure under tsunami disaster.

I.3.2. Proposed Analytical Model

In order to achieve the main objective of this thesis, A few analytical models were needed to propose. These proposed analytical models were included:

Analytical model considering nonlinear response of soil material and motion.

Analytical model considering nonlinear SSI effect using substructure approach under earthquake disaster.

Analytical model considering the nonlinear effect of near-field soil on the response of structure under tsunami disaster.

I.4. RESEARCH OUTLINE

In order to obtain the objective of this research, the FFGM analysis procedure was presented for both FD and TD. Then, these analysis procedures were integrated into Object-Based Structural Analysis (OBASAN), a structural analysis program but unable to perform FFGM analysis yet, in order to perform FFGM analysis under both domains.

- ***Nonlinear Response of Soil Material and Motion:***
  - The procedure considering nonlinear response of FFGM in TD was presented. FFGM analyses in TD were provided under two different soil columns. The accuracy of proposed analytical model was explained and compared to linear and equivalent-linear response of FFGM in FD.
- ***Response of Structure under Nonlinear SSI Effect*:**
  - The analytical model considering nonlinear SSI effect was presented. The comparison of existing and proposed analytical model was conducted. The response of structure was performed under linear response of base-shear, overturning-moment, relative displacement, and acceleration. The discussion of both analytical model was provided.
- ***Response of Structure under Near-Field Soil Effect Subjected to Tsunami:***
  - Tsunami Effect

    The analytical model considering the near-field soil column boundary was presented. In this case, the near-field soil column was not suffered from earthquake disaster. Thus, there was no any deformation of near-field soil under earthquake disaster. The response of structure under near-field soil effect was performed under hydrodynamic force. The deformation of near-field soil and response of structure were provided under linear and nonlinear response of near-field soil.

  - Earthquake-Tsunami Effect
    - Earthquake disaster

    The base-shear and overturning-moment of structure under nonlinear SSI effect was determined under nonlinear response of motion and soil material. The FIM, base-shear, and overturning-moment were applied at the surface of near-field soil column while the FFGM at the same depth of near-field soil was applied at the base in order to perform nonlinear response of near-field soil under earthquake disaster. The last response soil material was assigned as initial state of near-field soil material under tsunami effect.

- Tsunami disaster

  In this case, the near-field soil column was performed under linear, and nonlinear response analysis subjected to tsunami force. The effect of near-field soil on the response of structure was discussed.

These procedures were divided as into seven chapters which orderly introduced as in the following:

Chapter I: This chapter introduces the experiences of structural damage under the 2011 Great East Earthquake and Tsunami in Japan. The inadequateness of existing analytical model for structure response under earthquake and tsunami disaster was presented. The objective and research outline were described in this chapter.

Chapter II: This chapter presents the literature reviews which described about the existing analytical model of SSI problem under earthquake disaster and response of structure under tsunami disaster. The statement of problems from these analytical model were presented.

Chapter III: This chapter describes the integration procedure of FFGM analysis into OBASAN, which is a structural analysis program. This integration was conducted for both procedures of FFGM analysis in FD and TD. The analytical model considering nonlinear response of FFGM and soil material was proposed. The nonlinear response analysis of FFGM in TD was performed and corresponding soil material was obtained.

Chapter IV: This chapter shows about the seismic response of RC frame structure under equivalent-linear and nonlinear SSI effect using substructure approach. The responses of structure were included linear response of base-shear, overturning-moment, relative displacement, and acceleration of structure. The comparison of both analytical models was conducted and discussed.

Chapter V: This chapter proposes the analytical model considering the effect of near-field soil on the response of structure under tsunami disaster. The boundary of near-field soil column was presented. The near-field soil segment division was recommended. The response of structure under fixed-base condition and near-field soil were conducted. The comparison and discussion were presented from these responses.

Chapter VI: This chapter presents the effect of earthquake on the near-field soil column and the response of structure under subsequent tsunami disaster was conducted. The comparison and discussion of response of structure under tsunami disaster after and without earthquake disaster was provided.

Chapter VII: This chapter concludes the achievement and contribution of this thesis. The recommendation and further studies were presented.

CHAPTER II. LITERATURE REVIEWS

II.1. INTRODUCTION

The experiences of the 2011 Great East Earthquake and Tsunami disaster have remained an extreme concern for the future earthquake disaster that can occur anytime along Nankai Trough with the estimated magnitude 9.1. According to this magnitude, it can generate another subsequent powerful tsunami disaster. Due to this reason, many efforts have been conducted to improve the existing structural design guideline based on structural damage experienced from the 2011 Earthquake and Tsunami disaster.

In this chapter, the literature reviews of existing analytical model of SSI problem under earthquake disaster and the response of structure under tsunami disaster were presented. The inadequateness of existing analytical models was described.

II.2. SOIL-STRUCTURE INTERACTION UNDER EARTHQUAKE DISASTER

SSI problem is regarded as a crucial major in earthquake engineering domain. SSI analysis permits evaluating the seismic response of structure and foundation system including the interaction effect of soil medium. This analysis leads to an understanding the actual response of structure under earthquake disaster and controlling the damage response of structural elements.

In order to perform SSI analysis, there are three significant interaction effects that have to consider: kinematic interaction effect, inertial interaction effect, and soil-foundation flexibility effect [8]. To evaluate these interaction effects, various methods have been proposed and utilized as Finite Element Method (FEM), Boundary Element Method (BEM), the coupling of FEM-BEM, Discrete Element Method (DEM), etc. However, these methods can be categorized as direct and substructure approach [6].

II.2.1. Direct Approach

Direct approach is considered as a rigorous method and can deal with complicated structural geometry and soil condition. In the direct approach, as shown in Fig. 2.1, the structure and soil medium are simulated within the same model and analyzed as a complete system. Various studies have been performed base on this approach. These include:

FEM: Ottaviani [9] analyzed a group pile, Randolph [10] studied a single cylindrical pile, Lin et al. [11] conducted interaction between adjacent embedded foundations, etc.

BEM: Karabalis et al. [12] analyzed the dynamic response of rigid embedded

foundation of arbitrary, Estorff et al., [13] studied the interaction effects in underground traffic systems, Karabalis et al. [14] presented the interaction between adjacent rigid surface foundation, etc.

FEM-BEM: Padron et al. [15] studied the time harmonic dynamic analysis of piles and pile groups embedded in an elastic half-space, Padron et al. [16] investigated the interaction between nearby piles supported structure, Lehmann et al. [17] developed a reliable analysis of the dynamic behavior of high-rise buildings with fully considering of the SSI effect, etc.

However, this approach is rarely used in practical work especially for complex geometrical structure and nonlinearity behavior of soil medium as a result of large computer-storage, running time, and cost consumption [18].

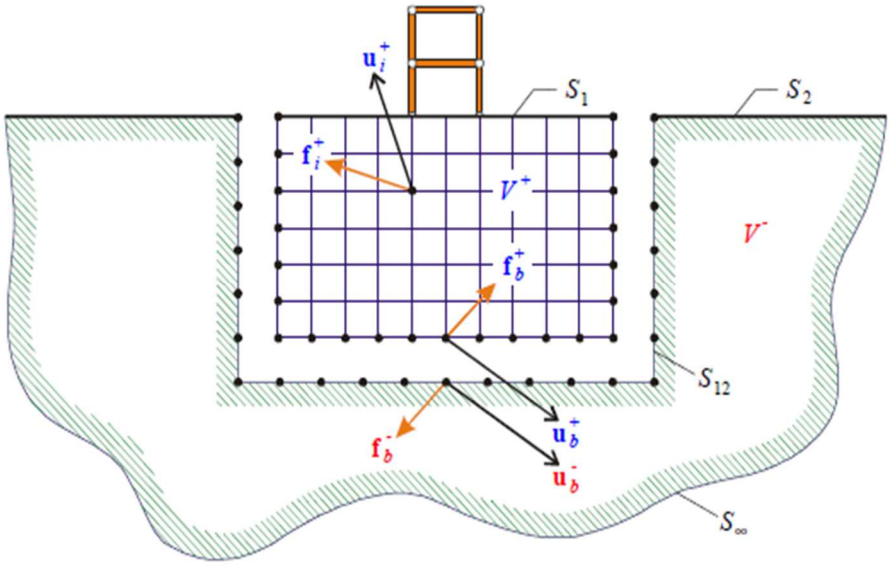

Figure II.1 Soil-structure interaction model under direct approach [6]

II.2.2. Substructure Approach

In substructure approach, SSI problem is commonly distinguished into three steps which are combined to a complete solution of the seismic response of structure base on law of superposition [8]. These evaluation steps include foundation input motion (FIM), dynamic impedance (spring-dashpot), and the seismic response of structure. However, free field ground motion analysis was another important factor that should be considered in these evaluation steps. The explanation of these steps was presented in the following [6]:

- *Free Field Ground Motion (FFGM)*: an evaluation of free vibration of ground motion without foundation or any structures. Generally, the ground motion analysis is performed with equivalent-linear of soil material, which can be obtained in FD based on equivalent-linear analysis method and use the Fast Fourier Transform (FFT) to transform the motion from FD to TD. However, the nonlinear response analysis of soil material in TD is favorable for improving this approach.

- *Foundation Input Motion (FIM)*: an evaluation of transfer function to convert the free field motion to the foundation input motion, which based on stiffness and type of foundation. In order evaluate FIM, the structure and foundation are supposed to be massless. This motion usually differs from FFGM due to the present of pile or/and embedment of foundation. This motion is generally involved with both translational and rotational components which represent the seismic demand applied to the foundation and structure system. The ratio of FIM and FFGM is named as a transfer function (TF), which expresses the effect of kinematic interaction only when the effect of inertial interaction is neglected. It makes sure that the FIM is varied along the depth of the foundation (such as pile foundation), therefore, the distributed of spring-dashpot should be used and the variation of ground motion should be considered along the depth of the foundation.

- *Dynamic Impedances*: an evaluation the characteristics of stiffness and damping which is represented by using a relatively simple function models or a series of distributed springs and dashpots. This impedance function is generally the frequency-dependent and represents the interaction between soil and foundation system. The dynamic impedance matrix is a complex value and can be a fully form matrix (translation, rotation, and coupling of translation-rotation) according to the condition of structure and foundation. The real-value expresses the stiffness of the soil-foundation system and represented by the spring as a function of frequency while the imaginary-value expresses the energy dissipation of soil due to the vibration of the foundation subjected to the earthquake loading and represented by dashpot with a frequency-dependent function. The distributed springs and dashpots are needed when the foundation is non-rigid or when internal force demands (shear, deformation, moment) are required for the analysis.

- *Seismic Response of Structure*: an evaluation the seismic response of the whole system, which the structure was supported by spring-dashpot element subjected to the FIM. The inertial interaction effect is taken into account in this step. The dynamic response analysis of the whole system can be performed by response spectrum method or time history method.

This approach is widely used in research and practical work due to the simplicity, time, and cost consumption. Various studies and investigations have been performed in order improve the seismic response of structure under this approach. These include Javier et al. [19] [20] investigated the effect of foundation embedment on the effective period, effective damping, and response of structure under different type of wave motion, Cristina et al. [21] proposed a simple and stable procedure for estimation of periods and damping of piled shear buildings, Mejia et al. [22] proposed the formulation of the substructure method of SSI analysis for the seismic evaluation of the Manhattan bridge in New York city, etc.

However, this approach can be performed only with equivalent-linear analysis of soil material in FD and the corresponding FFGM. This restriction can cause mismatched response and overestimated results compared to the actual response of structure under earthquake disaster.

Therefore, a new analytical model considering nonlinear response of soil material and corresponding motion should be proposed. This proposal would facilitate performing the seismic response of structure under nonlinear SSI effect.

The analytical procedure above was presented in the following section in each step.

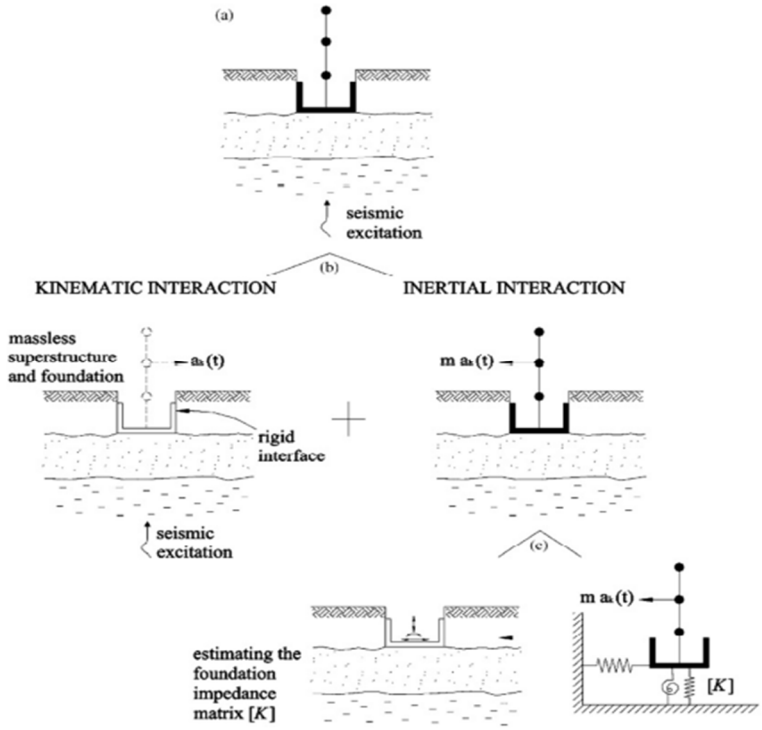

Figure II.2 Soil-structure interaction model under substructure approach [6]

II.2.3. Existing Analytical Model for SSI problem under Substructure Approach

· ***Foundation Input Motion Analysis***

As described above, FIM can be derived from the FFGM and transfer function. FIM component is composed by translational and rotational motion that can be expressed in Eq. (2.1) and (2.2) [23] [24], respectively.

$$u_{FIM} = f\left(H_u, u_g\right) \tag{2.1}$$

$$\phi_{FIM} = f\left(u_g, I_\phi, B\right) \tag{2.2}$$

Where

H_u, I_ϕ : Translational and rotational of transfer function

u_{FIM}, ϕ_{FIM} : Translational and rotational of FIM

u_g : FFGM response

B : Foundation half-width or equivalent radius

In this step, FFGM is performed in FD using equivalent-linear method analysis. This method is used and described in many programs such as SHAKE [25], EERA [26], etc. According to this method, the equivalent-linear values of soil material (G_{EL}, ξ_{EL}) and corresponding FFGM at the ground surface are achieved.

For the transfer function, various expressions related to foundation and wave motion types were described in NIST guideline for SSI problem [24], Mylonakis et al. [23], Nikolaou et al. [27], etc. According to this description, the FIM can be achieved corresponding to soil conditions, wave motions, and foundation types.

· ***Dynamic Impedances (Spring-Dashpot)***

Dynamic impedances function is an interaction function between foundation and soil medium. This function is represented by spring and dashpot of soil-foundation interaction system as shown in Fig. 2.3. The equation of this function is composed by stiffness and damping as expressed in Eq. (2.3) and (2.4) [18] [23] [24]:

$$\bar{K}_i = k_i + i\omega c_i \tag{2.3}$$

$$\bar{K}_i = k_i(1 + i2\beta_i) \tag{2.4}$$

$$\beta_i = \frac{\omega c_i}{2k_i} \tag{2.5}$$

Where

β_i: Radiation damping ratio

$\bar{K}_i$: Complex-valued impedance function

k_i, c_i : Frequency-dependent foundation stiffness and damping

In the Eq. (2.4), the foundation stiffness k_i can be expressed in function of equivalent-linear soil material obtaining from the FFGM analysis and foundation dimension while foundation damping can be expressed in function foundation stiffness and radiation damping ratio as expressed in Eq. (2.5).

There are various expressions proposed for both function (k_i, c_i) related to different types of foundation and soil conditions such as surface and embedded foundation [23] [28]-[30], and piles foundation [24].

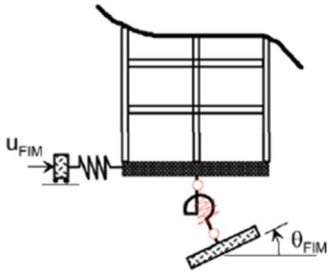

Figure II.3 Soil-foundation interaction system [24]

· ***Seismic Response of Structure***

The structure was assumed to support by spring-dashpot that computed in the second step and subjected to FIM in the first step, as shown in Fig. 2.4. The seismic response of structure under SSI effect can be solved in both TD and FD [31] as expressed in Eq. (2.6) and (2.7), respectively.

$$[M]\{\ddot{u}\}+[C]\{\dot{u}\}+[K]\{u\}=-[M]\{1\}\ddot{u}_0 \tag{2.6}$$

$$\left(-\omega^2[M]+i\omega[C]+[K]\right)\{U\}=\omega^2[M]\{1\}U_0 \tag{2.7}$$

Where

$[M],[C],[K]$: Mass, damping, stiffness of the whole structure

$\{\ddot{u}\},\{\dot{u}\},\{u\}$: Acceleration, velocity, displacement of structure

$\{\ddot{u}_0\},\{U_0\}$: Acceleration and displacement of FIM

According to the description, in the existing analytical model, the seismic response of structure considering SSI effect is solved under equivalent-linear of soil material and FFGM in FD. However, due to this condition, this analytical model might not represent the actual response of structure. Therefore, an analytical model considering the nonlinear response of soil material and FFGM in TD should be proposed and applied for the response of structure under nonlinear SSI effect.

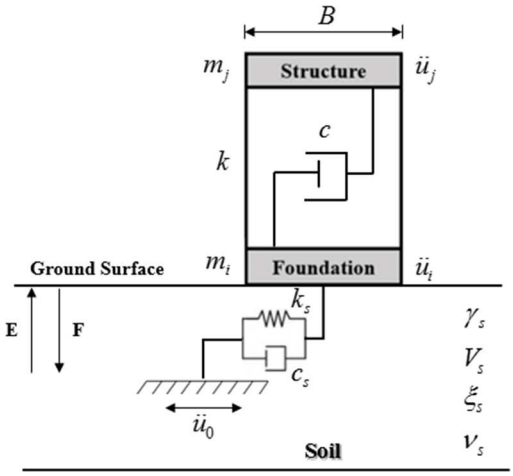

Figure II.4 Structural model under SSI effect

II.3. RESPONSE OF STRUCTURE UNDER TSUNAMI DISASTER

After the 2011 Great East Earthquake and Tsunami in Japan, the overturning of RC building, in Onagawa town, has become an impressive issue for structural design guideline. The resisting of structure to the overturning-moment was considered under four significant effects such as hydrostatic force, buoyant force, self-weight of structure, and tensile resistance of piles, as shown in Fig. 2.5.

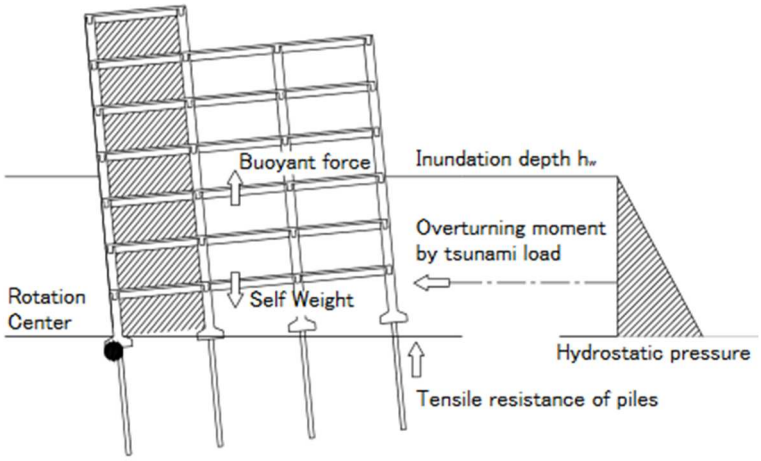

Figure II.5 Overturning mechanism of the building [4]

II.3.1. Hydrostatic Force

The hydrostatic force was supposed as tsunami load on the building. The design guideline considering the effect of hydrostatic force was proposed by Japan Cabinet Office [7], as shown in Fig. 2.6. This proposal was based on the experimental study or tsunami damage survey from the 2004 Sumatra Earthquake [4]. The hydrostatic

pressure equation is expressed in Eq. (2.8).

$$P_s = \int_0^{h_0} \left(\rho g \left(a h_w - z \right) B \left(1 - \zeta \right) \right) dz \tag{2.8}$$

Where

a : Water depth ratio
ρ : Density of water
g : Gravity acceleration
h_w : Inundation depth
B : Building width
h_0 : Minimum value within inundation depth and building height
ζ : Aerial opening ratio

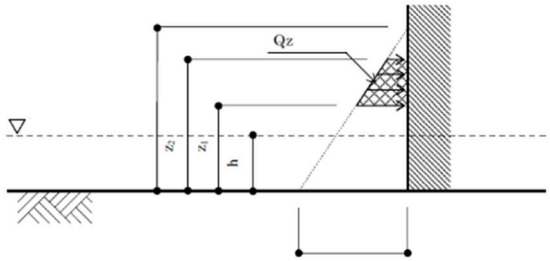

Figure II.6 Japanese design guideline for hydrostatic force [4]

II.3.2. Buoyant Force

Basically, buoyant force is equal to the weight of water sinking the building and can be expressed in Eq. (2.9).

$$F_b = \rho g h A \tag{2.9}$$

Where

ρ : Density of water
g : Gravity acceleration
h : Sinking depth of water
A : Sinking area of water

II.3.3. Tensile Resistance of Piles

According to AIJ design guideline [32], the tensile resistance of piles is expressed in Eq. (2.10).

$$R_{TC} = \left(\sum \tau_{ST} L_S + \sum \tau_{CT} L_C \right) \varphi + W_p \tag{2.10}$$

Where

τ_{ST} : Friction stress on peripheral surface of piles in sand layer

τ_{CT} : Friction stress on peripheral surface of piles in clay layer

L_s : Thickness of sand soil layer

L_c : Thickness of clay soil layer

φ: Peripheral length of pile

W_p : Pile weight

However, the nonlinear effect of near-field soil should be considered on the overturning-moment response of structure. This effect would contribute on the overturning-moment response of structure in case of earthquake-tsunami effect.

The detail of proposed analytical model considering nonlinear SSI effect and analytical model considering the effect near-field soil on the response of structure under tsunami disaster were described in the following chapters.

CHAPTER III. FREE FIELD GROUND MOTION ANALYSIS

III.1. INTRODUCTION

Many mega earthquake disasters, such as Michoacán Earthquake (Mexico, 1985), Northbridge Earthquake (US, 1994), and Great East Earthquake (Japan, 2011) have indicated how the effect of geological condition on the ground motion and the structure interaction response under these disasters.

In order to perform SSI effect, FFGM analysis is definitely significant. One-dimensional site response analysis methods are widely used approach to determine FFGM. These methods are divided into FD and TD analysis [33].

In this chapter, wave propagation analysis procedure was integrated into Object-Based Structural Analysis (OBASAN) program [50] [51] for both FD and TD. The analytical model considering nonlinear response of soil material was proposed and examples of FFGM analysis in TD were conducted at the end of this chapter.

III.2. GROUND MOTION ANALYSIS IN FREQUENCY DOMAIN (FD)

The FFGM analysis in FD is the most widely used method in earthquake engineering domain due to the simplicity, flexibility and low computational requirement [33]. This method was assumed that the cyclic soil behavior can be simulated using an equivalent-linear model, which is extensively described in the geotechnical earthquake engineering literature [34]. Many programs consisted this procedure such as SHAKE91 [25], EERA [26], DEEPSOIL [35], etc. This analytical procedure was presented briefly in the following section.

III.2.1. One-Dimensional Wave Propagation in Soil Deposits

The equation of 1D ground motion analysis subjected to vertically incident wave S can be expressed in Eq. (3.1) and (3.2).

$$E_{m+1} = \frac{1}{2} E_m (1+\alpha_m^*) e^{ik_m^* h_m} + \frac{1}{2} F_m (1-\alpha_m^*) e^{-ik_m^* h_m} \quad (3.1)$$

$$F_{m+1} = \frac{1}{2} E_m (1-\alpha_m^*) e^{ik_m^* h_m} + \frac{1}{2} F_m (1+\alpha_m^*) e^{-ik_m^* h_m} \quad (3.2)$$

Where

$$\alpha_m^* = \frac{k_m^* G_m^*}{k_{m+1}^* G_{m+1}^*} = \sqrt{\frac{\rho_m G_m^*}{\rho_{m+1} G_{m+1}^*}}, \quad k^{*2} = \frac{\rho\omega^2}{G^*}$$

$$G^* = G(1 + 2i\xi), \quad G = \rho V_s^2$$

E_m, F_m : Incident and reflected wave motion at layer m

α_m^* : Complex impedance ratio at layer m

k_m^* : Complex wave number at layer m

G_m^* : Complex shear modulus at layer m

ρ, V_s : Density and shear velocity of soil deposits

G, ξ : Shear modulus and ratio damping

The recursive algorithm is started at the top of free surface, the shear stress was assumed to be zero:

$$\tau_1(0,t) = 0 \tag{3.3}$$

Therefore: $E_1 = F_1$

The transfer function between the displacement at the top layer m and n can be expressed in Eq. (3.4)

$$A_{mn}(\omega) = \frac{u_m}{u_n} = \frac{\dot{u}_m}{\dot{u}_n} = \frac{\ddot{u}_m}{\ddot{u}_n} = \frac{E_m + F_m}{E_n + F_n} \tag{3.4}$$

The shear strain and stress at depth z and time t can be expressed in Eq. (3.5) and (3.6)

$$\gamma(z,t) = \frac{\partial u}{\partial z} = ik^*(Ee^{ik^* z} - Fe^{-ik^* z})e^{i\omega t} \tag{3.5}$$

$$\tau(z,t) = G^* \gamma(z,t) \tag{3.6}$$

At free surface, it was assumed that $E_1 = F_1 = 1$.

As shown in Fig. 3.1, the bedrock outcropping motion is $2E_N$, because there is no shear stress on free surface. The motion at the surface of bedrock is $E_N + F_N$ while the motion at free surface is $2E_1$.

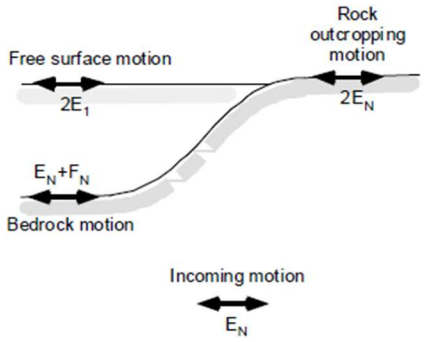

Figure III.1 Site response motion [26]

III.2.2. Equivalent-Linear Analysis Method

In the equivalent-linear analysis, shear modulus ratio and damping ratio was assumed as a function of effective shear strain. The value of shear modulus and damping ratio curve can be obtained from dynamic experimental of soil properties as shown in Fig. 3.2. The procedure of equivalent linear analysis was decribed as in the following several steps [34]:

- Step1: initialize value of $G_0 \& \xi_0$ at small strain
- Step2: calculate ground motion response in each layer of time step.
- Step3: calculate maximum shear strain in each layer.
- Step4: calculate effective shear strain: $\gamma_{eff} = \alpha.\gamma_{\max}$ which $\alpha = 0.65$ or $\alpha = \frac{M-1}{10}$, M is magnitude of earthquake.
- Step5: define new value of $G_i \& \xi_i$ corresponding to effective strain.
- Step6: repeat the procedure from step2 to step5 until no effective change of effective shear strain. Generally more than 8 iterations are adequate to obtain convergence.

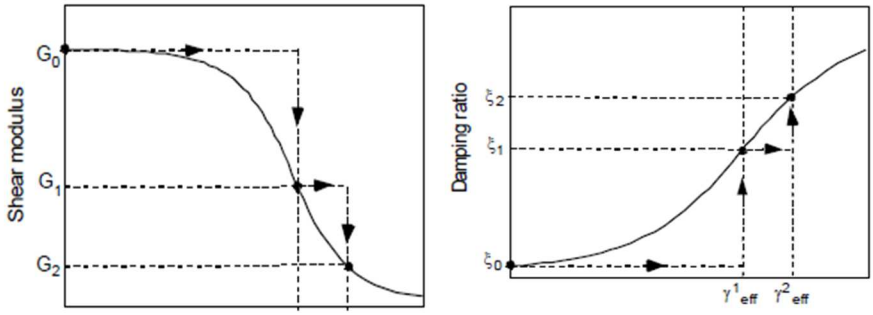

Figure III.2 Shear modulus and damping ratio curve [26]

III.3. GROUND MOTION ANALYSIS IN TIME DOMAIN

As mentioned above, FFGM analysis in FD is the most widely used method to analyze site motion response due to its simplicity and less computational time consumption. However, this method was performed in equivalent-linear method which might not perform the actual response of motion compared to the reality. Therefore, in this case, FFGM analysis in TD was conducted in order to obtain the nonlinear response of soil materials and motion.

In nonlinear analysis, the FFGM response motion can be solved by Eq. (3.7):

$$[M]\{\ddot{u}\}+[C]\{\dot{u}\}+[K]\{u\}=-[M]\{I\}\ddot{u}_g \tag{3.7}$$

Where

$[M],[C],[K]$: Mass, damping, and stiffness matrix of soil element

$\{\ddot{u}\},\{\dot{u}\},\{u\}$: Acceleration, velocity, and displacement of soil element

$\{\ddot{u}_g\}$: Acceleration of ground motion

$\{I\}$: Unit vector

In order to solve the Eq. (3.7), Newmark method [36] was used for numerically solving in each time step. In each soil layer was represented by consistent mass, spring, and dashpot as shown in Fig 3.3. Instead of using lumped mass, the consistent mass can represent the reality of soil behavior and perform a fully matrix as indicated in the following section. The stiffness value was updated in each time increment to represent the nonlinear behavior of soil deposits and damping matrix was expressed by viscous damping in the elastic range and updated in each time increment for nonlinear response of soil medium.

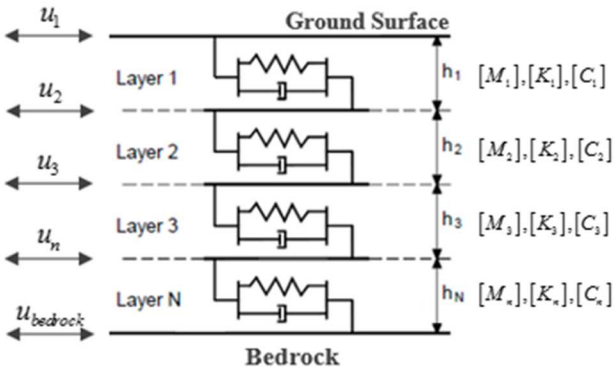

Figure III.3 Soil deposit model for FFGM analysis in TD

III.3.1. Soil Mass Matrix

As mentioned above, mass matrix of soil deposit was modeled as consistent matrix. This consistent mass matrix allowed performing a full mass matrix which can represent the actual behavior of soil deposit. The consistent mass matrix of soil deposit [45] for each layer is shown in the Eq. (3.8).

$$[M] = \frac{\rho h}{6}\begin{bmatrix} 2 & 1 \\ 1 & 2 \end{bmatrix} \tag{3.8}$$

Where

ρ : Density of soil in each layer

h : Thickness of soil in each layer

III.3.2. Soil Stiffness Matrix

The stiffness matrix was initialized by the Eq. (3.9) and updated in each time step to incorporate the non-linearity of soil behavior as expressed in Eq. (3.10).

$$[K] = \frac{G}{h}\begin{bmatrix} 1 & -1 \\ -1 & 1 \end{bmatrix} \tag{3.9}$$

$$K_i = \frac{G_i}{h_i} = \frac{\Delta\tau_i(\gamma_i)}{h_i \Delta\gamma_i} \tag{3.10}$$

Where

G : Shear modulus in each layer

h : Thickness of soil in each layer

$\Delta\tau_i, \Delta\gamma_i$: Stress and strain in each time step

III.3.3. Soil Damping Matrix

III.3.3.1. Viscous Damping

The original expression for small strain damping was proposed by Rayleigh [37] was the most widely used for wave propagation analysis in TD. This expression results from the addition of two matrices: stiffness and mass matrix as expressed in Eq. (3.11).

$$[C] = \alpha_R [M] + \beta_R [K] \tag{3.11}$$

Where

α, β: Scalar value selected to obtain given damping value for two control frequencies.

$[M], [K]$: Mass and stiffness matrix

α_R and β_R coefficient of Eq. (3.12) can be computed using two significant natural modes m and n [37] [38]:

$$\frac{1}{2}\begin{bmatrix} 1/\omega_m & \omega_m \\ 1/\omega_n & \omega_n \end{bmatrix}\begin{Bmatrix} \alpha_R \\ \beta_R \end{Bmatrix} = \begin{bmatrix} \xi_m \\ \xi_n \end{bmatrix} \tag{3.12}$$

This matrix can be solved as the following expression:

$$\alpha_R = 2\omega_m\omega_n\left(\frac{\omega_m\xi_n - \omega_n\xi_m}{\omega_m^2 - \omega_n^2}\right) \beta_R = 2\left(\frac{\omega_m\xi_m - \omega_n\xi_n}{\omega_m^2 - \omega_n^2}\right)$$

If the damping ratio is frequency independent, the both coefficients becomes:

$$\alpha_R = 2\xi\left(\frac{\omega_m\omega_n}{\omega_m + \omega_n}\right) \beta_R = 2\xi\left(\frac{1}{\omega_m + \omega_n}\right)$$

Where

ω_m, ω_n: Frequency mode m and n

ξ: Damping ratio

Generally, for the small strain damping, the first natural mode is widely used and supposed no the second relevant mode occurs $\omega_n = 0$. The damping matrix of small strain at each layer becomes:

$$[C] = \frac{2}{\omega}[\xi_i K_i] = \frac{2}{\omega}\begin{bmatrix} \xi_i K_i & -\xi_i K_i \\ -\xi_i K_i & \xi_i K_i \end{bmatrix} \quad (3.13)$$

However, according to Youssef [39], Eq. (3.13) was available only for short soil columns where only the first mode dominates. For thicker soil columns, Eq. (3.11) was available and showed a good agreement with FD analysis due to contribution of higher mode. As higher modes was used, α_R increased and β_R decreased.

For the site response analysis the natural frequency of the selected mode is commonly calculated as [34]:

$$f_n = (2n-1)\frac{\bar{V}_s}{4H} \quad (3.14)$$

Where

n : Mode number

H : Total thickness of soil column,

$\bar{V}_s$: Equivalent shear velocity.

III.3.3.2. Hysteretic Damping

The hysteretic damping is the equivalent viscous damping ratio that represents the dissipation due to the nonlinear behavior soil column. The concept of dissipated ($E_{dissipated}$) and stored (E_{stored}) energy is used to represent equivalent viscous damping as shown in Eq. (3.15) and Fig. 3.4:

$$\xi_{hysteretic} = \frac{1}{4\pi}.\frac{E_{dissipated}}{E_{stored}} = \frac{1}{2\pi}\frac{A_{hysteretic}}{\tau_0\gamma_0} \quad (3.15)$$

Where

τ_0, γ_0 : Reversal stress and strain

$A_{hysteretic}$: Area of hysteretic loop

$\xi_{hysteretic}$: Hysteretic damping

$E_{dissipated}$: Dissipated energy

E_{stored} : Stored energy

For nonlinear response of soil column, the modified Ramberg-Osgood model [40] was used in this study. The Ramberg-Osgood model, coupling with the extended

Masing criterion, is one of the most used constitutive relations in nonlinear analysis of FFGM as shown in Fig. 3.5.

Firstly, Ramberg-Osgood model [50] was proposed to describe the stress-strain curve of aluminums-alloy and steel sheets. Idriss et al. [41] were the first authors who proposed the use of the Ramberg-Osgood model to obtain the shear modulus reduction. At the same year, the modification of Ramberg-Osgood model for nonlinear analysis of FFGM was proposed by Tatsuoka et al. as mentioned above.

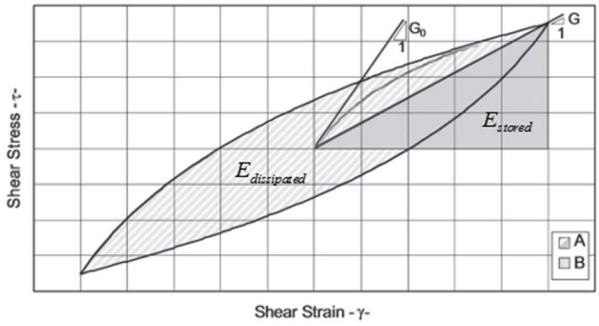

Figure III.4 Stress-strain relationship [33]

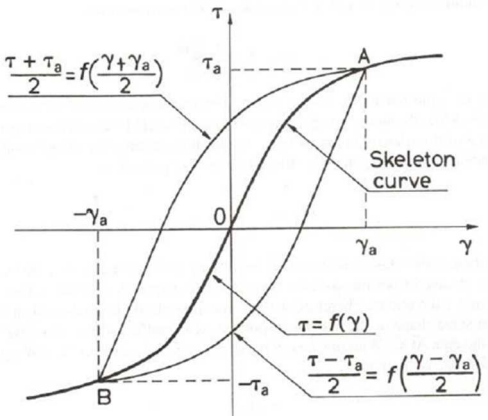

Figure III.5 Ramberg-Osgood model [42]

According to the modified Ramberg-Osgood, the hysteretic damping due to the nonlinear behavior of soil column is shown in Eq. (3.16).

$$h_{hystertic} = \frac{1}{2\pi}\frac{\beta}{\beta+2}\frac{\alpha\tau_0^{\beta}}{1+\alpha\tau_0^{\beta}} = \frac{2}{\pi}\frac{\beta}{\beta+2}\left(1-\frac{G}{G_0}\right) \tag{3.16}$$

Where

$$\beta = \frac{2\pi h_{\max}}{2 - h_{\max}} \quad \frac{G}{G_0} = \frac{1}{1 + \alpha|\gamma G|^{\beta}} \quad \alpha = \left(\frac{2}{\gamma_{0.5} G_0} \right)^{\beta}$$

$\gamma_{0.5}$: Corresponds to $\frac{G}{G_0} = 0.5$

$h_{\max}$: Maximum damping, when $\gamma \to \infty, so\ h \to h_{\max}, G \to 0$

The skeleton and hysteretic curve of modified Ramberg-Osgood can be expressed in Eq. (3.17) and (3.18):

- *Skeleton or Backbone curve*: $$\gamma = \frac{\tau}{G_0}\left(1 + \alpha|\tau|^{\beta}\right) \tag{3.17}$$

- *Hysteretic curve:* $$\frac{\gamma \pm \gamma_0}{2} = \frac{\tau \pm \tau_0}{2G_0}\left(1 + \alpha\left|\frac{\tau \pm \tau_0}{2}\right|^{\beta}\right) \tag{3.18}$$

Based on the hysteretic rule, the nonlinear response of shear modulus $G_i(t)$ can be derived from Eq. (3.19).

$$\frac{G_i(t)}{G_0} = \frac{\tau_i - \tau_{i-1}}{\gamma_i - \gamma_{i-1}} \tag{3.19}$$

Where

τ_i, τ_{i-1}: Reversal shear stress of point i and i-1

γ_i, γ_{i-1}: Reversal shear strain of point i and i-1

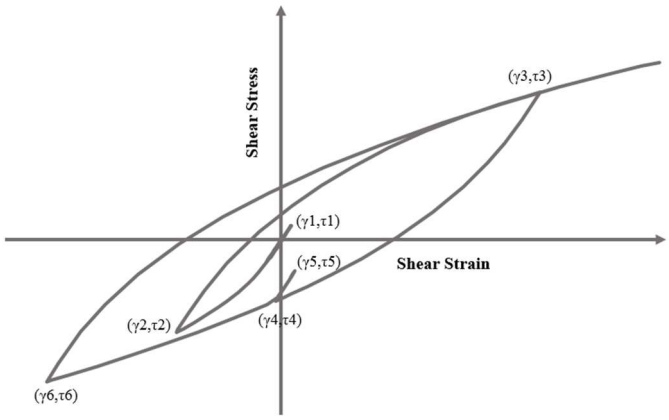

Figure III.6 Reversal points of shear stress-strain

III.4. PROPOSED ANALYTICAL MODEL FOR NONLINEAR RESPONSE OF SOIL MATERIAL AND MOTION

In order to perform FFGM in TD, the FFGM analysis in FD was necessary to obtain a properly input motion for FFGM in TD. The procedure of FFGM analysis in TD was presented under both linear and nonlinear analysis. Examples of FFGM analysis in TD were conducted at the end of this chapter.

III.4.1. Linear Response Analysis

In linear (LN) response analysis, the target earthquake motion was input at the base of soil column (or surface layer) as an outcrop motion (*2E*). Then, the FFGM analysis in FD was performed and the within output motion (*E+F*) was extracted at the base of soil column. This motion was applied at the same layer of soil column (as input motion) for FFGM analysis in TD, as shown in Fig. 3.7. The within motion (*E+F*) of any location is an actual motion of that location.

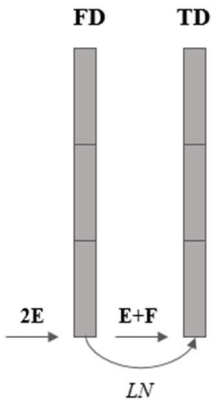

Figure III.7 Linear input motion for FFGM in TD

III.4.2. Nonlinear Response Analysis

In nonlinear (NL) response analysis, the procedure is the same as linear analysis but it was required to perform in both linear (LN) and equivalent-linear (EL) analysis in FD and the within output motion (*E+F*) of both analyses were significant to be the same or almost the same. Then, this motion was applied as the input motion at the same layer for FFGM analysis in TD.

Some extra layers might be needed in order to obtain the same or similar motion as described above. This procedure is shown in Fig. 3.8.

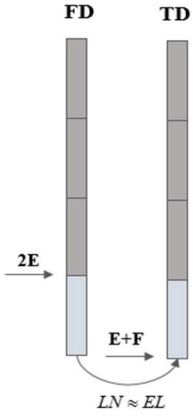

Figure III.8 Nonlinear input motion for FFGM in TD

Besides this, in order to validate the nonlinear response output motion in TD, the comparison of this motion with linear and equivalent-linear analysis in FD was immensely significant. This comparison leads to an understanding how correctly of this nonlinear response motion.

III.4.3. Example of Free Field Ground Motion Analysis in TD

III.4.3.1. First Soil Column

In this example, the uniform soil column in a depth of 40m was assumed resting on the rock. This uniform soil column consisted the same properties as in class D of IBC code [43] as shown in Table 3.1 and the nonlinear soil property $(G/G0-\gamma, \xi-\gamma)$ is shown in Table 3.2.

The Kobe earthquake record data were assumed as input motion at the base of soil column. The motion in X and Y direct were assumed as the motion in EW and NS of record data as shown in Fig. 3.9 while the UD motion was ignored in this study.

Table III.1 Uniform soil column properties

H (m)	Vs (m/s)	γ (kN/m^3)	ξ (%)
0.0-40.0	300	21.0	5
Rock	500	23.0	1

Table III.2 Dynamic soil property [25]

γ_{-soil} (%)	$G/G0_{-soil}$	ξ_{-soil} (%)	γ_{-rock} (%)	$G/G0_{-rock}$	ξ_{-rock} (%)
0.0001	1.000	0.24	0.0001	1.000	0.40
0.0003	1.000	0.42	0.0003	1.000	0.40
0.001	0.990	0.80	0.001	0.987	0.80
0.003	0.960	1.40	0.003	0.952	0.80
0.01	0.850	2.80	0.01	0.900	1.50
0.03	0.640	5.10	0.03	0.810	1.50
0.1	0.370	9.80	0.10	0.725	3.00
0.3	0.180	15.50	1.00	0.550	4.60
1	0.080	21.00			
3	0.050	25.00			
10	0.035	28.00			

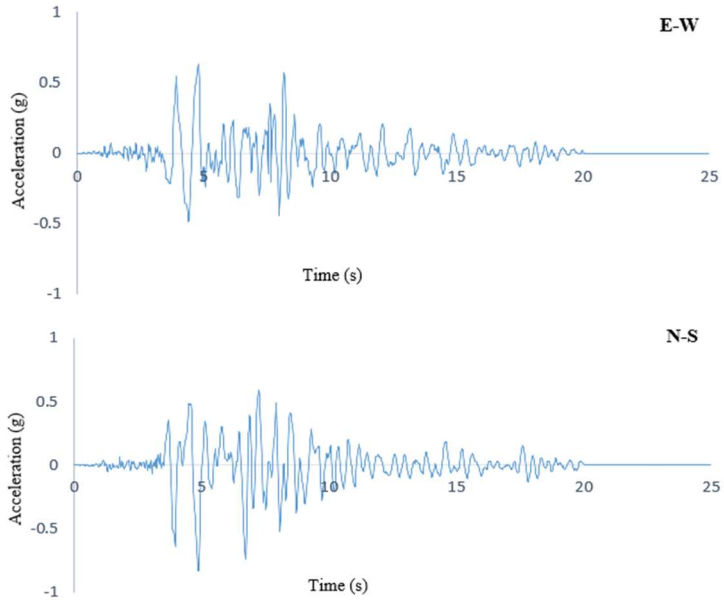

Figure III.9 Kobe earthquake record motion data

· **Linear Response of FFGM Analysis**

In linear analysis, based on the procedure described above, the output motion results at the ground surface for both analysis in FD and TD are shown in Fig. 3.10.

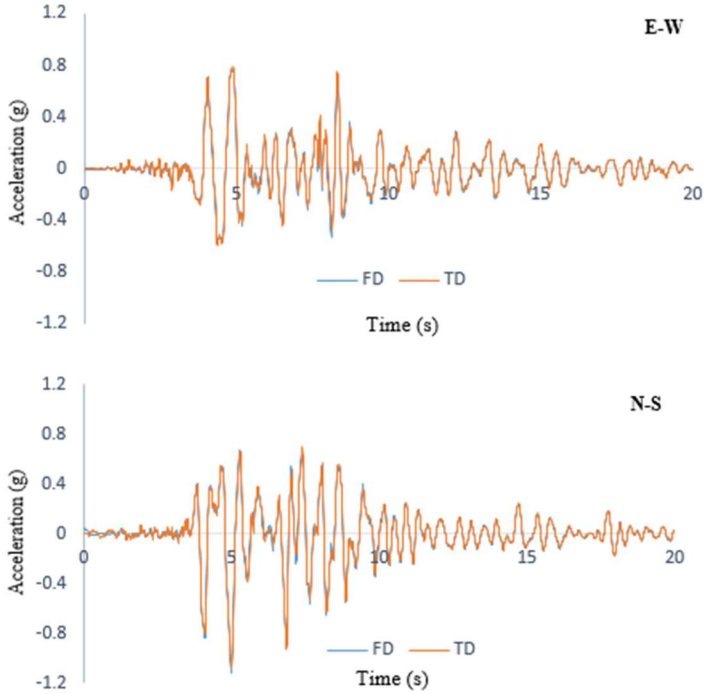

Figure III.10 Linear response analysis of FFGM in FD and TD

· **Nonlinear Response of FFGM Analysis**

In nonlinear analysis, based on the procedure described above, two extra layers were needed for this study as shown in Fig. 3.11. The first layer consisted 5m in depth and 500m/s for shear velocity while the second layer consisted 1000m in depth and 8km/s for shear velocity. The within output motion (*E+F*) in FD is shown in Fig. 3.12 and the output motion at the ground surface in TD is shown in Fig. 3.13.

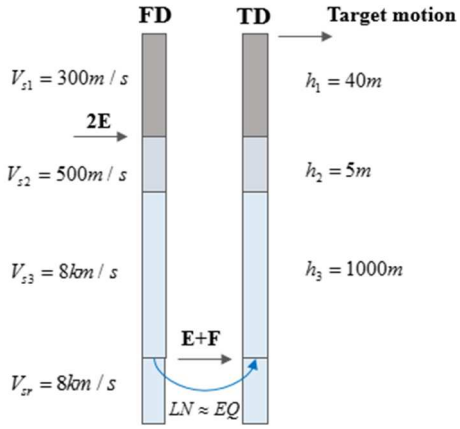

Figure III.11 Procedure for input motion in TD

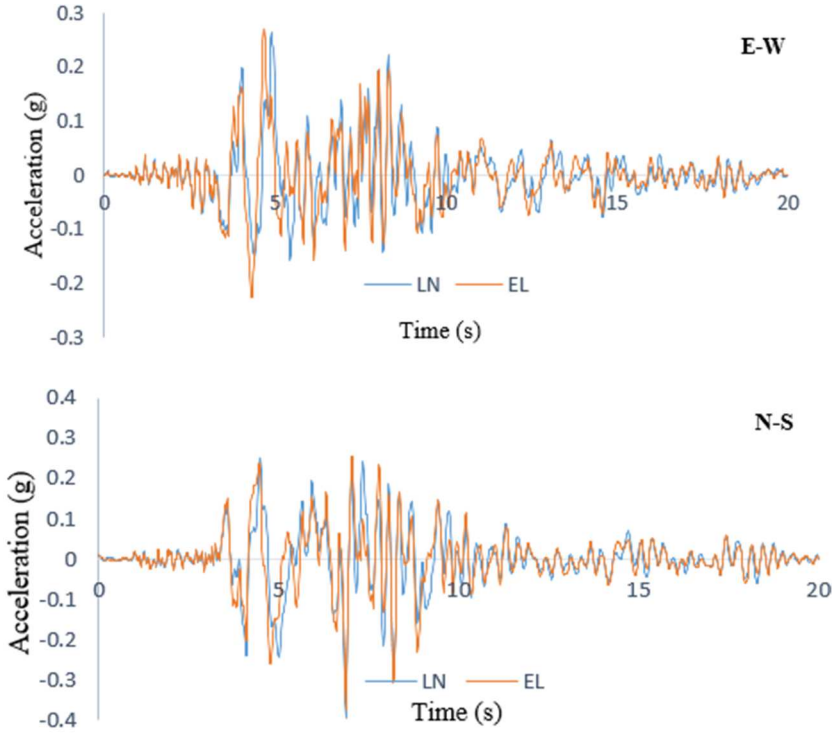

Figure III.12 Within output motion (*E+F*) in FD

As shown in Fig. 3.12, the within output motion (*E+F*) results from both analysis showed a good agreement and adequate for input motion in TD analysis. This motion was applied at the same layer and property for TD analysis. The FFGM at the ground surface for both direction, as shown in Fig. 3.13, and nonlinear response of soil stiffness G_{NL} were obtained. However, as mentioned above, the comparison of these nonlinear response motions with linear and equivalent-linear motions at the ground surface in FD was significant. These comparisons are shown in Fig. 3.14 and 3.15.

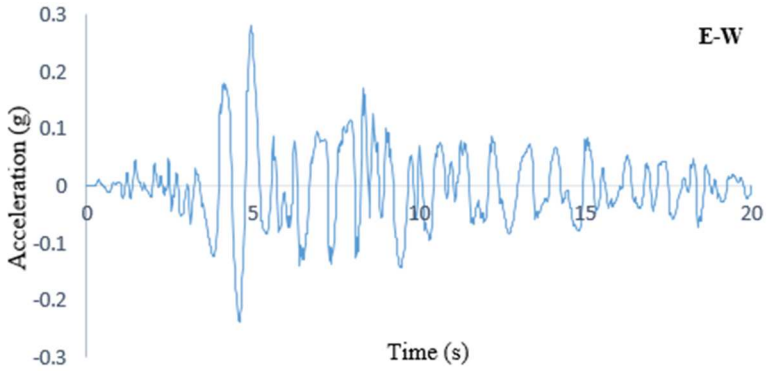

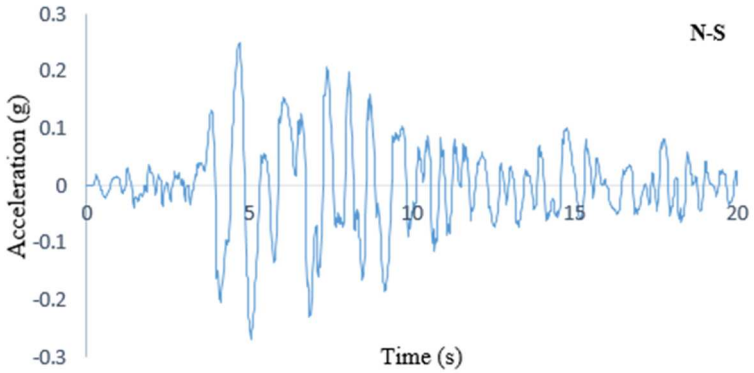

Figure III.13 Nonlinear response of FFGM analysis in TD

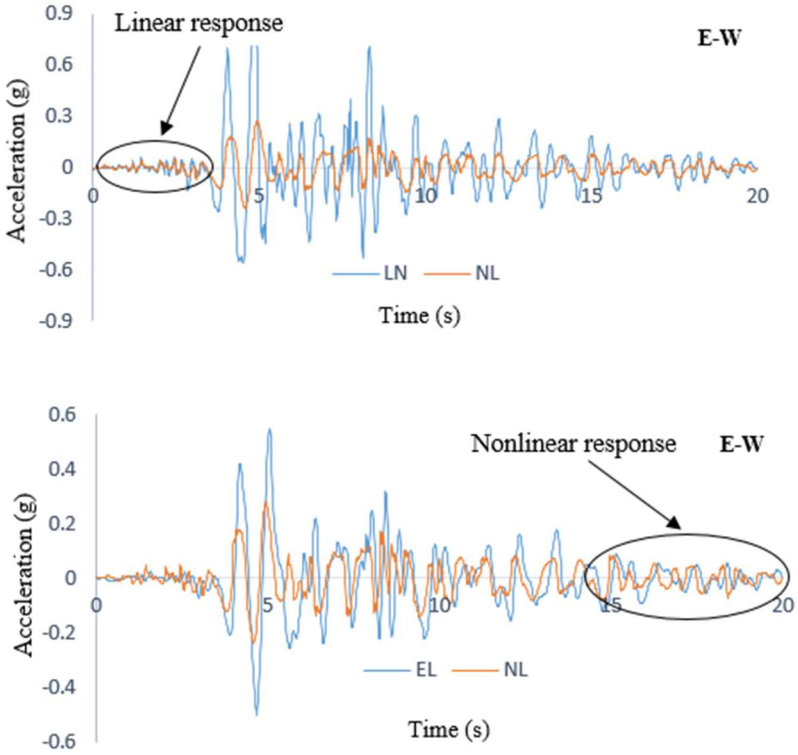

Figure III.14 Comparison between LN, EL, NL motion in EW direction

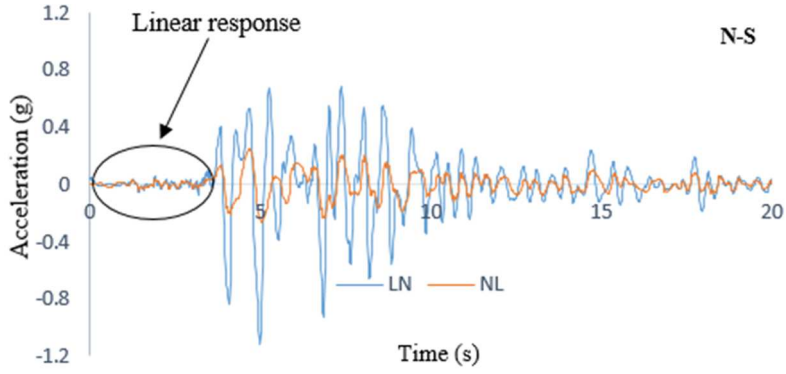

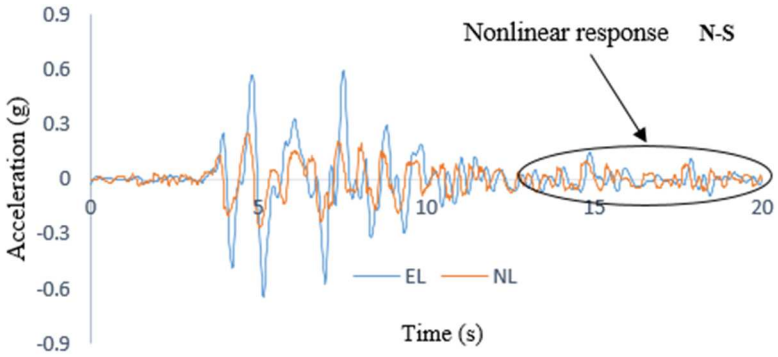

Figure III.15 Comparison between LN, EL, and NL motion in NS direction

As shown in Fig. 3.14 and 3.15, these comparisons indicated that the nonlinear response motion at the ground surface showed a good agreement with linear motion response for a few seconds from starting point and with equivalent-linear motion response for the last several seconds. These agreements confirmed that the nonlinear response at the ground surface in TD started from the linear to nonlinear response motion. This confirmation showed about the validation of proposed analytical model considering the nonlinear response of soil material. Furthermore, the hysteretic curve of nonlinear response motion at the ground surface is shown in Fig. 3.16 and the maximum strain in each layer is shown in Table 3.3.

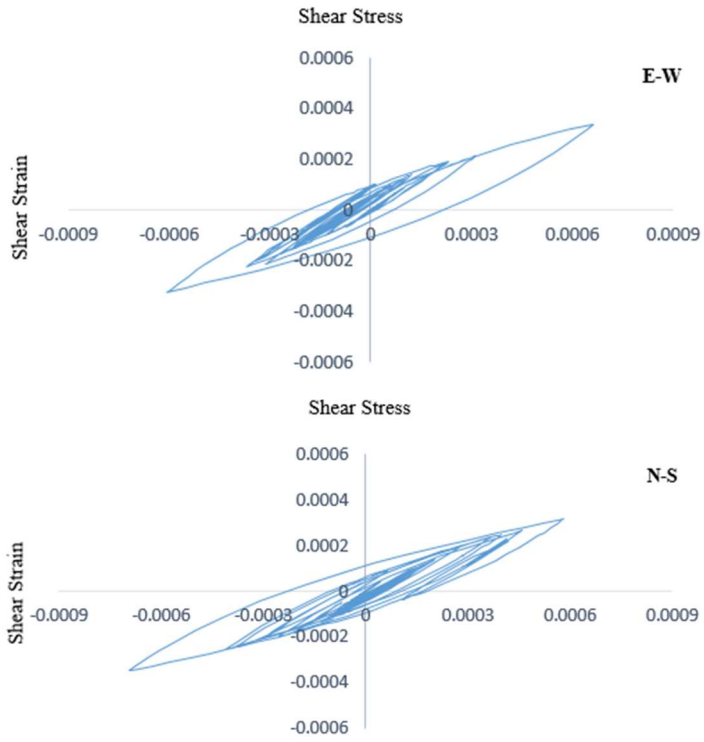

Figure III.16 Hysteretic curve of nonlinear response motion

Table III.3 Maximum strain in each layer

Layer	Max.strain (E-W)	Max. strain (N-S)
1	0.00066	0.00069
2	0.00391	0.00413
3	0.00823	0.00868
4	0.01281	0.01331
5	0.01747	0.01771
6	0.02217	0.02196
7	0.02707	0.02625
8	0.03247	0.03094

The nonlinear response of soil material for both directions is shown in Fig. 3.17.

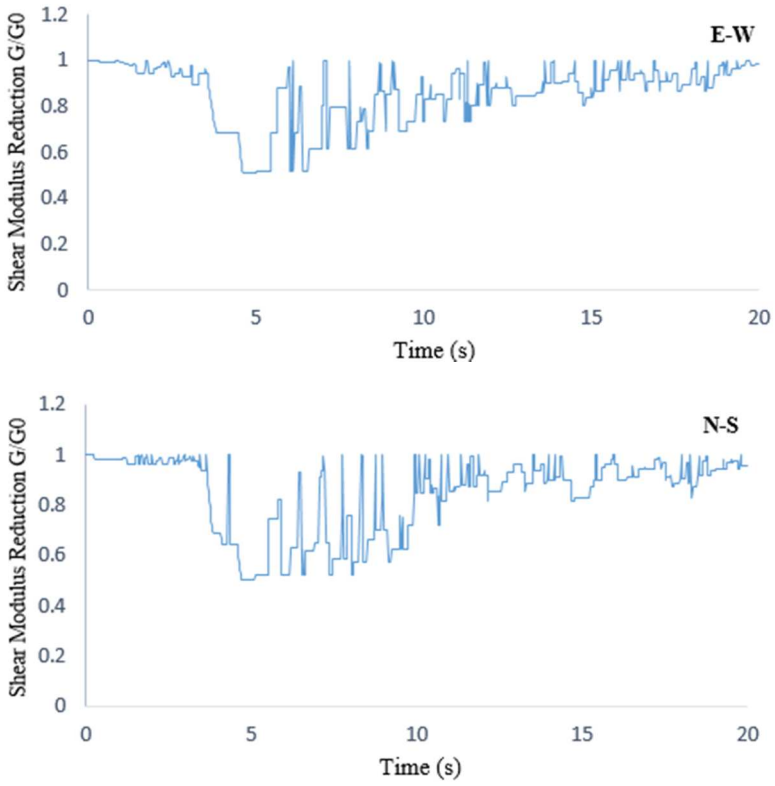

Figure III.17 Nonlinear response of soil material at surface layer

III.4.3.2. Second Soil Column

In this example, the uniform soil in depth 60m was assumed resting on the rock. The soil property was shown in Table 3.4 while the nonlinear soil property and earthquake input motion were the same as shown in Table 3.2 and Fig. 3.9. According to the same

procedure described above, the response of FFGM was achieved as in the following sections.

Table III.4 Uniform soil property

H (m)	Vs (m/s)	γ (kN/m^3)	ξ (%)
0.0-60.0	350	22.0	5
Rock	600	23.0	1

- **Linear Response of FFGM Analysis**

According to Fig. 3.18, the linear response of both FD and TD was the same as described above.

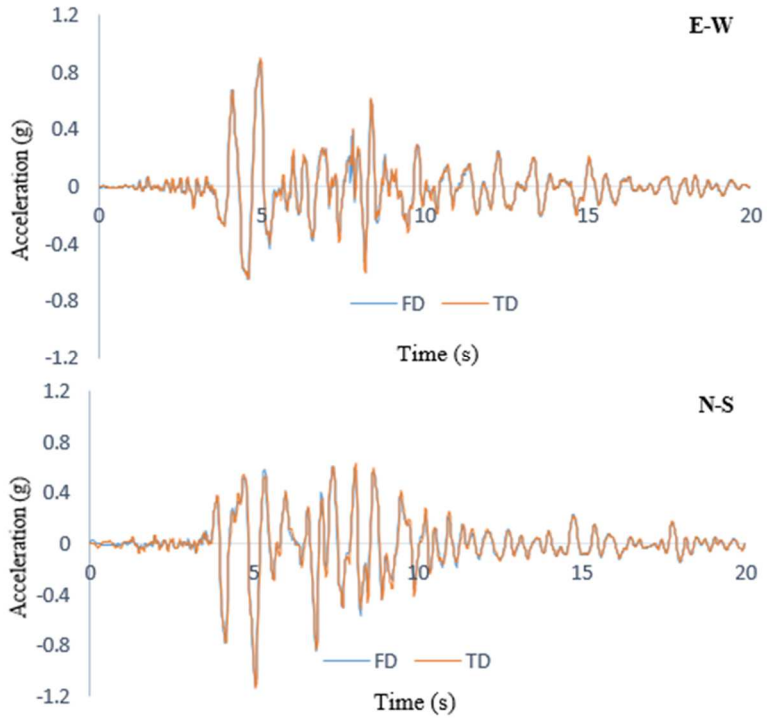

Figure III.18 Linear response analysis of FFGM in FD and TD

- **Nonlinear Response of FFGM Analysis**

For nonlinear response analysis, there were two extra layers added to existing layers as shown in Fig. 3.19. The first layer consisted h = 5m and V_s= 600m/s while the second layer consisted h = 800m and V_s= 5km/s.

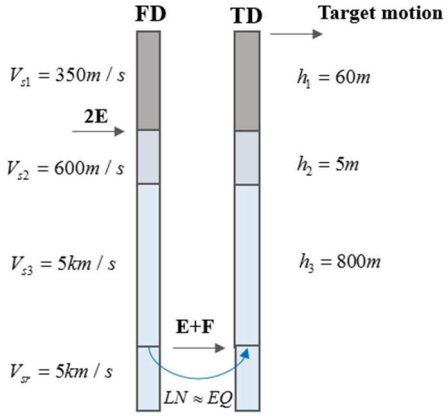

Figure III.19 Procedure for input motion in TD

The within output motion at the base of column for both directions is shown in Fig. 3.20. The response results showed a good agreement for both analytical model LN and EL, thus, these motions were adequate for assigning as input motion in TD.

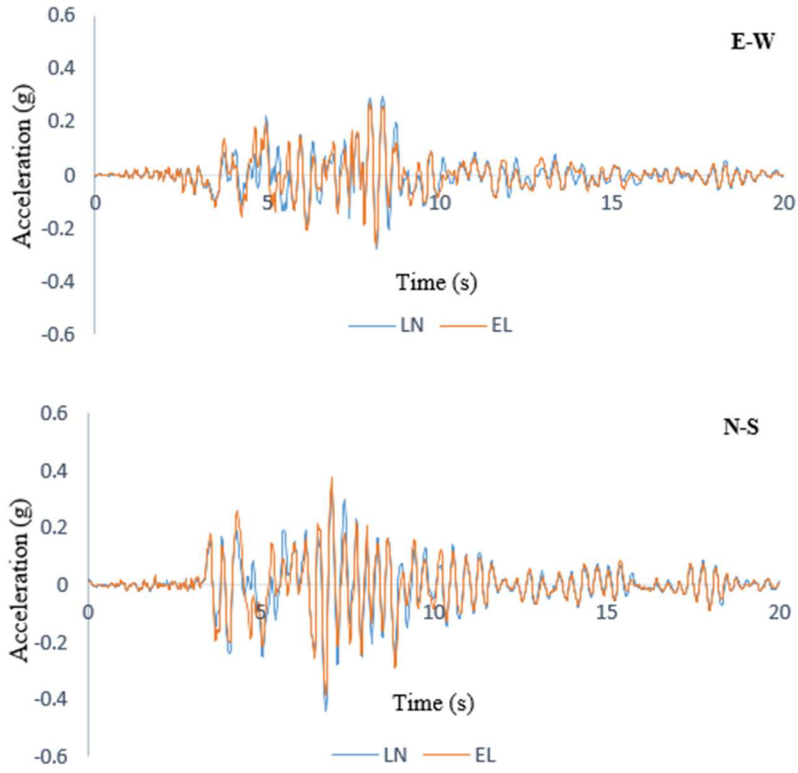

Figure III.20 Within output motion (*E+F*) in FD

The nonlinear response motion at surface layer for both directions was shown in Fig. 3.21 while the comparisons of both motions are shown in Fig. 3.22 and 3.23.

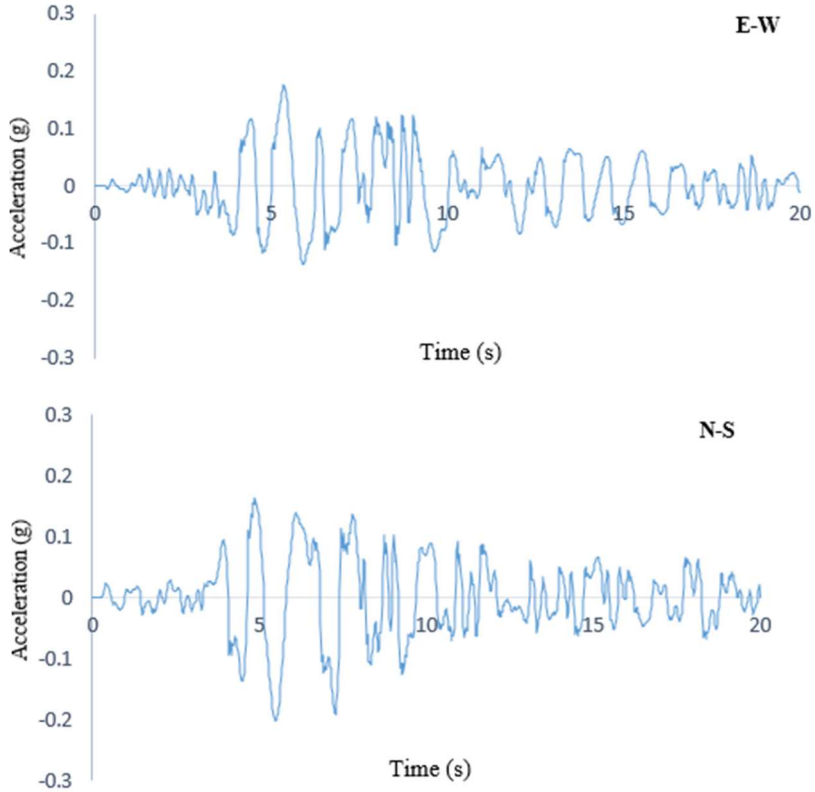

Figure III.21 Nonlinear response of FFGM analysis in TD

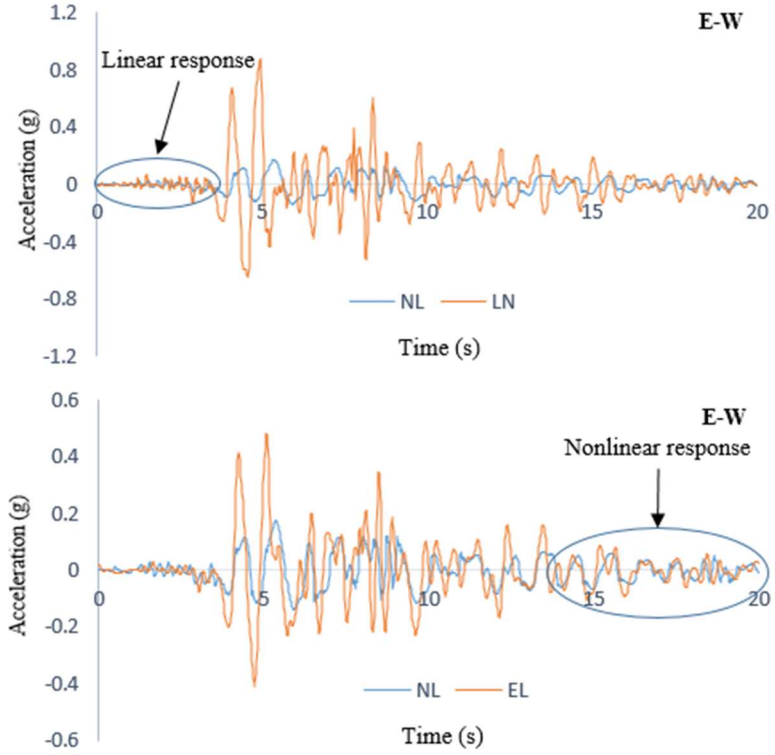

Figure III.22 Comparison between LN, EL, NL motion in EW direction

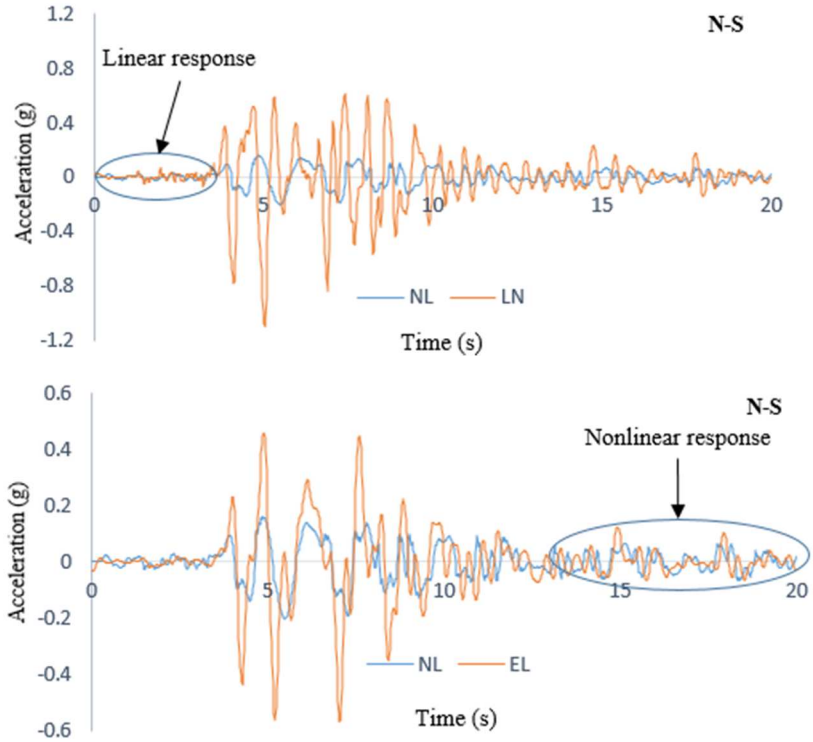

Figure III.23 Comparison between LN, EL, NL motion in NS direction

The hysteretic curves of nonlinear response motion at surface layer for both directions and maximum strain in each layer shown in Fig. 3.24 and Table 3.5 while nonlinear response of soil material is shown in Fig. 3.25.

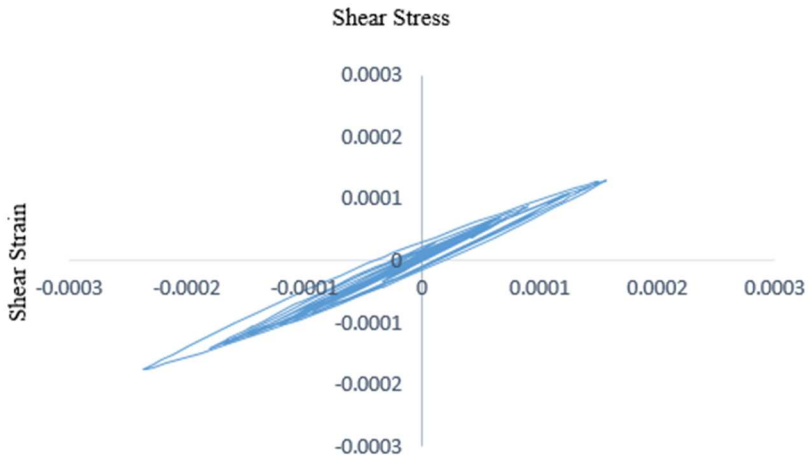

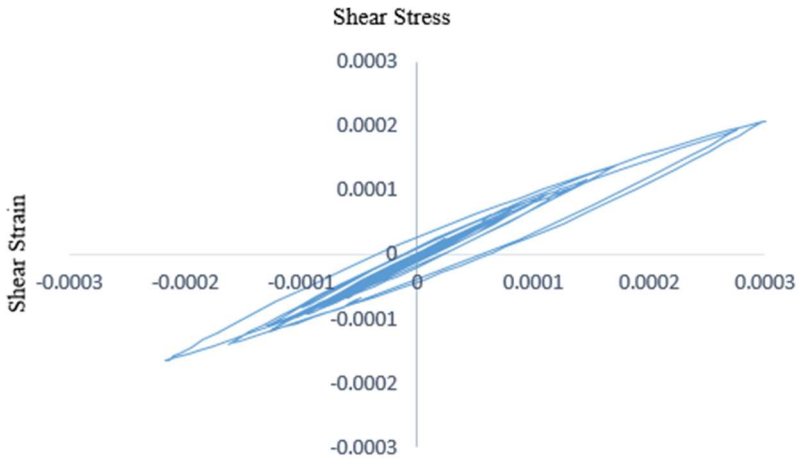

Figure III.24 Hysteretic curve of nonlinear response motion

Table III.5 Maximum strain in each layer

Layer	Max.strain (E-W)	Max. strain (N-S)
1	0.0002	0.0003
2	0.0013	0.0018
3	0.0031	0.0043
4	0.0053	0.0073
5	0.0077	0.0105
6	0.0101	0.0138
7	0.0124	0.0171
8	0.0147	0.0203
9	0.0168	0.0233
10	0.0186	0.0262
11	0.0204	0.0290
12	0.0223	0.0319

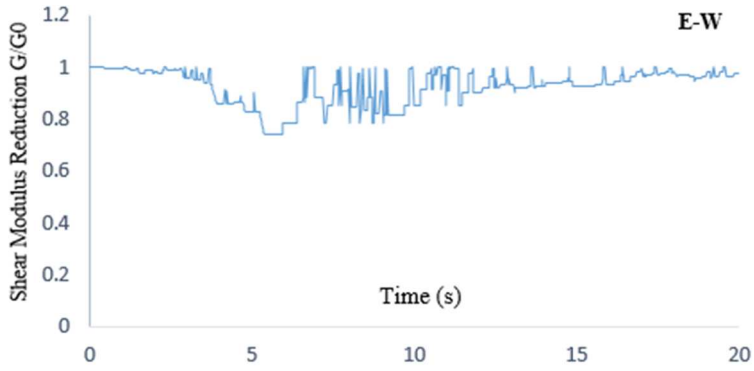

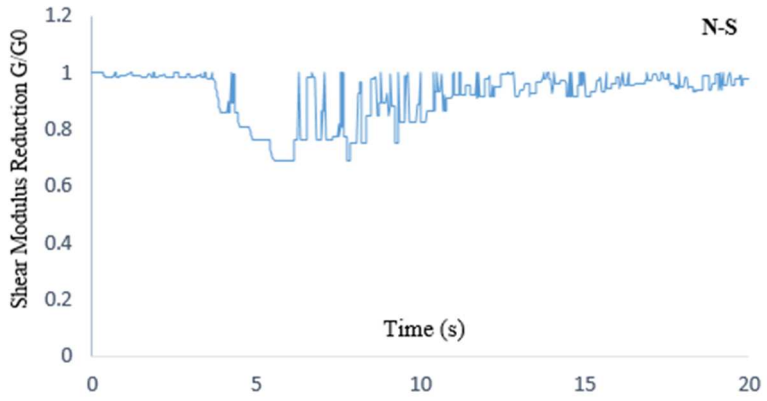

Figure III.25 Nonlinear response of soil material at surface layer

III.5. CONCLUSIONS

The conclusion of this chapter was presented as in the following:

- The necessity of FFGM analysis was introduced and the integration of FFGM analysis into OBASAN was presented for both FD and TD. The verification of FFGM analysis in OBASAN was provided in Appendix.
- An analytical model considering nonlinear response of soil material was proposed and examples of FFGM analyses were provided. The nonlinear response motion of FFGM at the ground surface in TD was compared to linear and equivalent-linear response motion in FD. The nonlinear response results showed a good agreement with linear response for a few seconds from starting point and with equivalent-linear response for the last several seconds. The agreement confirmed about the validation of proposed analytical model considering nonlinear response motion and soil material.

According to the description above, this proposed analytical model considering nonlinear response of soil material and motion would be adequate and a potential model for nonlinear FFGM analysis in TD. This nonlinear response of soil material and motion was a significant part for conducting the seismic response of structure considering nonlinear SSI effect using substructure approach.

CHAPTER IV. SEISMIC RESPONSE OF STRUCTURE UNDER NONLINEAR SOIL-STRUCTURE INTERACTION EFFECT

IV.1. INTRODUCTION

Generally, the seismic response of structure considering SSI effect under substructure approach can be performed only with equivalent-linear response of soil material and corresponding motion in FD. This restriction can cause mismatched response and overestimated results compared to the actual response of structure under earthquake. Therefore, the objective of this chapter is to present analytical model considering nonlinear SSI effect on the response of structure using substructure approach. In order to achieve this objective, the analytical model was divided into four steps: FFGM, FIM, dynamic impedance, and response of structure. For better understanding, an example of 3D RC frame structure model supported by rigid surface foundation was conducted. The soil column models and input earthquake motion from Chapter III were used in this study. The relevant parameters were provided in the following sections.

IV.2. NONLINEAR SOIL-STRUCTURE INTERACTION EFFECT

IV.2.1. Free Field Ground Motion (FFGM)

In order to obtain the target, the nonlinear response of soil material and motion was very important. Based on the analytical procedure from Chapter III, the nonlinear response of soil material $G_i(t)$ and motion can be achieved with corresponding input data of soil deposits.

IV.2.2. Foundation Input Motion (FIM)

FIM is an evaluation of transfer functions to convert the FFGM to the FIM. This motion is generally composed by both translational and rotational component which represent the seismic demand applied to the foundation and structure system. The translational and rotational of FIM can be expressed in the Eq. (4.1) and (4.2).

- ***Translation Motion***: $$u_{FIM} = H_u.u_g \quad (4.1)$$

Where

$$H_u = \frac{\sin\left(a_0^k\left(\frac{V_s}{V_{app}}\right)\right)}{a_0^k\left(\frac{V_s}{V_{app}}\right)} \quad \text{if} \quad a_0^k \le \frac{\pi}{2}\frac{V_{app}}{V_s}$$

$$H_u = \frac{2}{\pi} \quad \text{if} \quad a_0^k > \frac{\pi}{2}\frac{V_{app}}{V_s}$$

$$a_0^k = \frac{\omega B_e^A}{V_s}$$

- ***Rotation Motion:*** $$\phi_{FIM} = \frac{u_g}{B_e^A} I_\phi \tag{4.2}$$

Where

$$I_\phi = 0.30\left[1 - \cos\left(a_0^k\left(\frac{V_s}{V_{app}}\right)\right)\right] \text{if} \quad a_0^k \le \frac{\pi}{2}\frac{V_{app}}{V_s}$$

$$I_\phi = 0.30 \quad \text{if} \quad a_0^k > \frac{\pi}{2}\frac{V_{app}}{V_s}$$

$$a_0^k = \frac{\omega B_e^A}{V_s}$$

H_u, I_ϕ: Translation and rotation of transfer function

u_{FIM}, ϕ_{FIM} : Translation and rotation of FIM

a_0^k: Dimensional of frequency

u_g : Free field ground motion

V_s, V_{app} : Shear velocity and apparent shear velocity

B_e^A: Foundation half-width or equivalent radius

To determine V_{app}, there are various solutions have been proposed according to wave motion types and geology conditions such as incident S wave [23], surface wave [53], multiple layers of soil deposits [54]-[56], and the increasing stiffness with depth [54]. However, apart from these theoretical proposal, there were numerous indirect measurement of apparent velocity in body wave and indicated that the apparent velocity for a typical soil site ranges from 2.0km/s to 3.5km/s, thus, $V_{app} / V_s \approx 10$ [24].

IV.2.3. Dynamic Impedance

The dynamic impedance is an evaluation the interaction section between soil and structure. This function can be expressed in Eq. (4.3) and (4.4) [24].

$$\bar{k}_j = k_j + i\omega c_j \tag{4.3}$$

$$\bar{k}_j = k_j(1 + 2i\beta_j) \tag{4.4}$$

$$\beta_j = \frac{\omega c_j}{2k_j} \tag{4.5}$$

Where

$\bar{k}_j$: Complex-valued impedance function

k_j, c_j : Foundation stiffness and dashpot

β_j : Radiation damping

IV.2.3.1. Foundation Stiffness

The equation of foundation stiffness can be expressed according to the type of foundation [24]. Due to the scope of this study, nonlinear SSI effect, the simply equation of surface foundation was expressed in this study. The foundation stiffness of surface foundation rested on the uniform soil medium is expressed in Eq. (4.6).This foundation stiffness is composed by static stiffness, dynamic stiffness modifiers, and embedment modifier.

$$k_j = K_j . \alpha_j . \eta_j \tag{4.6}$$

Where

K_j : Static foundation stiffness at zero frequency

α_j : Dynamic stiffness modifiers

η_j : Embedment modifier

· ***Static Foundation Stiffness***

The static foundation stiffness is expressed in Eq. (47)-(4.12) for six directions.

$$K_x = K_y - \frac{0.2}{0.75 - \upsilon} GL\left(1 - \frac{B}{L}\right) \tag{4.7}$$

$$K_y = \frac{2GL}{2 - \upsilon}\left[2 + 2.5\left(\frac{B}{L}\right)^{0.85}\right] \tag{4.8}$$

$$K_z = \frac{2GL}{1-\upsilon}\left[0.73+1.54\left(\frac{B}{L}\right)^{0.75}\right] \tag{4.9}$$

$$K_{xx} = \frac{G}{1-\upsilon}\left(I_x\right)^{0.75}\left(\frac{L}{B}\right)^{0.25}\left[2.4+0.5\left(\frac{B}{L}\right)\right] \tag{4.10}$$

$$K_{yy} = \frac{G}{1-\upsilon}\left(I_y\right)^{0.75}\left[3\left(\frac{L}{B}\right)^{0.15}\right] \tag{4.11}$$

$$K_{zz} = GJ_t^{0.75}\left[4+11\left(1-\frac{B}{L}\right)^{10}\right] \tag{4.12}$$

- ***Rigid Surface Foundation Stiffness Modifiers***

  The foundation stiffness modifiers are expressed in Eq. (4.13)-(4.18).

$$\alpha_x = 1.0 \tag{4.13}$$

$$\alpha_y = 1.0 \tag{4.14}$$

$$\alpha_z = 1-\left[\frac{\left(0.4+\frac{0.2}{\left(\frac{L}{B}\right)}\right)a_0^2}{\left(\frac{10}{1+3\left(\frac{L}{B}-1\right)}\right)+a_0^2}\right] \tag{4.15}$$

$$\alpha_{xx} = 1-\left[\frac{\left(0.55+0.11\sqrt{\frac{L}{B}-1}\right)a_0^2}{\left(2.4-\frac{0.4}{\left(\frac{L}{B}\right)^3}+a_0^2\right)}\right] \tag{4.16}$$

$$\alpha_{yy} = 1 - \left[\frac{0.55 a_0^2}{\left(0.6 + \frac{1.4}{\left(\frac{L}{B} \right)^3} \right) + a_0^2} \right] \tag{4.17}$$

$$\alpha_{zz} = 1 - \left[\frac{\left(0.33 - 0.33 \sqrt{\frac{L}{B} - 1} \right) a_0^2}{\left(\frac{0.8}{1 + 0.33 \left(\frac{L}{B} - 1 \right)} \right) + a_0^2} \right] \tag{4.18}$$

· **Rigid Surface Foundation Embedment Modifiers**

Due to the scope of this study, as mentioned above, the embedment modifier is $\eta_i = 1.0$.

IV.2.3.2. Radiation Damping

The radiation damping is expressed in Eq. (4.19)-(4.24).

$$\beta_x = \left[\frac{4 \left(\frac{L}{B} \right)}{\frac{K_x}{GB}} \right] \left[\frac{a_0}{2\alpha_x} \right] \tag{4.19}$$

$$\beta_y = \left[\frac{4 \left(\frac{L}{B} \right)}{\frac{K_y}{GB}} \right] \left[\frac{a_0}{2\alpha_y} \right] \tag{4.20}$$

$$\beta_z = \left[\frac{4\psi \left(\frac{L}{B} \right)}{\frac{K_z}{GB}} \right] \left[\frac{a_0}{2\alpha_z} \right] \tag{4.21}$$

$$\beta_{xx} = \left[\frac{\left(\frac{4\psi}{3}\right)\left(\frac{L}{B}\right)a_0^2}{\left(\frac{K_{xx}}{GB^3}\right)\left[2.2 - \frac{0.4}{\left(\frac{L}{B}\right)^3} + a_0^2\right]} \right] \left[\frac{a_0}{2\alpha_{xx}} \right] \tag{4.22}$$

$$\beta_{yy} = \left[\frac{\left(\frac{4\psi}{3}\right)\left(\frac{L}{B}\right)^3 a_0^2}{\left(\frac{K_{yy}}{GB^3}\right)\left[\left(\frac{1.8}{1+1.75\left(\frac{L}{B}-1\right)}\right) + a_0^2\right]} \right] \left[\frac{a_0}{2\alpha_{yy}} \right] \tag{4.23}$$

$$\beta_{zz} = \left[\frac{\left(\frac{4}{3}\right)\left[\left(\frac{L}{B}\right)^3 + \left(\frac{L}{B}\right)\right]a_0^2}{\left(\frac{K_{zz}}{GB^3}\right)\left[\frac{1.4}{1+3\left(\frac{L}{B}-1\right)^{0.7}} + a_0^2\right]} \right] \left[\frac{a_0}{2\alpha_{zz}} \right] \tag{4.24}$$

Where

G, ν : Shear modulus and Poisson's coefficient

B, L : Width and length of rectangular foundation

I_x, I_y : Area moment of inertia of soil-foundation contact

$J_t = I_x + I_y$: Polar moment of inertia of soil-foundation contact surface

$\psi = \sqrt{2(1-\upsilon)/(1-2\upsilon)}, \ \psi \le 2.5$

$a_0 = \dfrac{\omega B}{V_s}, \ B \le L$

In this section, the soil stiffness value, G , was varied according to each time step in order to perform nonlinear SSI effect. The variation of soil stiffness, $G_i(t)$, can be achieved from the analytical procedure in Chapter III.

IV.2.4. Seismic Response of Structure under Nonlinear SSI Effect

In order to perform seismic response of structure considering SSI effect under substructure approach, the upper structure was connected to soil spring-dashpot and subjected to the FIM which were determined in the previous sections, as shown in literature reviews. In this section, the seismic response of structure under SSI effect was performed using nonlinear response value of interaction section with the corresponding motions. The seismic response of structure was performed in TD, as expressed in Eq. (4.23). The analytical procedure allowed performing the seismic response of structure under nonlinear SSI effect.

$$[M]\{\ddot{u}\}+[C]\{\dot{u}\}+[K]\{u\}=-[M]\{1\}\ddot{u}_0 \tag{4.23}$$

Where

$[M],[C],[K]$: Mass, damping, and stiffness matrix of whole structure

$\{\ddot{u}\},\{\dot{u}\},\{u\}$: Acceleration, velocity, and displacement vector of whole structure

$\ddot{u}_0$: Foundation input motion

IV.3. EXAMPLE OF SEISMIC RESPONSE OF STRUCTURE UNDER NONLINEAE SSI EFFECT

For better understanding, an example of 3D RC frame under SSI effect was provided. This structure was assumed as a rigid surface foundation and supported by uniform soil medium. The interaction between structure and soil was represented by spring-dashpot, which was performed for both equivalent-linear and nonlinear value in order to evaluate the response of structure under nonlinear SSI effect. This frame structure was rested on the two types of soil columns and subjected to vertically S wave, as described in Chapter III.

IV.3.1. Structural Model Outline

This 3D frame structural model was the same model of the E-Defense test structure [44] [45], as shown in Fig. 4.1. This structure consisted six stories 3.5m for height in each floor. There were two spans in X-direction and three spans in Y-direction with the same length 5m in each span. In this study, the column C1 section was 0.5mx0.5m with 8-D19 and C2 section was 0.3mx0.3m with 4-D19, beam section was 0.3mx0.5m with 5-D19, and both shear-wall and sidewalls thickness were 0.15m with doubly reinforcing bar D10@300. Furthermore, the shear reinforcing bar of column was D10@100 while

beam element was D10@200. The nominal strength of reinforcing bars were SD345 and SD295 for D19 and D10, respectively, and concrete strength was 21MPa for all structural elements. Besides this, the non-structural element load was assumed 3.0kPa and live load 2.5kPa for each floor.

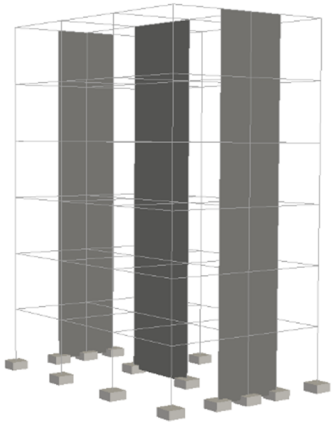

(a) Perspective view of frame structural model

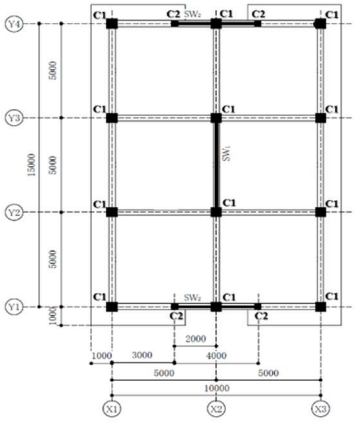

(b) Top view of structure

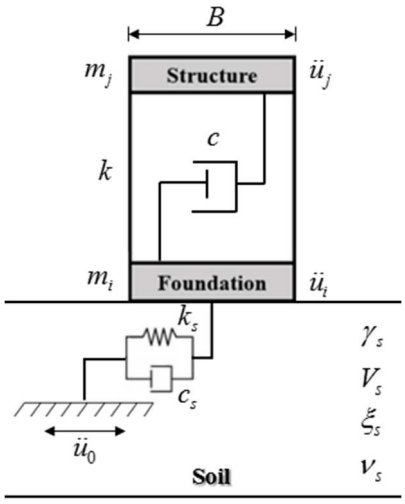

(c) Soil-structure interaction analytical model

Figure IV.1 3D RC frame structural model

IV.3.2. Uniform Soil Medium and Earthquake Input Motion

In this study, the uniform soil was assumed to support the structure and the soil property was described in the previous chapter and repeated here again in Table 4.1 and 4.2.

Table IV.1 Uniform soil property of first column

H (m)	Vs (m/s)	γ (kN/m^3)	ξ (%)
0.0-40.0	300	21	5
Rock	500	23	1

Table IV.2 Uniform soil property of second column

H (m)	Vs (m/s)	γ (kN/m^3)	ξ (%)
0.0-60.0	350	22	5
Rock	600	23	1

Moreover, the Kobe earthquake record motion was assumed as input motion at the base of soil column in both direction E-W and N-S while the motion in U-D direction was ignored in this study. The motion from both directions was shown in Fig. 4.2.

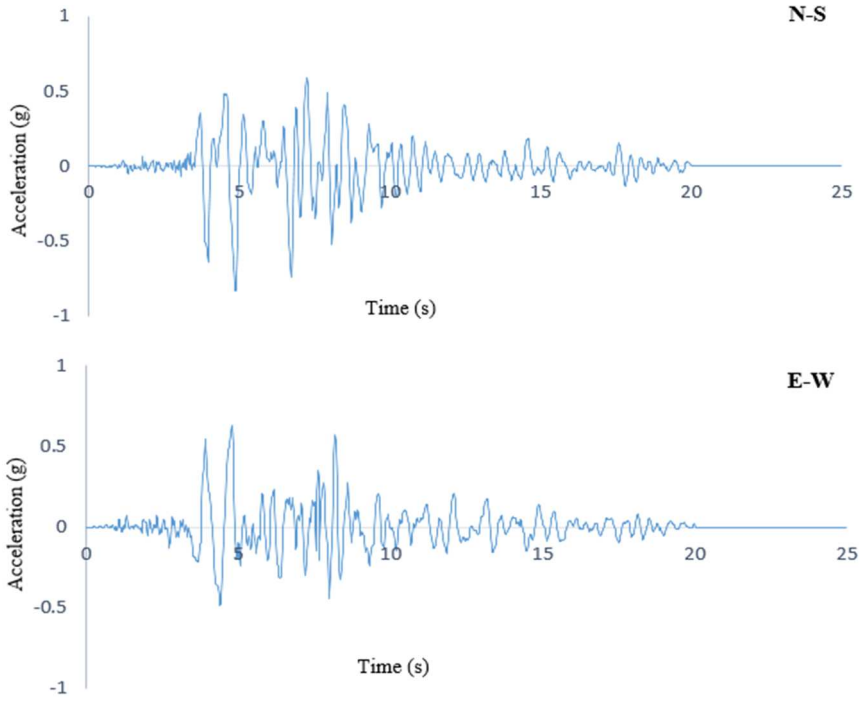

Figure IV.2 Kobe earthquake input motion

IV.3.3. Foundation Input Motion (FIM)

As described above, the frame structure was supported by surface foundation and subjected to vertically S wave. Thus, the $\ddot{u}_{FIM} = \ddot{u}_g$ and $\theta_{FIM} = 0$. The FIM of both soil columns are shown in Fig. 4.3 and 4.4, respectively for FD and TD.

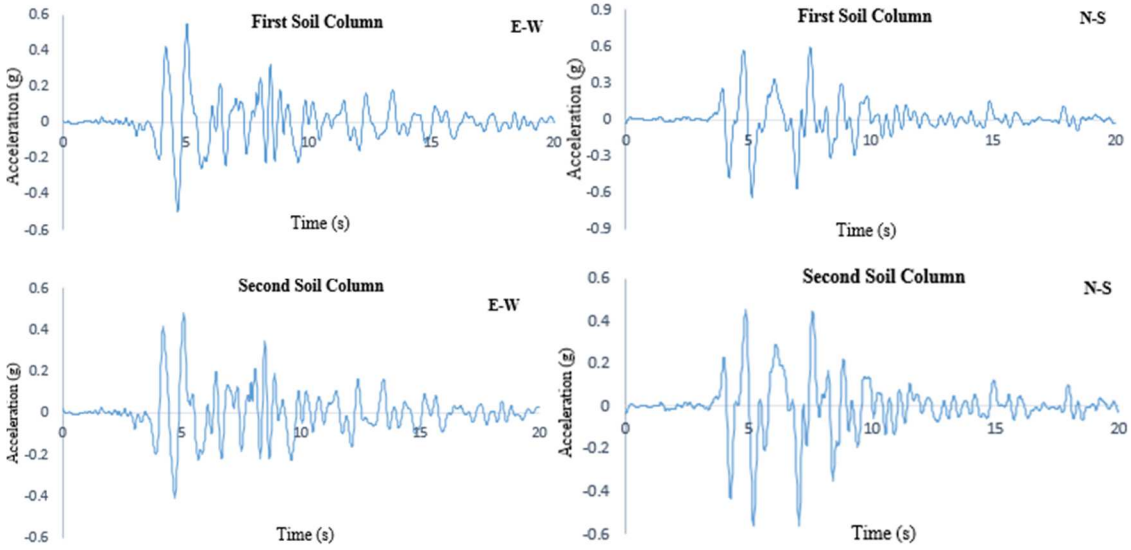

Figure IV.3 Foundation Input Motion in FD

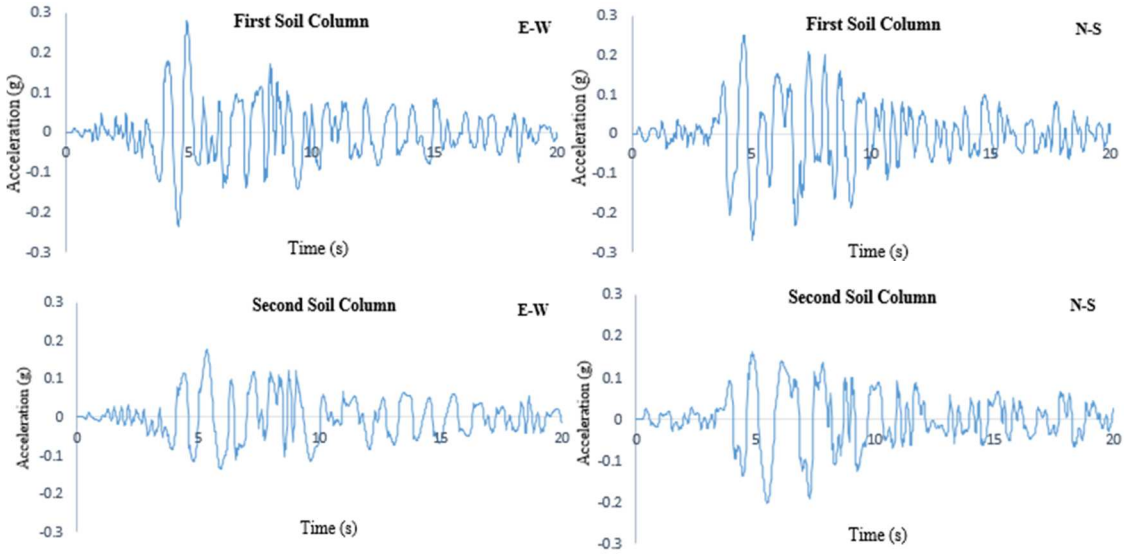

Figure IV.4 Foundation Input Motion in TD

IV.3.4. Dynamic Impedance

As described above, the dynamic impedance of both analytical models were achieved. The comparison of foundation stiffness-damping under both analytical models was conducted. There were six directions of stiffness k_i and damping c_i as shown in Fig. 4.5 for both soil columns. Furthermore, this comparison also included the linear response of foundation stiffness-damping.

- *Direction X:*

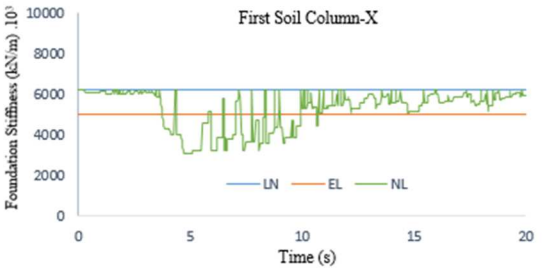

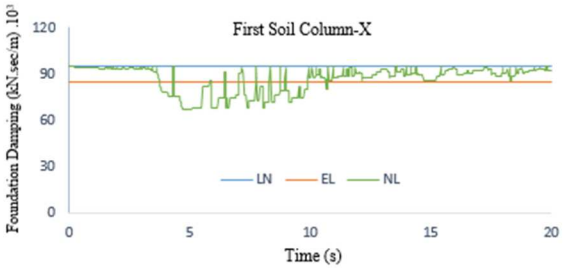

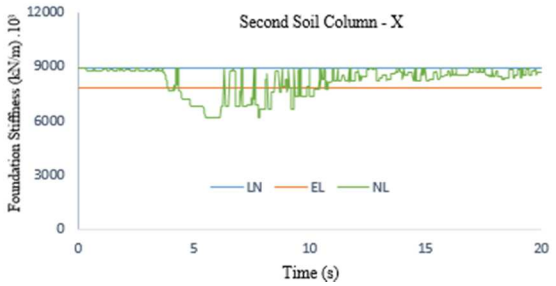

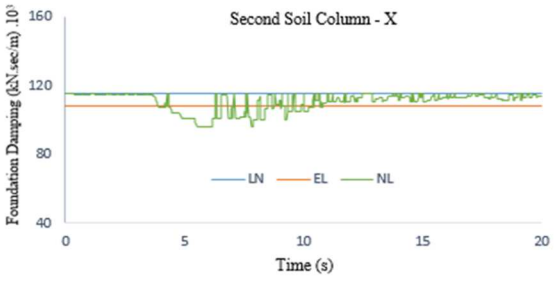

- *Direction Y:*

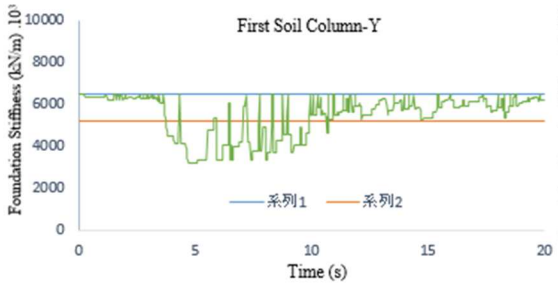

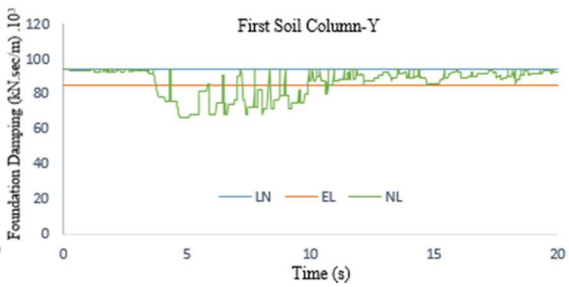

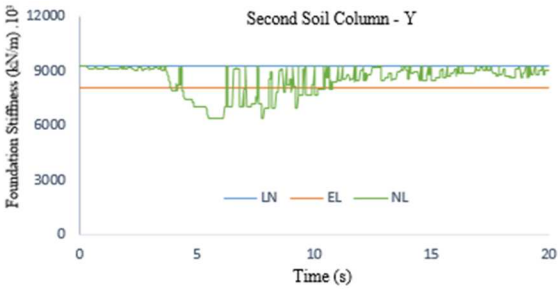

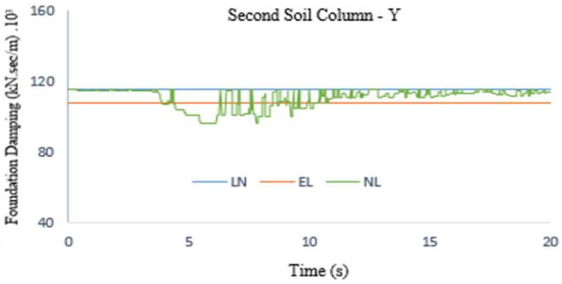

- *Direction Z:*

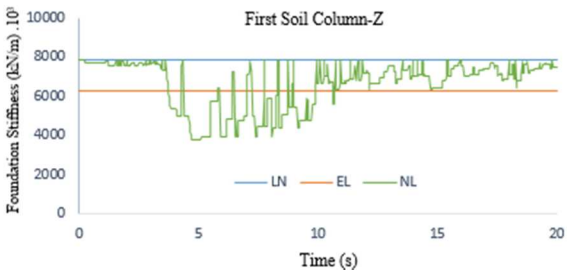

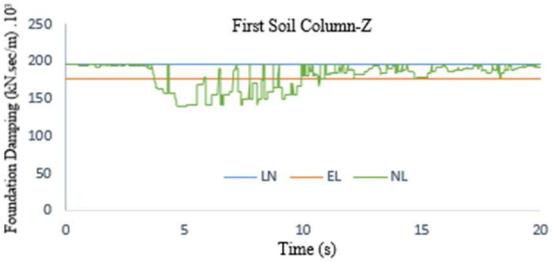

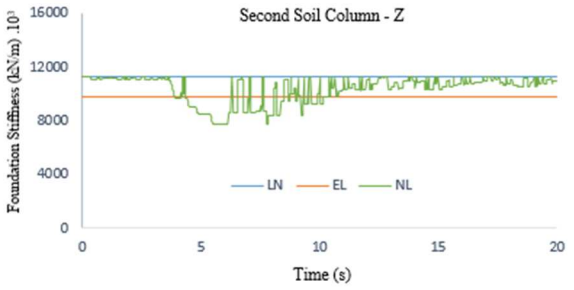

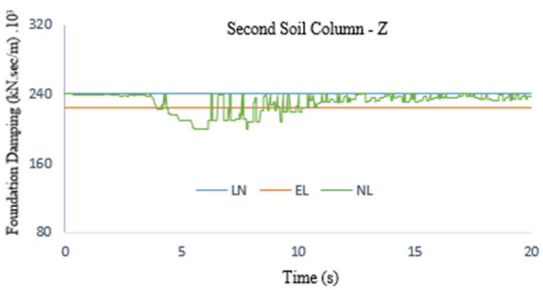

- *Direction XX:*

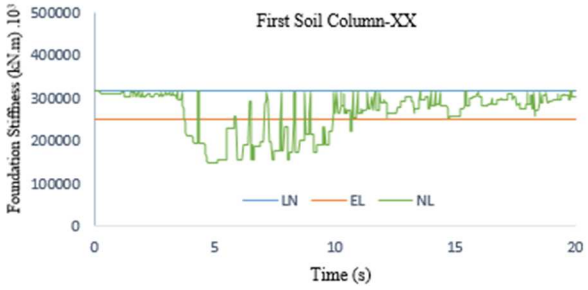

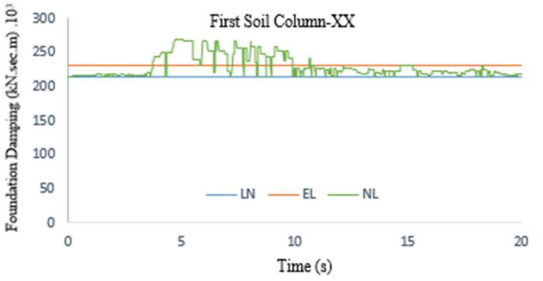

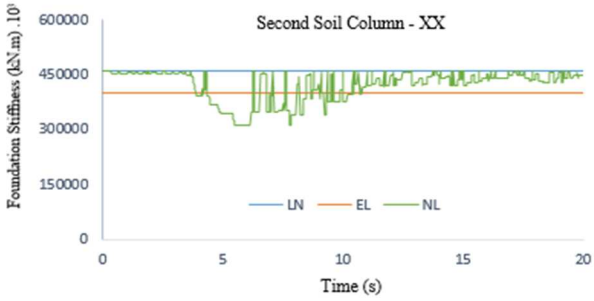

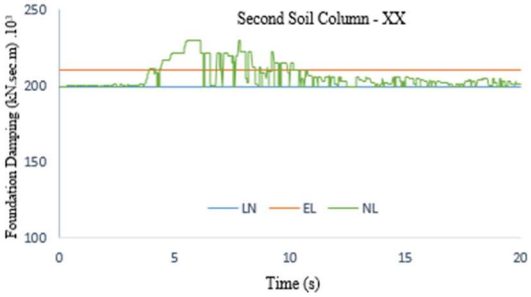

- *Direction YY:*

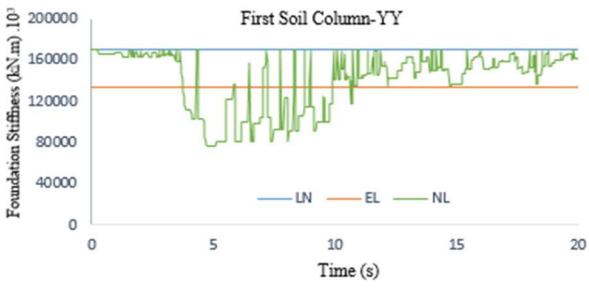

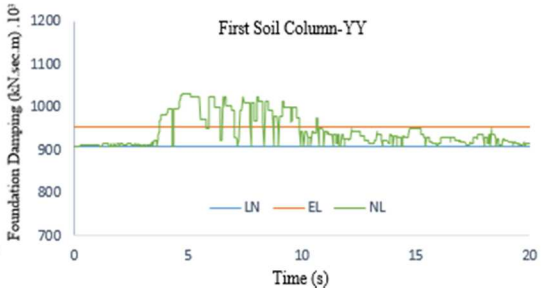

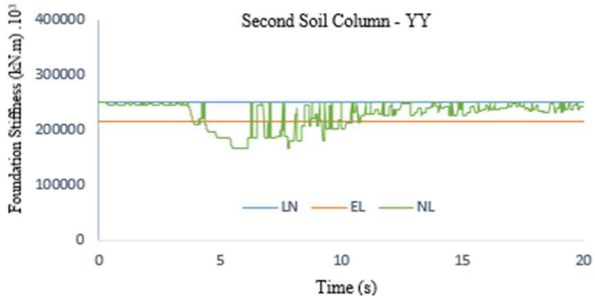

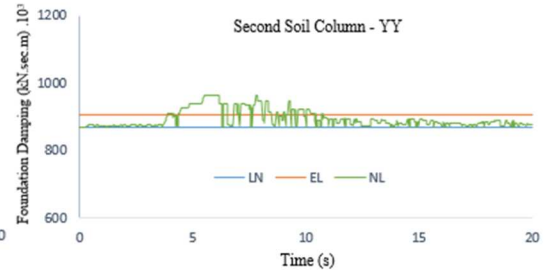

- *Direction ZZ:*

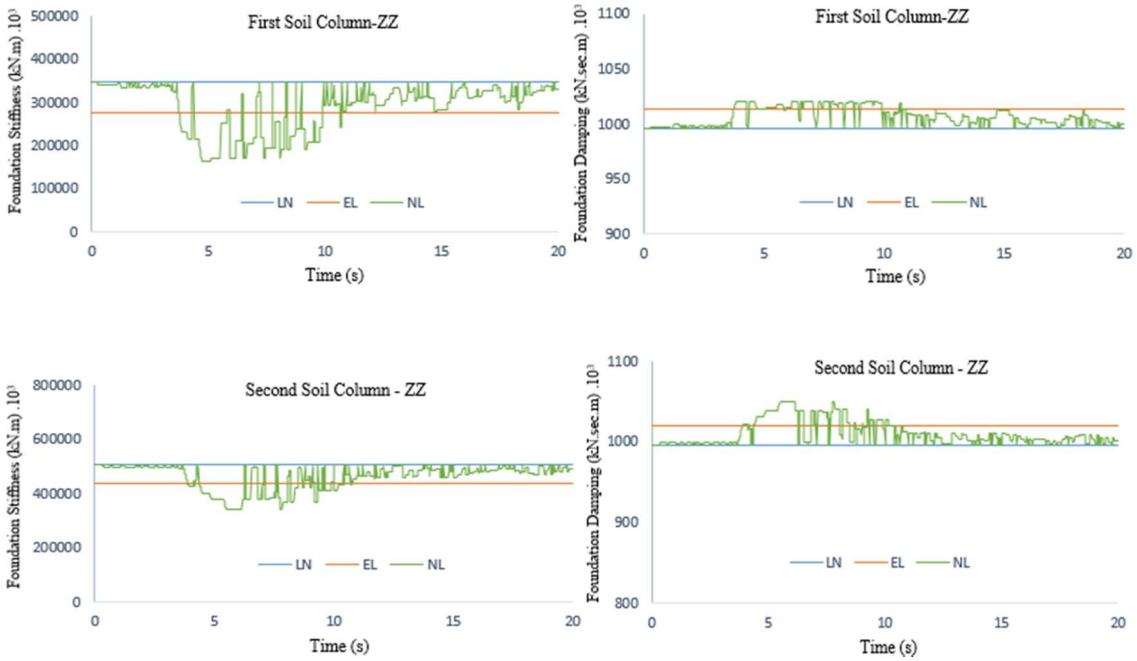

Figure IV.5 Comparison of foundation stiffness-damping under both analytical models

The hysteretic curve of foundation-soil system under both analytical models was also provided. There were six directions of foundation-soil system hysteretic curve as shown in Fig. 4.6 for both soil columns. Due to the absence of motion in vertical direction, there was no force in this direction.

- *Direction X:*

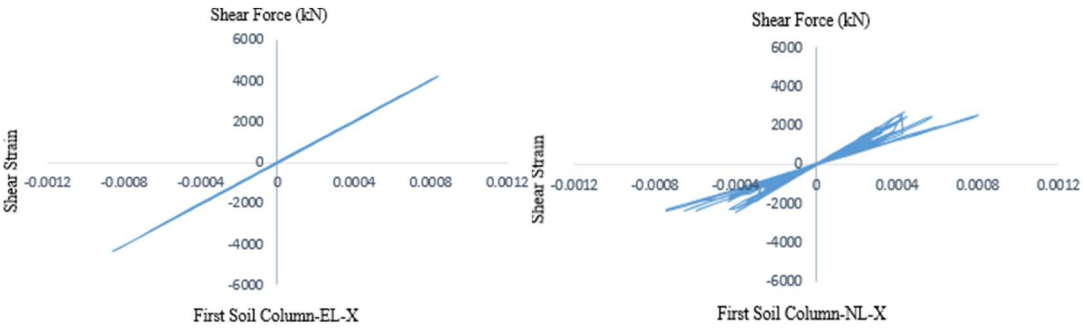

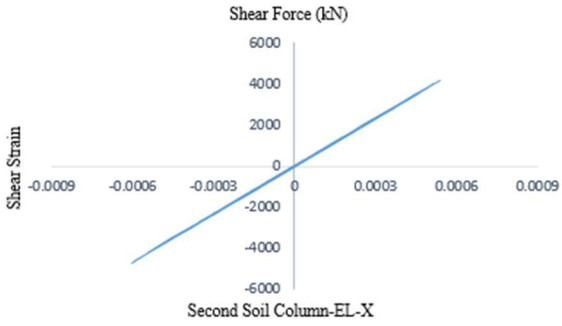

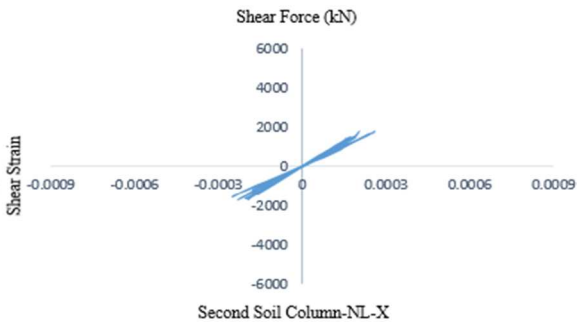

- *Direction Y:*

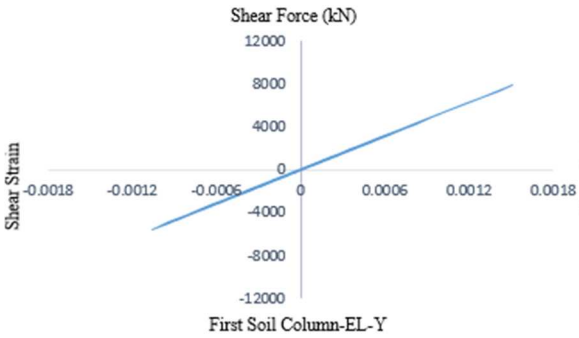

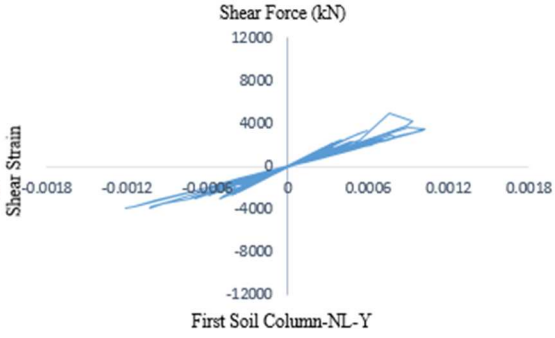

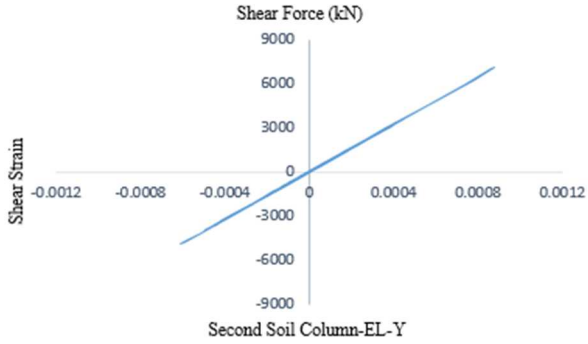

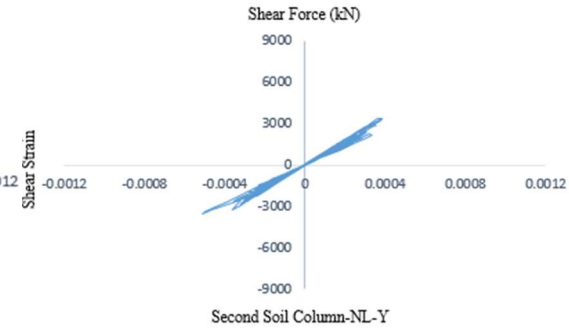

- *Direction XX:*

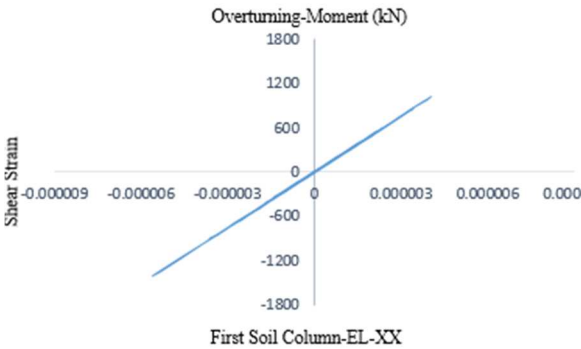

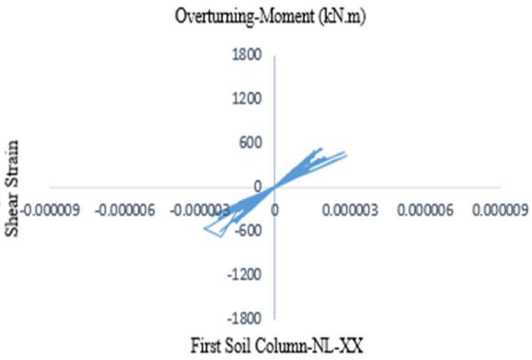

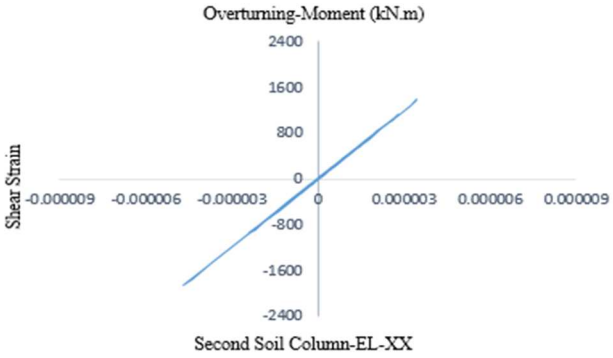

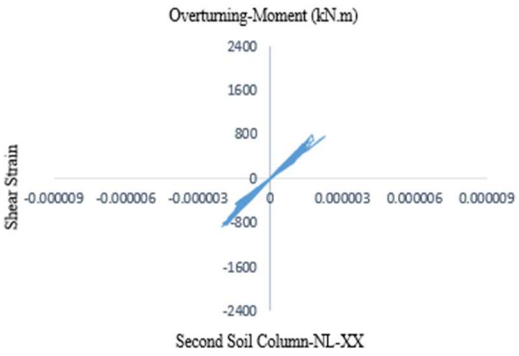

Direction YY:

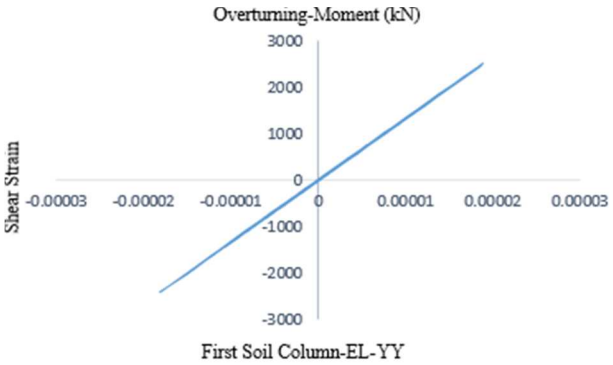

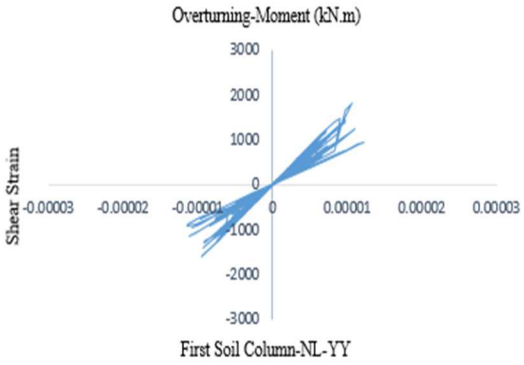

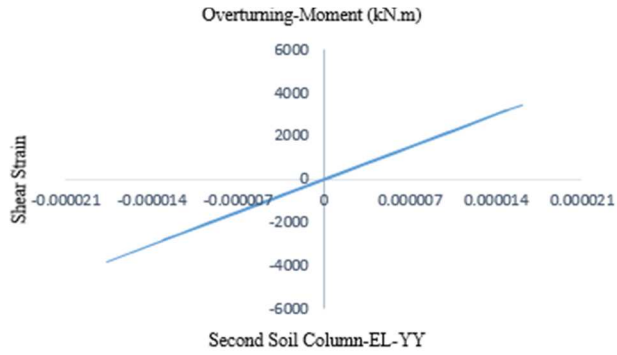

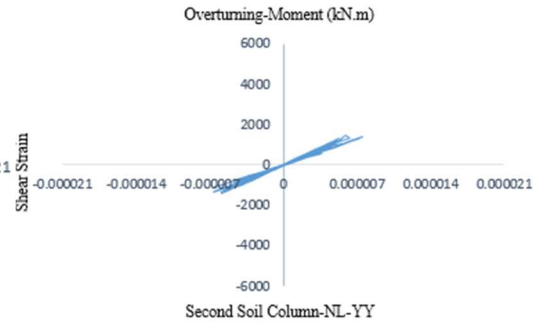

- *Direction ZZ:*

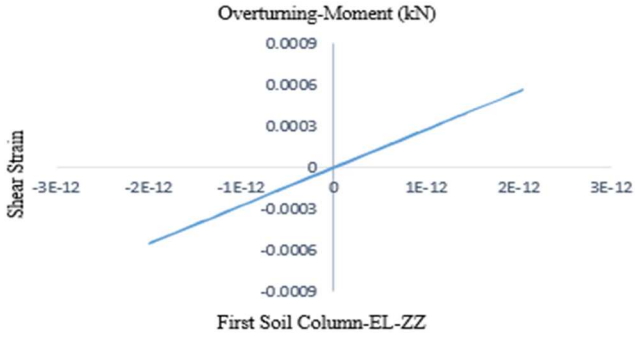

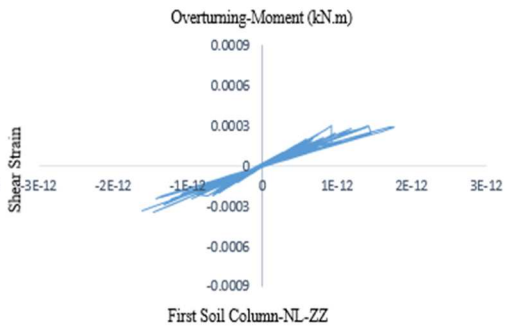

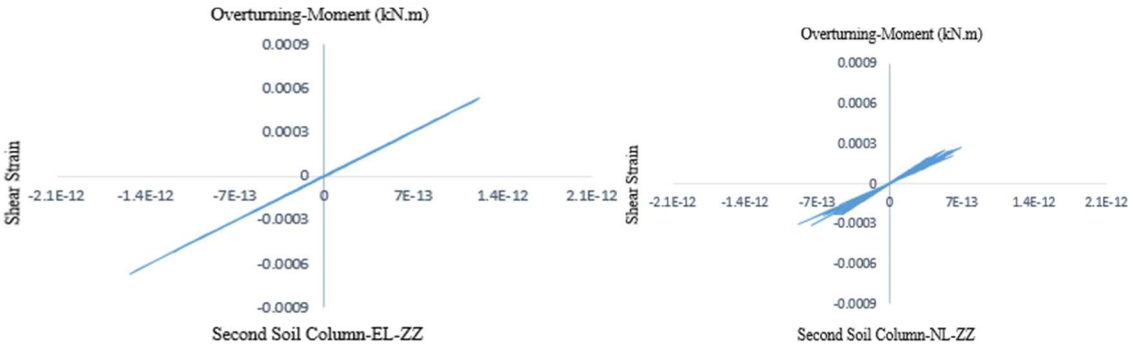

Figure IV.6 Hysteretic curve of foundation-soil system under both analytical models

IV.3.5. Seismic Response of RC Frame Structure under SSI Effect

The structural responses were provided under linear response of base-shear, overturning-moment, acceleration, and relative displacement. The comparison of both analytical model responses were conducted under two different soil columns and the evaluation was presented at the end of this chapter.

IV.3.5.1. Base-Shear of Structure

The base-shear response of structure under both analytical models was conducted. The comparison results from both analytical models showed that the base-shear response under equivalent-linear SSI effect was larger than the response from the nonlinear SSI effect. This discrepancy showed about overestimated result of using existing analytical model under substructure approach. The both response results is showed in Fig. 4.7 and the maximum values of base-shear response was shown in Table 4.3.

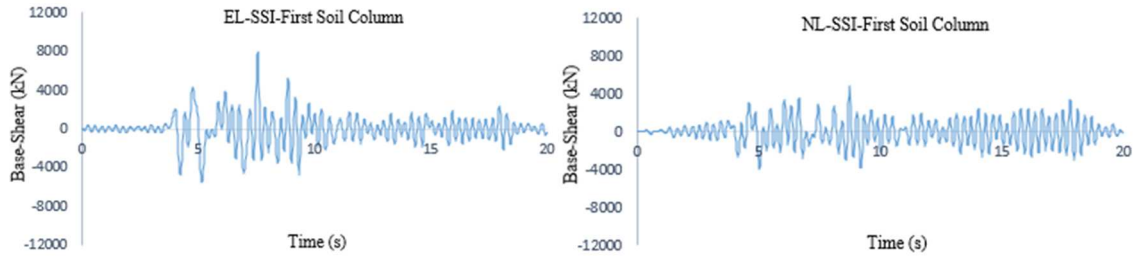

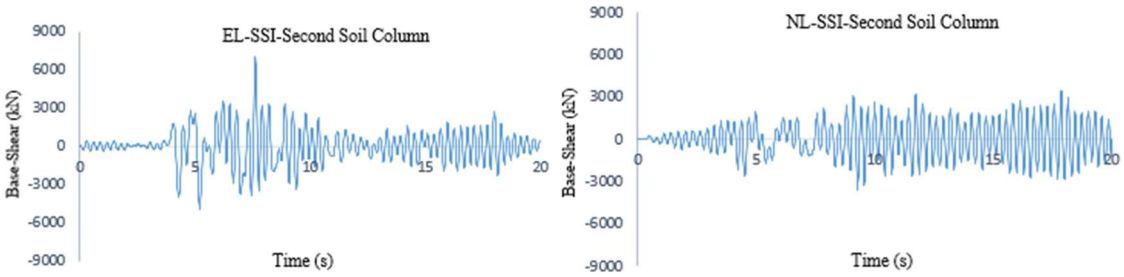

Figure IV.7 Base-shear responses under both analytical models

Table IV.3 Maximum base-shear of structure under both analytical models

Analytical model	First soil column (kN)	Second soil column (kN)
EL-SSI	7898.1	7079.8
NL-SSI	4893.9	3553.6

IV.3.5.2. Overturning-Moment of Structure

The overturning-moment response of structural under both analytical models was performed. The comparison from both analytical models showed that the response result under equivalent-linear SSI effect was larger than the response from the nonlinear SSI effect. This different response showed about overestimated result of using existing analytical model. The both response results is showed in Fig. 4.8 and the maximum of value of overturning-moment response is shown in Table 4.4

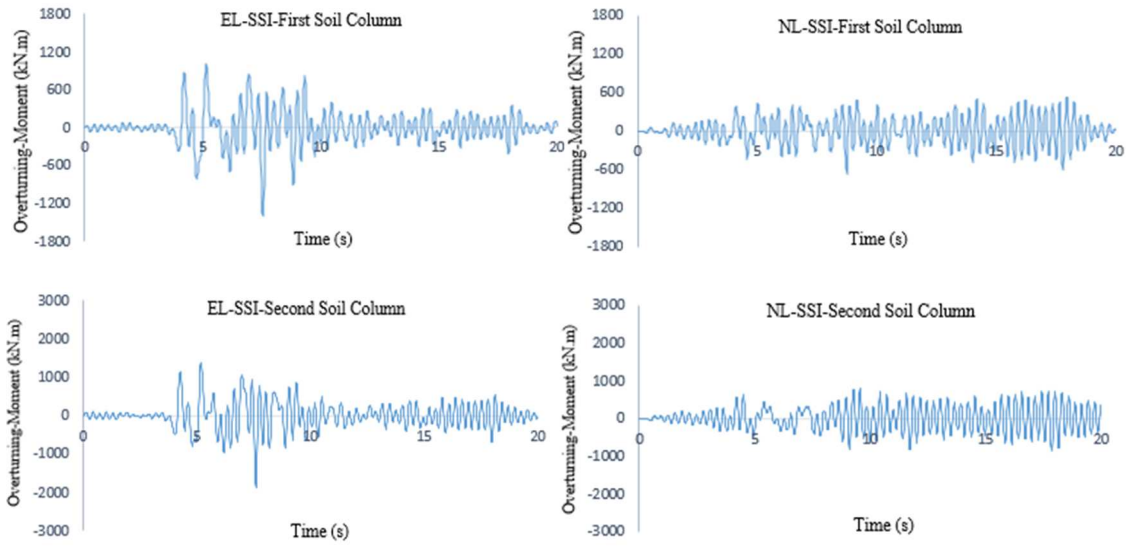

Figure IV.8 Overturning-moment responses under both analytical models

Table IV.4 Maximum value of overturning-moment

Analytical model	First soil column (kN.m)	Second soil column (kN.m)
EL-SSI	1409.50	1864.00
NL-SSI	669.96	867.76

IV.3.5.3. Acceleration of Structure

The acceleration response in each floor under both analytical model was performed. The comparison from both analytical models showed that the response result under equivalent-linear SSI effect was larger than the response from the nonlinear SSI effect. This different response showed about overestimated result of using existing analytical model. The both response result is showed in Fig. 4.9 and maximum value of acceleration in each floor is shown in Table 4.5.

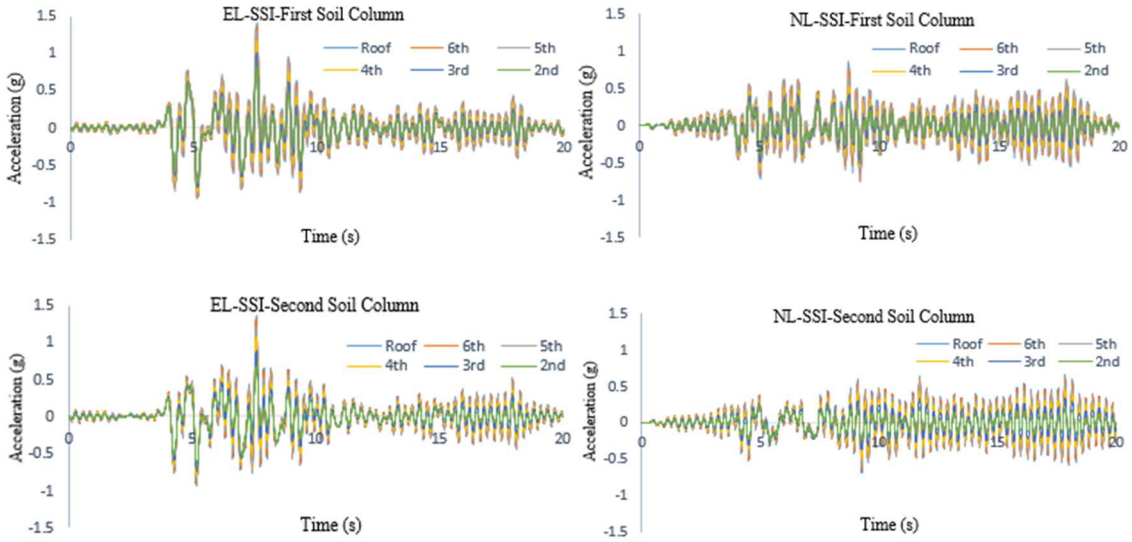

Figure IV.9 Acceleration responses in each floor under both analytical models

Table IV.5 Maximum value of acceleration

Floor	EL-SSI-First soil column (g)	NL-SSI-First soil column (g)
Roof	1.411	0.857
6	1.371	0.761
5	1.290	0.641
4	1.169	0.568
3	1.008	0.502
2	0.816	0.373
Floor	EL-SSI-Second soil column (g)	NL-SSI-Second soil column (g)
Roof	1.356	0.684
6	1.308	0.654
5	1.211	0.616
4	1.072	0.506
3	0.889	0.372
2	0.675	0.251

IV.3.5.4. Relative Displacement of Structure

The relative displacement of structure under both analytical models was performed. The comparison of both analytical model showed that the response result under equivalent-linear SSI effect was larger than the response from the nonlinear SSI effect. This different response showed about the overestimated result of using existing analytical model of SSI problem. The both response result is shown in Fig. 4.10 and maximum value of relative displacement in each floor is shown in Table 4.6.

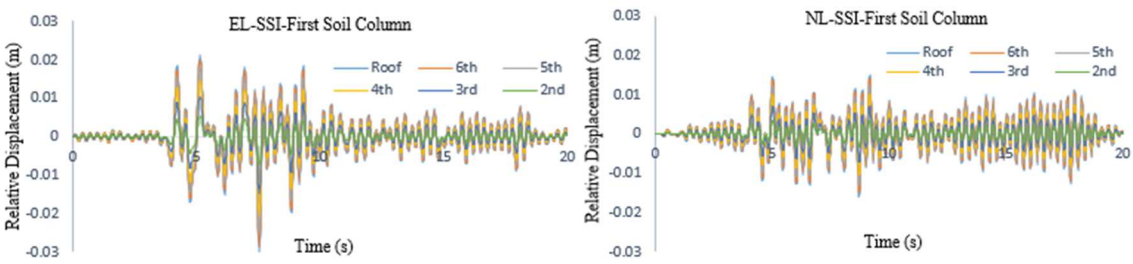

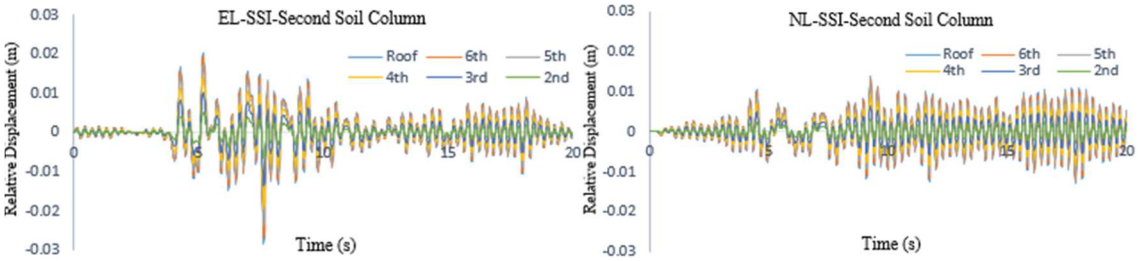

Figure IV.10 Relative displacement responses under both analytical models

Table IV.6 Maximum value of relative displacement

Floor	EL-SSI-First soil column (m)	NL-SSI-First soil column (m)
Roof	0.030	0.016
6	0.028	0.015
5	0.025	0.013
4	0.021	0.010
3	0.015	0.007
2	0.007	0.003
Floor	EL-SSI-Second soil column (m)	NL-SSI-Second soil column (m)
Roof	0.028	0.014
6	0.026	0.013
5	0.024	0.011
4	0.019	0.009
3	0.013	0.006
2	0.006	0.003

IV.4. CONCLUSIONS

The conclusion of this chapter was presented as in the following:

- The seismic response of structure considering nonlinear SSI effect under substructure approach was presented.
- The seismic response of structure under existing analytical model and proposed analytical model were conducted. The response results were showed under linear response of base-shear, overturning-moment, acceleration, and relative displacement. Furthermore, the foundation stiffness-damping and hysteretic curve were also provided.
- The response results showed that the structural responses under existing analytical model using substructure approach were larger than the responses under the proposed analytical model. There were two significant factors that

caused the differences between both analytical models:

- Nonlinear response of soil material
- Nonlinear response of FFGM.

These discrepancies showed about the overestimated results of using existing analytical model compared to the actual response of structure under earthquake loading.

Therefore, the proposed analytical model would be a potential model for SSI problem using substructure approach. This analytical model was taken into account the nonlinear response of soil material and motion, and showed about the adequateness of using substructure approach compared to actual response of structure under earthquake disaster. Furthermore, this analytical model facilitated performing the structural response under nonlinear response of near-field soil effect subjected to tsunami force by taken into account the effect of pre-earthquake disaster.

CHAPTER V. EFFECT OF NEAR-FIELD SOIL NONLINEARITY ON THE RESPONSE OF STRUCTURE UNDER TSUNAMI DISASTER

V.1. INTRODUCTION

After the 2011 Great East Earthquake and Tsunami in Japan, the response of structure under tsunami force has become an impressive issue for structural design guidelines. The overturning of RC buildings in Onagawa town was an example of the effect of tsunami force on the response and stability of structure. The response of structure during tsunami force was composed by two main factors: tsunami force and the effect of soil interaction. Many analytical studies and guidelines have proposed various relative parameters for design the effect of tsunami force on the structure such as lateral force [7] and buoyant force [4]. However, the nonlinear effect of near-field soil on the response of structure subjected to tsunami force has not been studied and deeply investigated yet. During tsunami disaster, the near-field soil around the structure can perform a significant role on the response of structure during tsunami disaster, especially nonlinear response behavior. Thus, the objective of this chapter is to propose an analytical model considering the nonlinear effect of near-field soil on the response of structure under tsunami force.

However, in order to achieve this objective, the nonlinear response analysis of soil deposits from Chapter III was indispensable. In this chapter, the procedure considering the boundary and analytical model of near-field soil were presented. For better understanding, an example of 3D RC frame structure supported by two types of soil column subjected to tsunami force was provided. The comparison between the effect of near-field soil and fixed-base condition on the response of structure was conducted in order to evaluate the nonlinear effect of near-field soil.

V.2. NEAR-FIELD SOIL COLUMN BOUNDARY

The procedure considering the near-field soil boundary, as shown in Fig. 5.1, was described as in the following:

- Area of the near-field soil at surface layer was the same as the area of the structural base.
- Effective angle was assumed $\alpha = 45^o$
- Area of near-field soil for the second segment was extended corresponding to the effective angle α and assumption depth H.

- Keeping the same procedure for other segments until the base of soil column or any favorable segment.
- Near-field soil column boundary was achieved in form of truncated rectangular pyramid but round at the edge as shown in Fig 5.1.
- Area, volume, and mass of soil column were determined based on the size of soil segment.

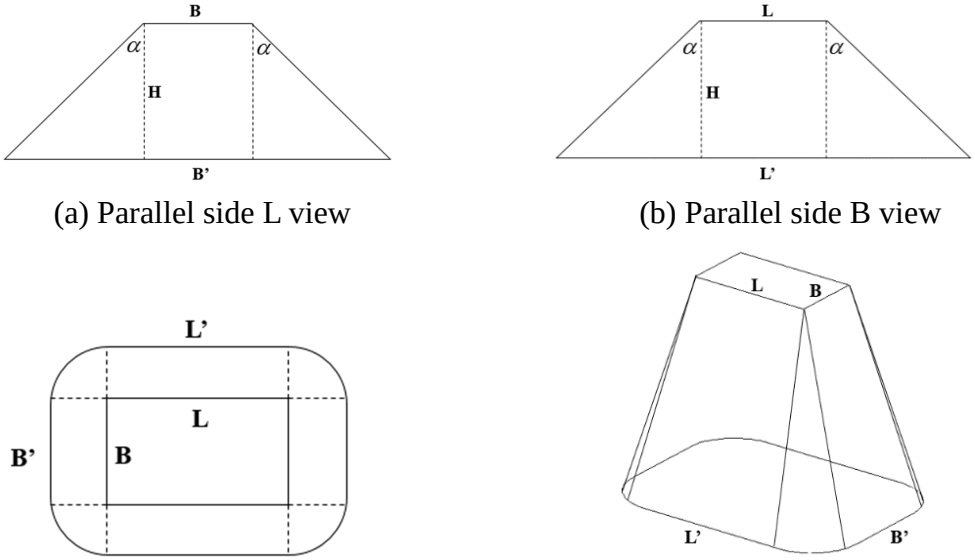

(a) Parallel side L view (b) Parallel side B view

(c) Top view (d) Perspective view

Figure V.1 Near-field soil column boundary

V.3. ANALYTICAL MODEL OF NEAR-FIELD SOIL COLUMN

Based on the soil column segment, the lumped mass, shear and bending stiffness can be computed and expressed in Eq. (5.1)-(5.3).

$$M_i = V_i.\rho_i \tag{5.1}$$

Where

$$V_i = \left(BL + (B+L).(H_{i+1} + H_i) + \frac{\pi}{3}(H_{i+1}^2 + H_{i+1}.H_i + H_i^2) \right).(H_{i+1} - H_i)$$

V_i : Volume of near-field soil segment between heights H_i and H_{i+1}

ρ_i : Soil density of near-field soil segment

B, L : Width and length of structural base

$$K_{si} = \frac{G_i A_i}{(H_{i+1} - H_i)} \tag{5.2}$$

Where

$$A_i = BL + (B+L).(H_{i+1} + H_i) + \frac{\pi}{4}\left(H_{i+1}^2 + 2H_{i+!}H_i + H_i^2\right)$$

$$G_i = \rho_i V_i^2$$

K_{si} : Shear stiffness of near-field soil segment

G_i : Shear modulus of near-field soil segment

A_i : Average area of near-field soil segment between H_i and H_{i+1}

V_{si} : Shear velocity of near-field soil segment

ρ_i : Density of near-field soil segment

B, L : Width and length of near-field soil segment

$$K_{\theta i} = \frac{E_i I_i}{(H_{i+1} - H_i)} \tag{5.3}$$

Where

$$I_i = \frac{\pi}{4}((H_i + H_{i+1})/2)^4 + \frac{\pi}{4}B^2((H_i + H_{i+1})/2)^2 + \frac{B^3}{12}(H_i + H_{i+i}) + \frac{L}{12}(H_i + H_{i+1} + B)^3$$

$$E_i = 2G_i(1+\upsilon_i)$$

I_i : Inertia moment of near-field soil segment for horizontal direction between H_i and H_{i+1}

E_i : Young's modulus of near-field soil segment

G_i: Shear modulus of near-field soil segment

υ_i : Poisson's ratio of near-field soil segment

$K_{\theta i}$: Bending stiffness of near-field soil segment

B, L : Width and length of near-field soil segment

According to the expressions above, the near-field soil column can be shown as in Fig. 5.2 by lumped mass, connected by shear and bending springs from one segment to another segment.

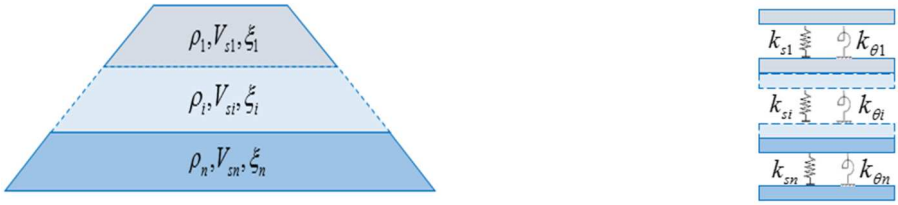

(a) Near-field soil column (b) Analytical model of near-field soil

Figure V.2 Near-field soil column analytical model

For nonlinearity of near-field soil segment analysis, the modified Ramberg-Osgood model [40] was utilized in this study. The skeleton and hysteretic curve was expressed in Eq. (5.4) and (5.5), respectively.

$$\gamma = \frac{\tau}{G_o}\left(1+\alpha|\tau|^{\beta}\right) \tag{5.4}$$

$$\frac{\gamma \pm \gamma_0}{2} = \frac{\tau \pm \tau_0}{2G_0}\left(1+\alpha\left|\frac{\tau \pm \tau_0}{2}\right|^{\beta}\right) \tag{5.5}$$

Where

$$\alpha = \left(\frac{2}{\gamma_{0.5}G_0}\right)^{\beta}, \quad \beta = \frac{2\pi h_{\max}}{2-\pi h_{\max}}$$

τ, γ: Stress and strain of near-field soil segment

τ_0, γ_0 : Reversal of stress and strain

β, α: Parameters of modified Ramberg-Osgood

G_0, $h_{\max}$: Initial shear modulus and maximum damping soil

$\gamma_{0.5}$: Half strain corresponds to $G/G_o = 0.5$

According to hysteretic rule of modified Ramberg-Osgood model, the nonlinear response of shear modulus $G_i(t)$ can be derived from Eq. (5.6) and shown in Fig. 5.3.

$$\frac{G_i}{G_0} = \frac{\tau_i - \tau_{i-1}}{\gamma_i - \gamma_{i-1}} \tag{5.6}$$

Where

G_i / G_0 : Secant shear modulus for nonlinear response

τ_i, τ_{i-1} : Reversal shear strain of point i and i-1

γ_i, γ_{i-1} : Reversal shear strain of point i and i-1

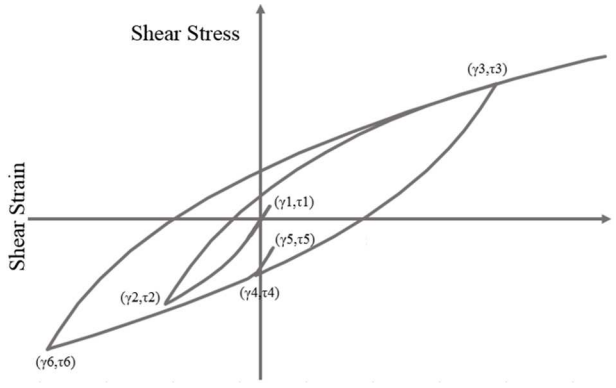

Figure V.3 Stress-strain relationship of modified Ramberg-Osgood model

This nonlinear response analysis can be achieved by using OBASAN program [50], which can perform for both structural and ground motion analysis.

V.4. ANALYTICAL PROCEDURE OF STRUCTURE UNDER NEAR-FIELD SOIL EFFECT SUBJECTED TO TSUNAMI FORCE

According to the boundary and analytical model of near-field soil above, the upper structure was connected to near-field soil by shear and bending spring, as shown in Fig. 5.4. Under tsunami disaster, the input tsunami force should be divided into striking and receding wave attacking the structure, as shown in Fig.5.5. The analytical procedure of tsunami force on structure in Panon's work [47] was used in this study.

Based on the description above, the response of structure can be obtained under linear and nonlinear effect of near-field soil. Besides this, the equivalent-linear response of near-field soil was assumed to be the same as response of near-field soil due to tsunami force, which was a push over loading.

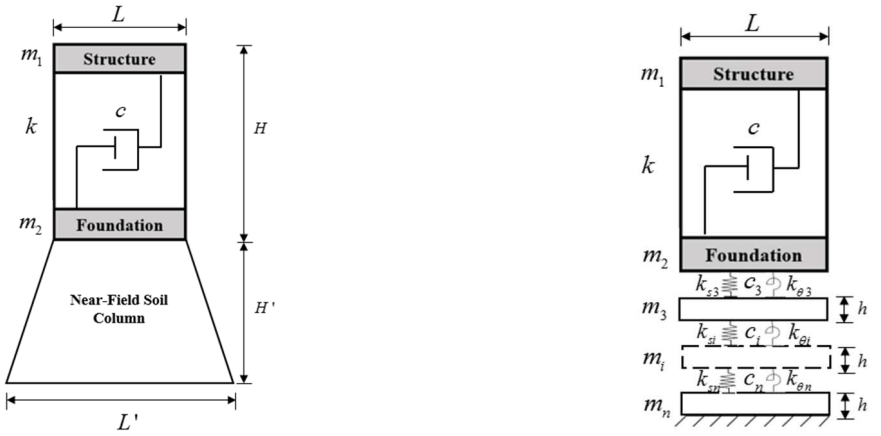

(a) Upper structure rested on near-field soil (b) Analytical model assumption

Figure V.4 Analytical model of structure under near-field soil effect

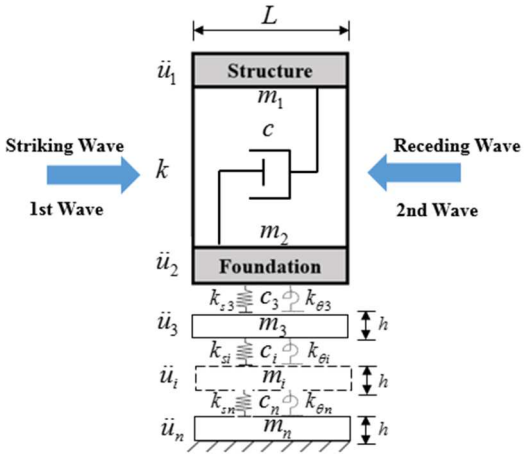

Figure V.5 Analytical model of structure subjected to tsunami force

V.5. EXAMPLE OF 3D RC FRAME STRUCTURE SUBJECTED TO TSUNAMI FORCE

For better understanding the nonlinear effect of near-field soil on the response of structure subjected to tsunami force, an example of 3D RC frame structure from chapter IV was used in this study. This frame structure was assumed to subject to hydrodynamic force as input tsunami force. The relevant parameters were presented in the following sections.

V.5.1. Input Tsunami Force

In this study, the hydrodynamic force was regarded as input tsunami force attacking on the structure. This hydrodynamic force was divided into striking (1st wave) and receding wave (2nd wave), as shown in Fig. 5.6, which was applied as distribution pressure from the first floor to the roof in Y direction of structure [48]. The hydrodynamic pressure was obtained from the inundation simulation [46] [47], as shown in Fig 5.7.

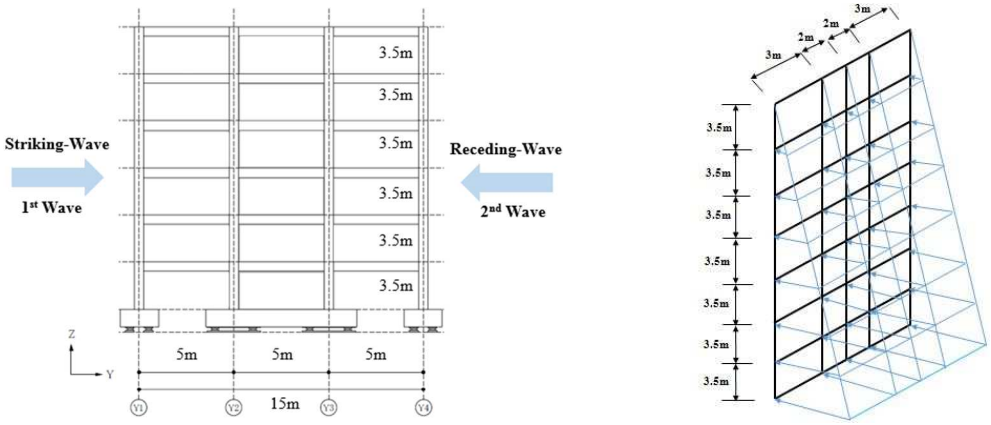

(a) Direction of input tsunami load (b) Distribution of tsunami pressure

Figure V.6 Input tsunami forces on the structure

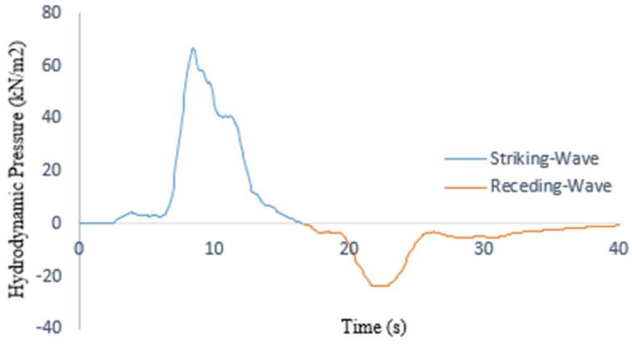

Figure V.7 Input hydrodynamic pressure

V.5.2. Response of Structure under Near-Field Soil Effect

According to the description above, the near-field soil column was achieved based on the effective angle $\alpha = 45^{o}$ [59] and the depth of soil column for both conditions, as shown in Fig. 5.8 and 5.9.

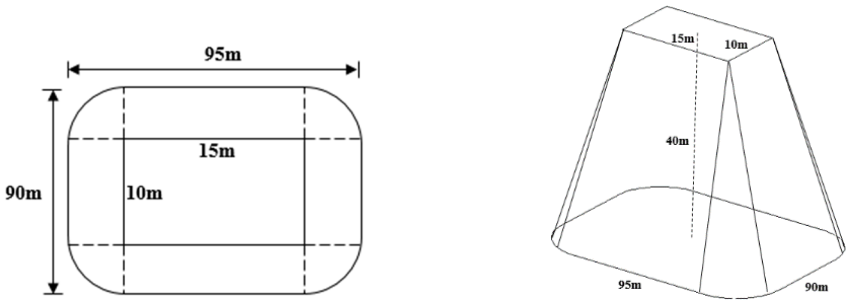

(a) Top view (b) Perspective view

Figure V.8 First column of near-field soil condition

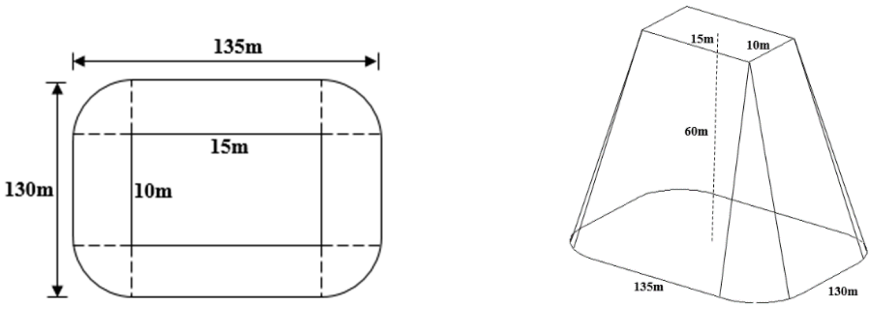

(a) Top view (b) Perspective view

Figure V.9 Second column of near-field soil condition

V.5.2.1. Near-Field Soil Segment Divisions

After obtaining the near-field soil column, the near-field segment division was another significant factor that impacted on the response of structure during tsunami disaster. In order to achieve a proper division of near-field segment, several divisions were tested including 0.5m, 1m, 2m, 4m, 5m, and 10m. The response of structure under these divisions were shown in Fig. 5.10 and 5.11 while the maximum of shear strain at surface layer under these divisions were shown in Table 5.1 for both soil columns.

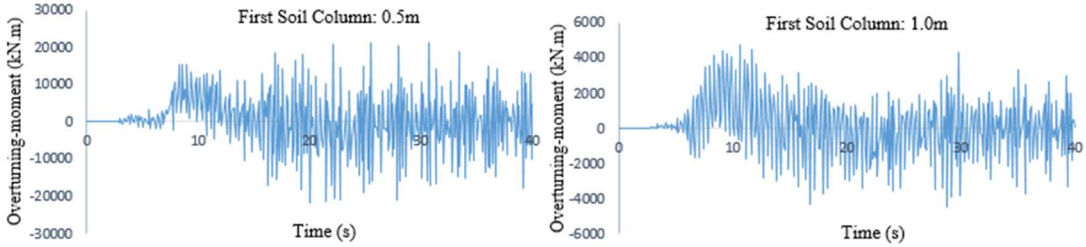

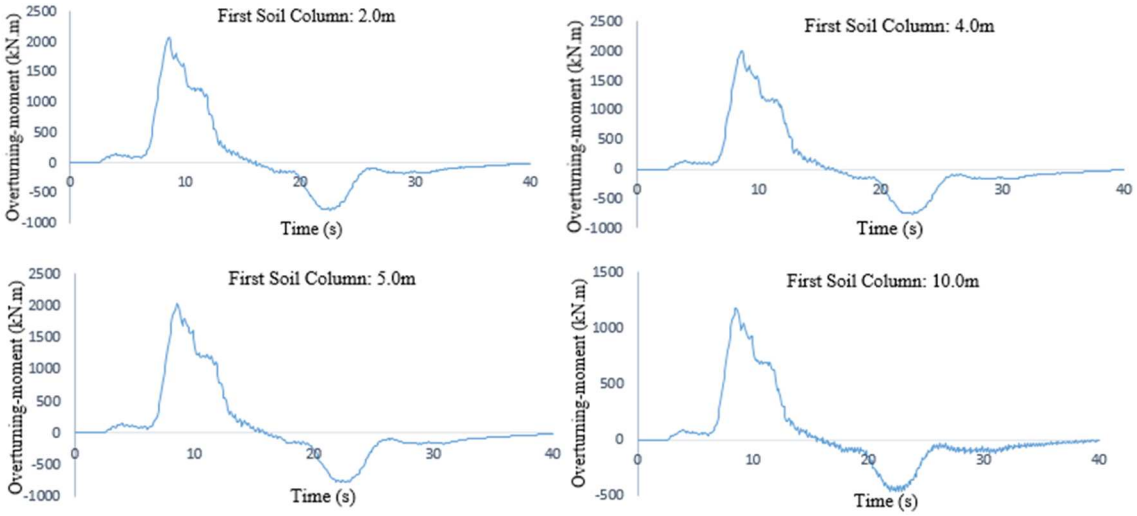

Figure V.10 Overturning-moment response of structure under different segment divisions of first near-field soil column

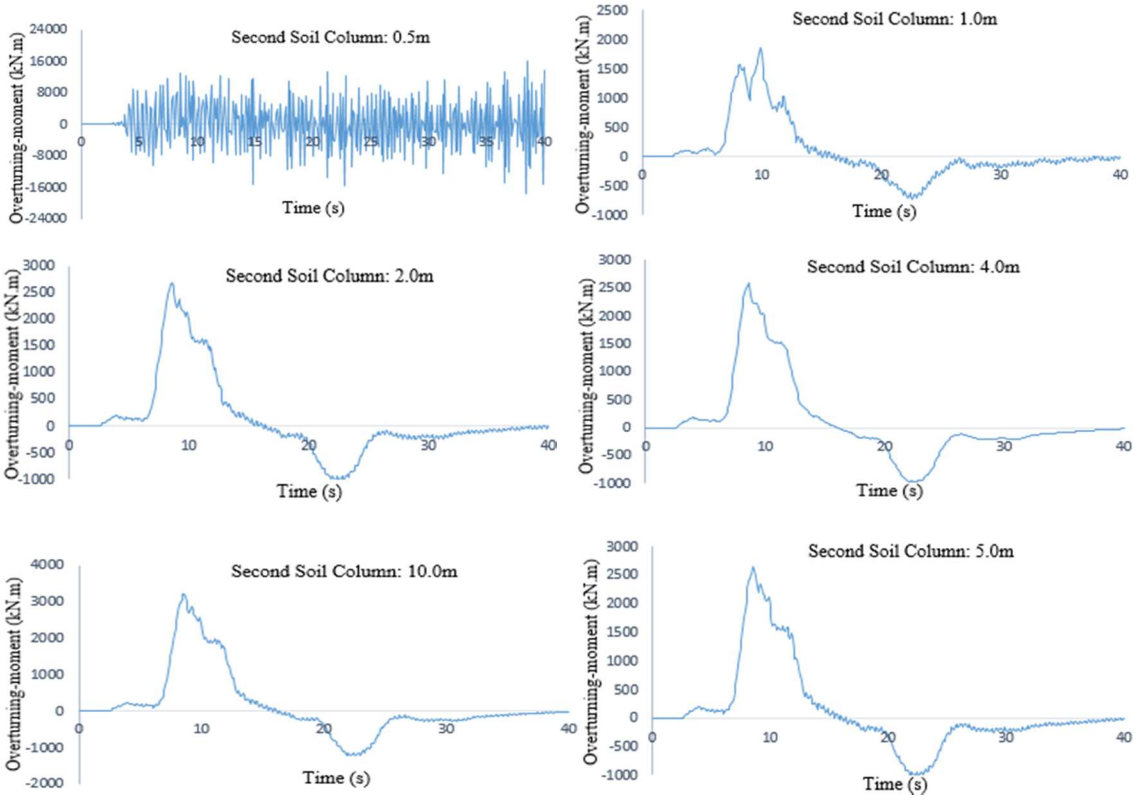

Figure V.11 Overturning-moment response of structure under different segment divisions of second near-field soil column

Table V.1 Maximum shear strain at surface layer under different segment divisions

Segment Division	First Soil Column	Second Soil Column
0.5m	0.001229	0.001125
1.0m	0.001202	0.000451
2.0m	0.001197	0.000814
4.0m	0.001926	0.001306
5.0m	0.002173	0.001468
10.0m	0.004625	0.001845

According to the response of structure under different segment division of near-field soil column, the segment division with 2m, 4m, and 5m showed almost response while the segment division with 0.5m and 1.0m showed a complicated response under tsunami disaster, which was like the push over excitation.

Besides this, the maximum shear at surface under segment division of near-field soil column from 0.5m to 5.0m showed a similar response compared to 10.0m.

Thus, based response results above, the proper segment division of near-field soil should be 2m, 4m, and 5m. However, in this study, the recommendation of near-field soil segment was 4m, which was the average value between these values.

The both near-field soil columns were divided into 10 and 15 segment, respectively, with the thickness of 4m in each segment, as shown in Fig 5.12. Then, the lumped mass, shear and bending spring were obatined, as shown in Table 5.2 and 5.3.

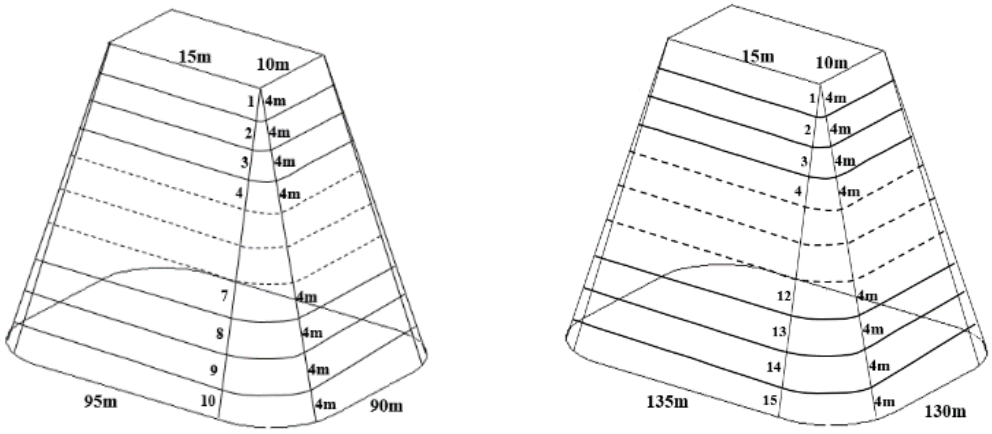

(a) First column of near-field soil (b) Second column of near-field soil

Figure V.12 Near-field soil segment divisions

Table V.2 Lumped mass, shear and bending stiffness of first near-field soil column

H(m)	Vs (m/s)	γ (kN/m3)	ξ (%)	M (t)	K_s (kN/m)	K_θ (kN.m)
0	300	21	5	0.11e5	1.24e10	5.22e11
4				0.54e5	4.82e10	8.64e12
8				1.38e5	1.07e11	4.36e13
12				2.63e5	1.88e11	1.37e14
16				4.28e5	2.93e11	3.33e14
20				6.34e5	4.20e11	6.89e14
24				8.81e5	5.70e11	1.27e15
28				11.68e5	7.43e11	2.17e15
32				14.96e5	9.39e11	3.47e15
36				18.65e5	1.16e12	5.28e15
40				10.30e5		

Table V.3 Lumped mass, shear and bending stiffness of second near-field soil column

H(m)	Vs (m/s)	γ (kN/m3)	ξ (%)	M (t)	K_s (kN/m)	K_θ(kN.m)
0	350	22	5	0.12e5	1.77e10	7.44e11
4				0.57e5	6.87e10	1.23e13
8				1.45e5	1.52e11	6.22e13
12				2.75e5	2.69e11	1.95e14
16				4.48e5	4.17e11	4.75e14
20				6.64e5	5.99e11	9.82e14
24				9.23e5	8.13e11	1.82e15
28				12.24e5	1.06e12	3.09e15
32				15.67e5	1.34e12	4.94e15
36				19.54e5	1.65e12	7.52e15
40				23.83e5	2.00e12	1.10e16
44				28.54e5	2.37e12	1.56e16
48				33.69e5	2.78e12	2.14e16
52				39.26e5	3.23e12	2.88e16
56				45.25e5	3.70e12	3.79e16
60				24.18e5		

The linear response of structure was performed under the effect of near-field soil and fixed-based condition in order to evaluate the nonlinear effect of near-field soil. In this study, the linear response of structure was included overturning-moment and story shear of structure, which controlled the stability and damage response of structure during tsunami disaster.

V.5.2.2. Shear modulus reduction and shear strain of near-field soil

The shear modulus reduction and shear strain of both near-field soil columns at surface layer (top segment) subjected to tsunami force are shown in Fig. 5.13 and 5.14, respectively. Moreover, the maximum shear strain in each layer of both soil columns are shown in Fig. 5.15.

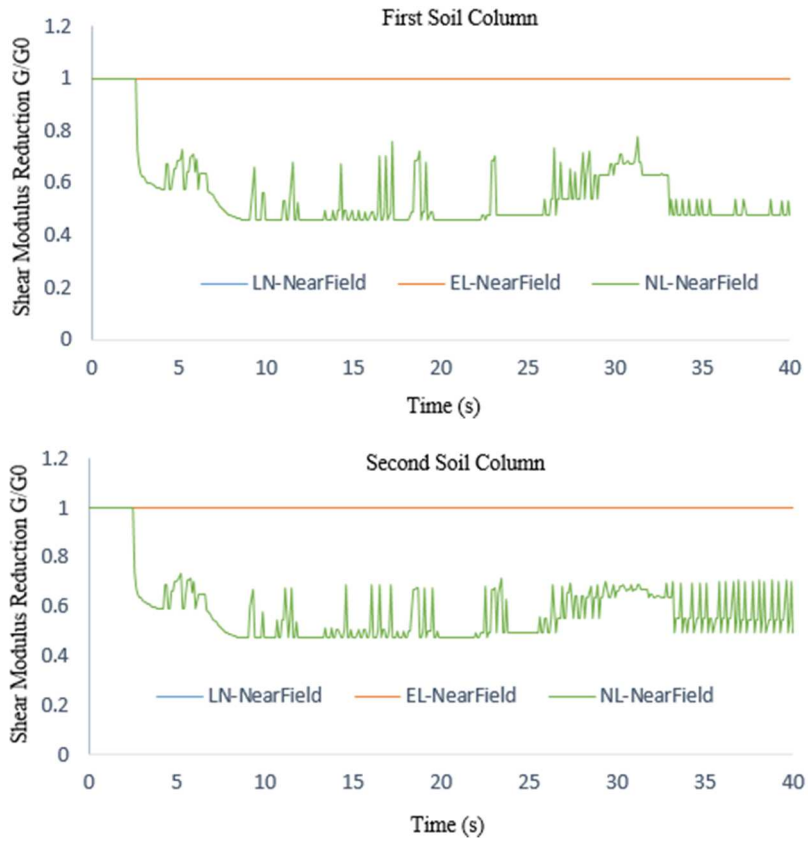

Figure V.13 Shear modulus reductions G/G0 of near-field soil at surface layer

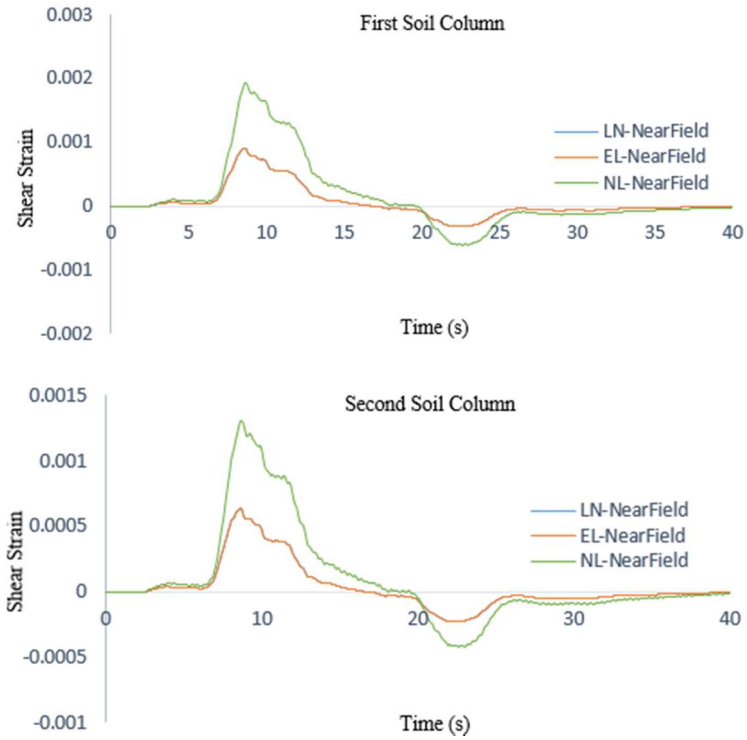

Figure V.14 Shear strain of near-field soil at surface layer

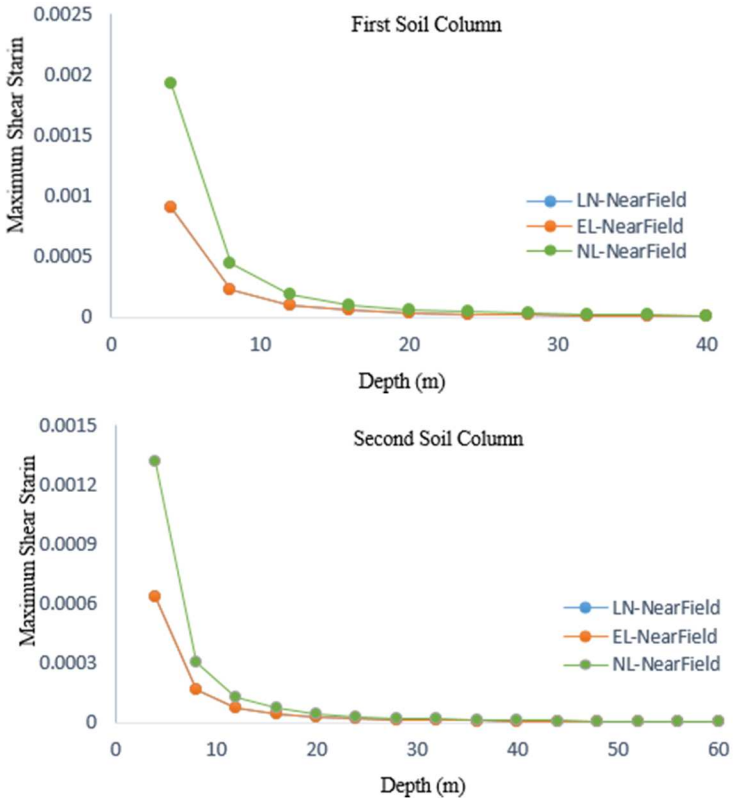

Figure V.15 Maximum shear strain in each layer of near-field soil

According to the response results above, the maximum shear strain in each layer was under 5%. Thus, the near-field soil column was not failed and can support the structure subjected to tsunami force.

V.5.2.3. Overturning-Moment Response of Structure

The overturning-moment response of structure under near-field soil effect and fixed-base condition subjected to tsunami force is shown in Fig. 5.16.

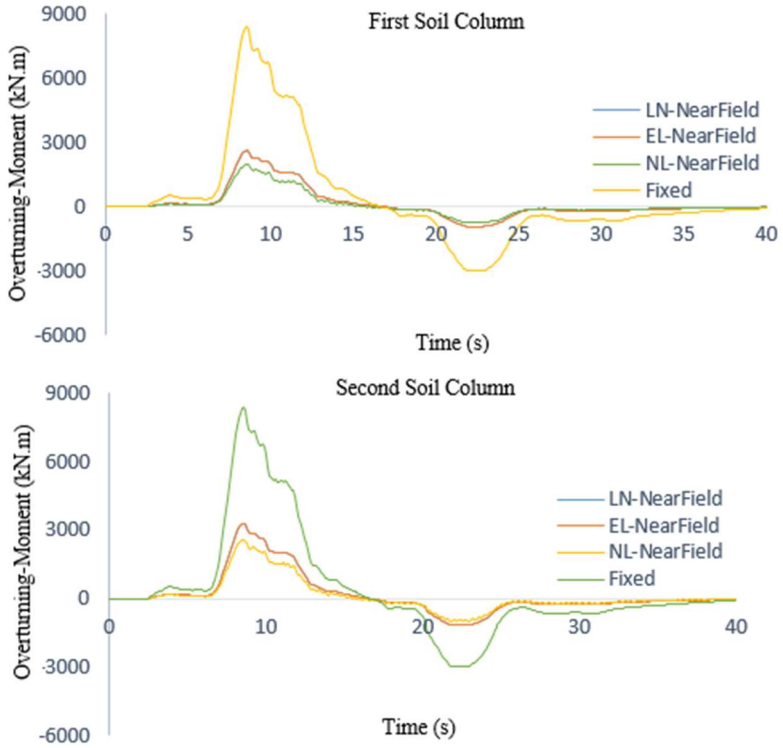

Figure V.16 Overturning-moment of structure under near-field soil effects and fixed-base condition

Based on the results above, it was shown that the overturning-moment response of structure under fixed-base structure was larger than the response under the effect of near-field soil. Besides this, the overturning-moment response of structure under linear response of near-field soil was larger than the response under nonlinear response of near-field soil. These output results showed about the overestimated results of using fixed-base structure condition without considering the nonlinear effect of near-field soil around the structure. Thus, the nonlinear effect of near-soil on the overturning-moment response of structure subjected to tsunami force should be considered and taken into account.

V.5.2.4. Story Shear Response of Structure

The story shear responses of structure under near-field soil effect and fixed-base condition subjected to tsunami force are shown in Fig. 5.17 and 5.18 for both soil conditions, respectively.

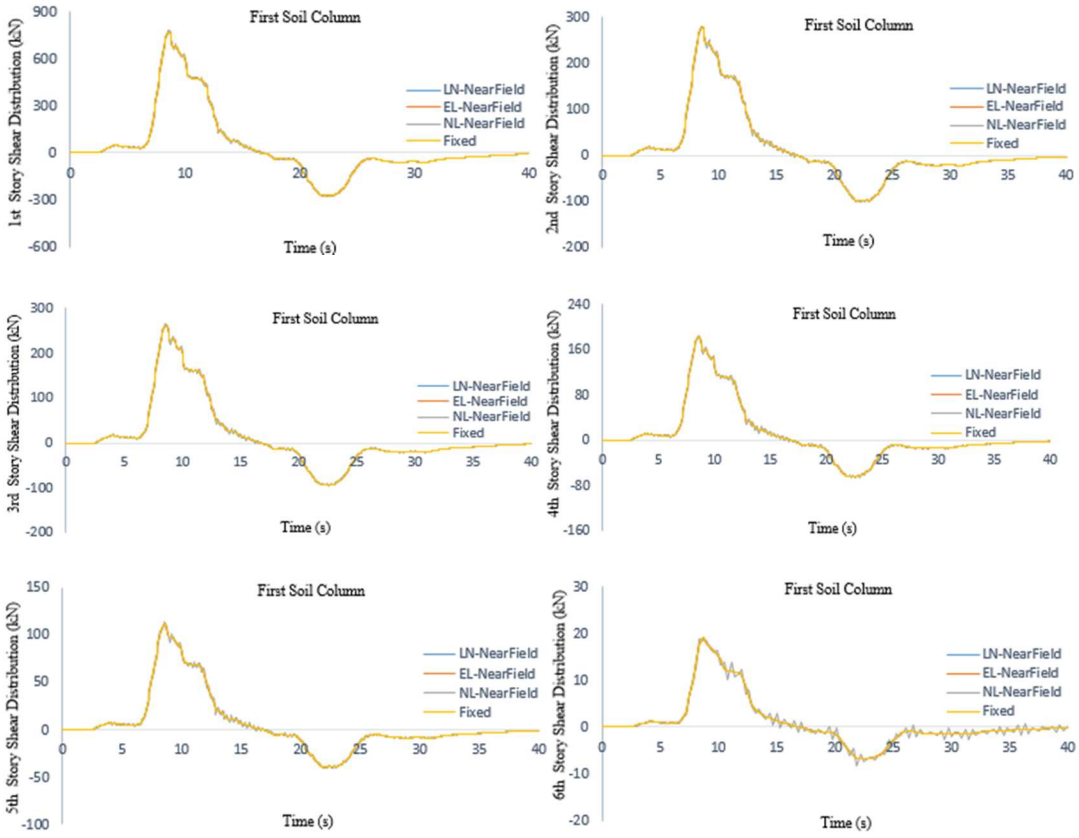

Figure V.17 Story shear response of structure under first column of near-field soil

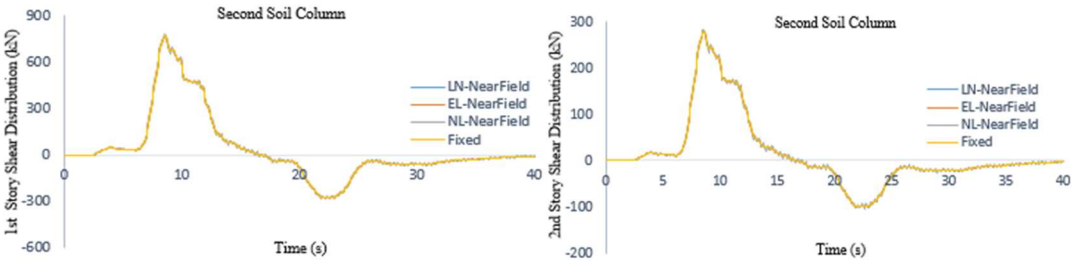

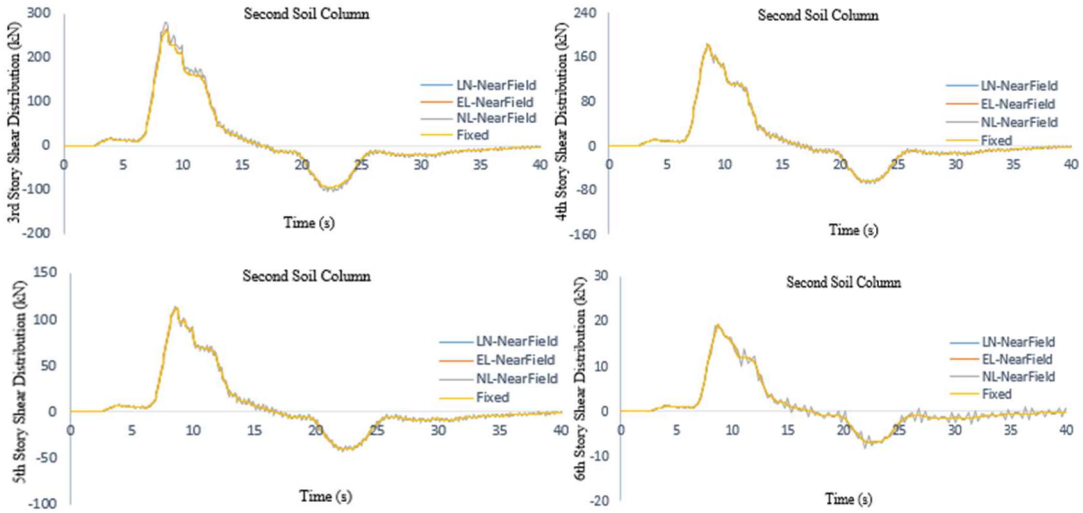

Figure V.18 Story shear response of structure under second column of near-field soil

Based on the response results above, it was shown that the story shear responses of structure under near-field soil effect and fixed-base condition were slightly different. There was no any significant effect for story shear response of structure under near-field soil effect and fixed-base condition under tsunami force.

These response results showed about the inefficacy of near-field soil nonlinearity on the story shear response of structure under tsunami force. However, further study should be conducted to investigate for further understanding.

Furthermore, the effect of near-field soil on the response of structure under tsunami force was applicable for some conditions of soil medium such as:

- *Tsunami Disaster*: all types of soil condition
- *Earthquake-Subsequent Tsunami Disaster*: applicable for sandy soil condition that can recover quickly after earthquake disaster. So, the deformation of near-field soil during earthquake disaster would not impact on the overturning-moment response of structure during subsequent tsunami disaster. Thus, it meant that the effect of near-field soil on the response of structure under both disasters were independent.

According to the description above, the nonlinear effect of near-field soil on the response of structure was significant and should be considered, especially overturning-moment response of structure.

V.6. CONCLUSION

The conclusion of this chapter was presented as in the following:

- *Near-field soil boundary*: the near-field soil boundary was proposed based on

the effective angle α and depth H. In this study, the effective angle α was proposed 45^o. This value was recommended by guidebook on excavation works considering neighboring structures.

- *Near-field soil segment division*: based on the variety of near-field soil segment divisions, the segment division of 4m was recommended. This segment division value allowed the correctly response of structure under tsunami disaster and applicable for the most of soil conditions.

- *Overturning-moment response of structure*: the overturning-moment response of structure under fixed base structure was larger than the response under near-field soil effect. Besides this, the overturning-moment response under linear response of near-field soil was larger than the response under nonlinear response of near-field soil. These results showed about the significant effect of near-field soil nonlinearity on the overturning-moment of structure under tsunami force. Thus, the nonlinear effect of near-field soil should be considered and taken into account on the overturning-moment response of structure under tsunami force. The ignoring of this effect can cause the overestimated resistance of structure during tsunami disaster.

- *Story shear response of structure*: the story shear response of structure subjected to tsunami force under fixed-base condition and near-field soil nonlinearity effect were slightly different. These response results showed about the inefficacy of near-field soil nonlinearity on the story shear response of structure. However, further investigation should be conducted to understand deeply about the effect of near-field soil on the response of structure under tsunami disaster.

In conclusion, the near-field soil boundary was proposed in this chapter. Based on the effective angle α, segment division, and the analytical model of near-field soil, this proposed analytical model was adequate and can utilize for practical work. In this study, the nonlinear effect of near-field soil has showed the significant impact on the response of structure during tsunami disaster, such as overturning-moment response of structure, which was utilized to evaluate the stability of structure during tsunami disaster.

However, during the 2011 Great East Earthquake and Tsunami in Japan, the tsunami disaster was occurred after the mega earthquake disaster. This subsequent

disaster can bring for another consideration and discussion on the effect of near-field soil during tsunami after earthquake disaster. This phenomenon will be discussed in the next chapter for further understanding on the nonlinear effect of near-field soil.

CHAPTER VI. EFFECT OF NEAR-FIELD SOIL NONLINEARITY ON THE RESPONSE OF STRUCTURE UNDER EARTHQUAKE AND SUBSEQUENT TSUNAMI DISASTER

VI.1. INTRODUCTION

In the previous chapter, the analytical model and effect of near-field soil on the response of structure subjected to tsunami force have been clarified. The response of structure, overturning-moment, have shown remarkable decreasing under the nonlinear effect of near-field soil. However, according to the experience of the 2011 disaster in Japan, the tsunami disaster was occurred after the great earthquake disaster. These subsequent disasters have raised the question for the nonlinear effect of near-field soil on the response of structure during tsunami disaster. During earthquake disaster, the near-field soil around the structure might be deformed and impacted on the response of structure during subsequent tsunami disaster. Thus, the objective of this chapter is to present the analytical procedure considering the effect of earthquake and subsequent tsunami disaster on the response of near-field soil column, which impacted on the response of structure.

In this chapter, the procedure considering the effect of earthquake force on the near-field soil column was presented while the effect of tsunami force was the same as presented in the previous chapter. An example of 3D RC frame structure subjected to both disasters was conducted subsequently. The comparison and discussion for the response of structure under the nonlinear effect of near-field soil subjected to tsunami force without and after earthquake disaster was provided for further understanding about these impacts on the response of near-field soil and structure.

VI.2. EARTHQUAKE EFFECT ON NEAR-FIELD SOIL COLUMN

In case of earthquake disaster, several effects should be considered and taken into account. These effects included earthquake motion at base of near-field soil, FIM, base-shear, and overturning-moment response of structure. For better understanding about these effects, the procedure of substructure approach for SSI effect was presented briefly again in this section. Commonly, substructure approach was divided into three steps of analysis procedure: FIM, dynamic impedance, and response of structure.

FIM was the required motion that needed to apply at the base of structure as input motion. This FIM was significant for both structure and near-field soil response.

Dynamic impedance was the interaction section between soil and structure

represented by spring-dashpot. From this interaction section, the FIM was transferred to structure and the response back from the structure on the top of near-field soil was achieved such as base-shear, and overturning-moment, which were other significant effects on the top of near-field soil column.

Furthermore, the earthquake motion at the base of near-field soil column was another crucial effect to maintain the same motion between FFGM and near-field soil column. This motion can be achieved from the FFGM at the same depth.

According to the description above, the significant effects on the near-field soil column were achieved. The FIM, base-shear, and overturning-moment were applied at the top of near-field soil column as the interaction response from the structure while the earthquake motion from FFGM at the same depth was applied to the base of near-field soil column, as shown in Fig. 6.1b. The nonlinear response analysis of near-field soil column under earthquake effect was conducted based on the procedure described in the previous chapter.

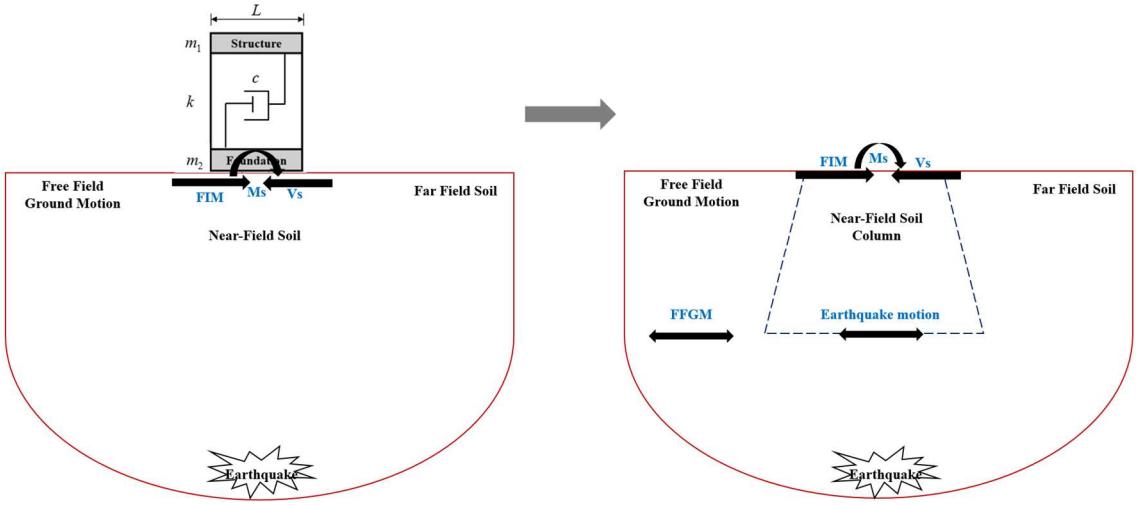

(a) Soil-structure interaction effect (b) Excitations on near-field soil column

Figure VI.1 Near-field soil column under earthquake effect

VI.3. EARTHQUAKE AND SUBSEQUENT TSUNAMI EFFECT ON NEAR-FIELD SOIL COLUMN

The analytical procedure of the effect of earthquake and subsequent tsunami force on the near-field soil column was another objective of this chapter. According to the nonlinear response analysis under earthquake effect, the nonlinear response of near-field soil material was achieved and assigned as initial state of near-field soil material under tsunami disaster. Under tsunami effect, the near-field soil column was connected to upper structure by shear and bending spring, as described in the previous chapter. The

response of structure subjected to subsequent tsunami force was conducted under the effect of near-field soil, as shown in Fig. 6.2. The response of near-field soil can be performed under linear and nonlinear response analysis. Besides this, the equivalent-linear response of near-field was assumed to be the same as linear response of near-field soil.

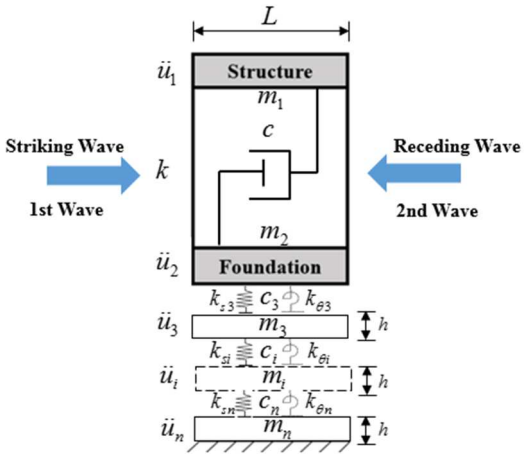

Figure VI.2 Analytical model of structure under tsunami force

VI.4. EXAMPLE OF 3D RC FRAME STRUCTURE SUBJECTED TO EARTHQUAKE AND SUBSEQUENT TSUNAMI DISASTER

For further comprehension the response of structure under near-field soil effect subjected earthquake and subsequent tsunami force, an example of 3D RC frame structure supported by two types of soil condition, from previous chapter, was conducted again under both subsequent disasters. Moreover, FIM, base-shear, and overturning-moment response of structure under nonlinear SSI effect [49] were achieved from Chapter IV while the earthquake at base of near-field soil column was achieved from Chapter III. Besides this, other relevant parameters were presented in the following sections.

VI.4.1. Excitations of Earthquake Effect on Near-Field Soil

The FIM, base-shear, and overturning-moment response from structure were the important effects on the top of near-field soil under earthquake disaster while the earthquake motion at the base of near-field soil column was another significant effect on the near-field soil column. These motions are shown in Fig. 6.3-6.6 for both soil conditions.

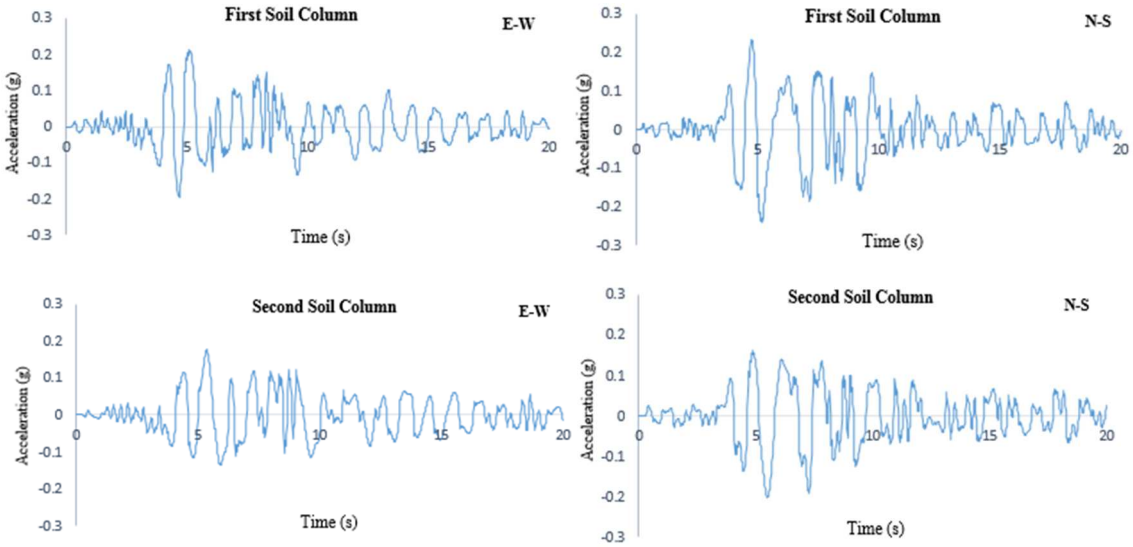

Figure VI.3 Foundation input motion for both soil columns

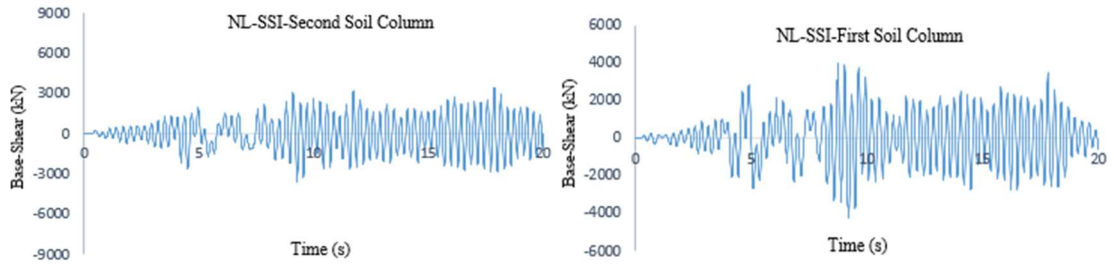

Figure VI.4 Base-shear of structure under nonlinear SSI effect

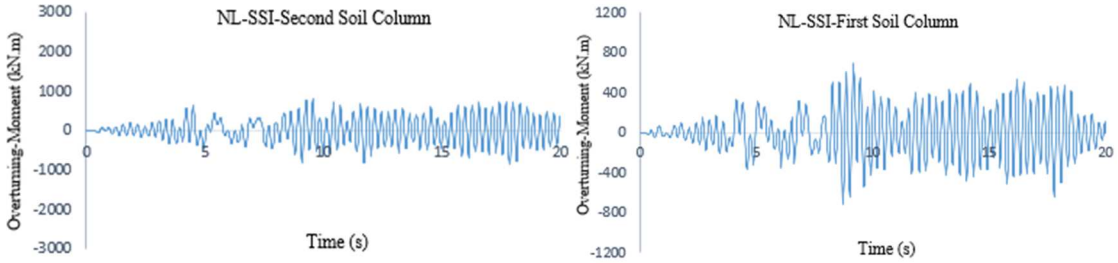

Figure VI.5 Overturning-moment of structure under nonlinear SSI effect

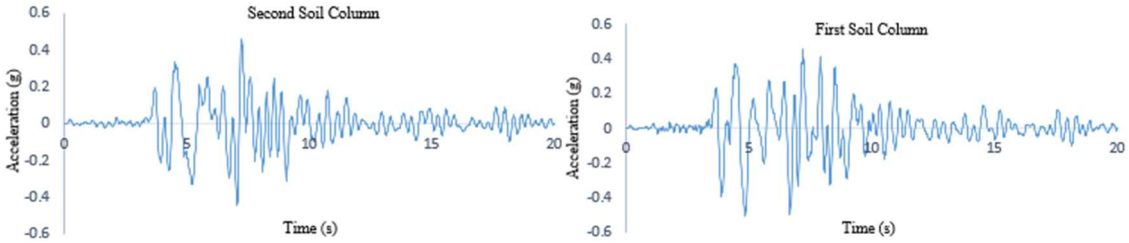

Figure VI.6 Earthquake input motion at the base of near-field soil column

Under these excitations, the nonlinear response of near-field soil was performed and the corresponding material was achieved.

VI.4.2. Near-Field Soil Response under Earthquake Excitations

The nonlinear response of near-field soil material at surface layer was achieved in Y-direction, as shown in Fig. 6.7, while the maximum shear strain in each segment of near-field soil is shown in Fig. 6.8. The tables of both initial near-field soil segment properties are shown in Table 6.1 and 6.2.

Table VI.1 Initial lumped mass, shear and bending stiffness of the first near-field soil column before earthquake disaster

H(m)	Vs (m/s)	γ(kN/m3)	ξ(%)	M (t)	K_s (kN/m)	K_θ(kN.m)
0	300	21	5	0.11e5	1.24e10	5.22e11
4				0.54e5		
8				1.38e5	4.82e10	8.64e12
12				2.63e5	1.07e11	4.36e13
16				4.28e5	1.88e11	1.37e14
20				6.34e5	2.93e11	3.33e14
24				8.81e5	4.20e11	6.89e14
28				11.68e5	5.70e11	1.27e15
32				14.96e5	7.43e11	2.17e15
36				18.65e5	9.39e11	3.47e15
40				10.30e5	1.16e12	5.28e15

Table VI.2 Initial lumped mass, shear and bending stiffness of the second near-field soil column before earthquake disaster

H(m)	Vs (m/s)	γ(kN/m3)	ξ(%)	M (t)	K_s (kN/m)	K_θ (kN.m)
0	350	22	5	0.12e5	1.77e10	7.44e11
4				0.57e5	6.87e10	1.23e13
8				1.45e5	1.52e11	6.22e13
12				2.75e5	2.69e11	1.95e14
16				4.48e5	4.17e11	4.75e14
20				6.64e5	5.99e11	9.82e14
24				9.23e5	8.13e11	1.82e15
28				12.24e5	1.06e12	3.09e15
32				15.67e5	1.34e12	4.94e15
36				19.54e5	1.65e12	7.52e15
40				23.83e5	2.00e12	1.10e16
44				28.54e5	2.37e12	1.56e16
48				33.69e5	2.78e12	2.14e16
52				39.26e5	3.23e12	2.88e16
56				45.25e5	3.70e12	3.79e16
60				24.18e5		

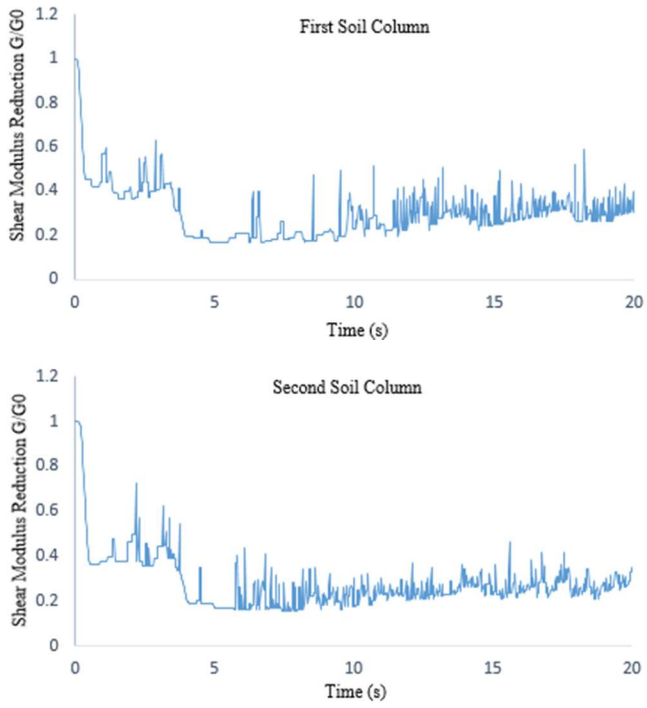

Figure VI.7 Shear modulus reductions G/G0 of near-field soil at surface layer

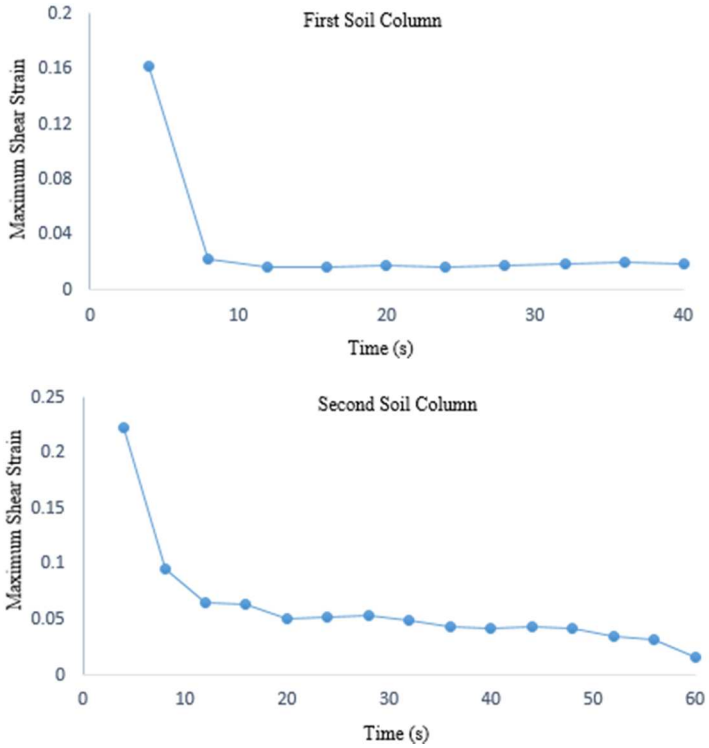

Figure VI.8 Maximum shear strains in each segment for both soil columns

As shown in Fig. 6.8, the first segment of both near-field soil columns showed a large response of shear strain more than 5% while the subsequent segments showed a small response of shear strain. In this case, the top segment of near-field soil column might be failed and needed for some kind of stability analysis. However, the objective of this chapter tends to express the effect of near-field soil on the response of structure rather than focusing on the stability of structure. Thus, the stability analysis was not discussed in this study.

The last nonlinear response of both near-field soil columns were assigned as initial material of near-field soil under tsunami disaster, as shown in Table 6.3 and 6.4.

Table VI.3 Lumped mass, shear and bending stiffness of the first near-field soil column after earthquake disaster

H(m)	Vs (m/s)	γ(kN/m3)	ξ(%)	M (t)	K_s (kN/m)	K_θ (kN.m)
0	165	21	5	0.11e5	3.73e9	1.57e11
4				0.54e5		
8	166			1.38e5	1.47e10	2.63e12
12	167			2.63e5	3.30e10	1.35e13
16	165			4.28e5	5.70e10	4.15e13
20	165			6.34e5	8.85e10	1.01e14
24	164			8.81e5	1.26e11	2.06e14
28	164			11.68e5	1.71e11	3.82e14
32	166			14.96e5	2.27e11	6.62e14
36	170			18.65e5	3.02e11	1.12e15
40	189			10.30e5	4.59e11	2.09e15

Table VI.4 Lumped mass, shear and bending stiffness of the first near-field soil column after earthquake disaster

H(m)	Vs (m/s)	γ (kN/m3)	ξ(%)	M (t)	K_s (kN/m)	K_θ (kN.m)
0	207	22	5	0.12e5	6.21e9	2.61e11
4				0.57e5		
8	198			1.45e5	2.19e10	3.93e12
12	188			2.75e5	4.38e10	1.79e13
16	194			4.48e5	8.27e10	6.02e13
20	183			6.64e5	1.15e11	1.31e14
24	186			9.23e5	1.70e11	2.78e14
28	191			12.24e5	2.42e11	5.40e14
32	204			15.67e5	3.59e11	1.05e15
36	190			19.54e5	3.96e11	1.46e15
40	185			23.83e5	4.62e11	2.10e15
44	182			28.54e5	5.43e11	2.99e15
48	181			33.69e5	6.31e11	4.14e15
52	179			39.26e5	7.28e11	5.60e15
56	186			45.25e5	9.07e11	8.09e15
60	202			24.18e5	1.23e12	1.26e16

VI.4.3. Response of Structure under Near-Field Soil Effect Subjected to Subsequent Tsunami Disaster

In case of subsequent tsunami disaster, the linear response of structure was performed under the effect of near-field soil. The responses of structure were included overturning-moment and story shear of structure, which was used to control the stability and damage response of structure.

VI.4.3.1. Shear Modulus Reduction and Shear Strain of Near-Field Soil

The shear modulus reduction and shear strain of both near-field soil columns at surface layer (top segment) subjected to subsequent tsunami force are shown in Fig. 6.9 and 6.10, respectively. Furthermore, the maximum strain in each layer is shown in Fig. 6.11.

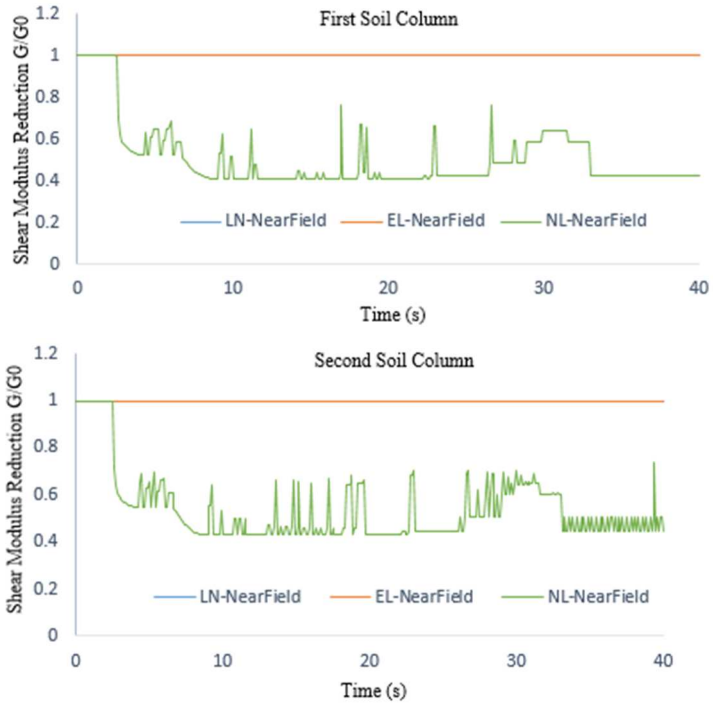

Figure VI.9 Shear modulus reductions under subsequent tsunami force at surface layer

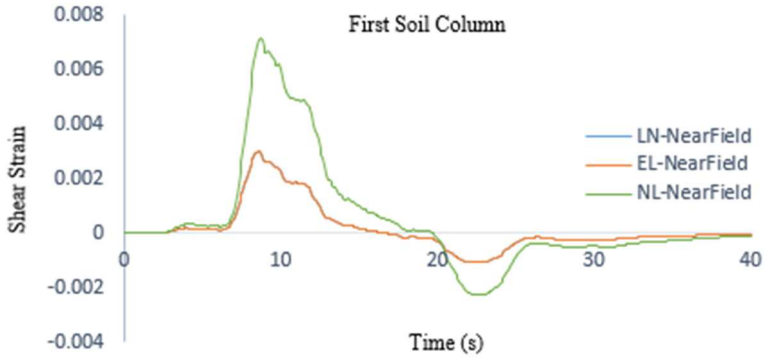

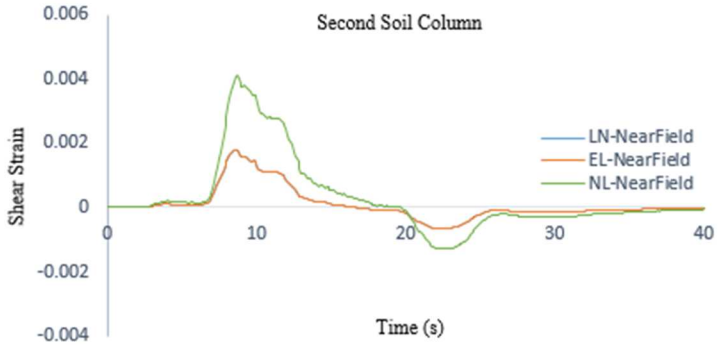

Figure VI.10 Shear strain of near-field soil at surface layer

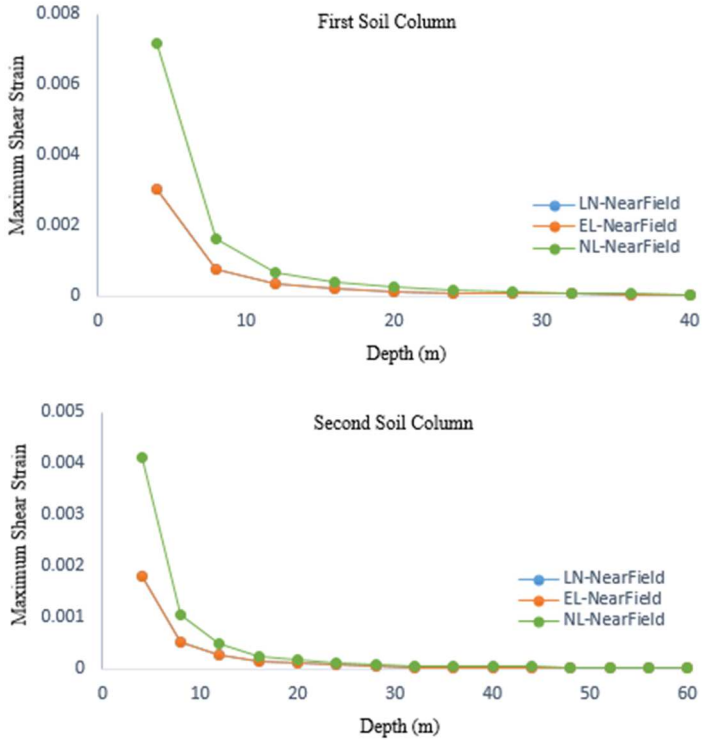

Figure VI.11 Maximum shear strains in each layer of near-field soil

As shown in Fig. 6.11, the maximum shear strain in each layer was smaller than 5%. Thus, the near-field soil can support the structure under subsequent tsunami disaster.

VI.4.3.2. Overturning-Moment Response of Structure

The overturning-moment response of structure under near-field soil effect for both soil columns were conducted, as shown in Fig. 6.12. The near-field soil was performed under linear and nonlinear response analysis while the equivalent-linear analysis was the same as linear response analysis.

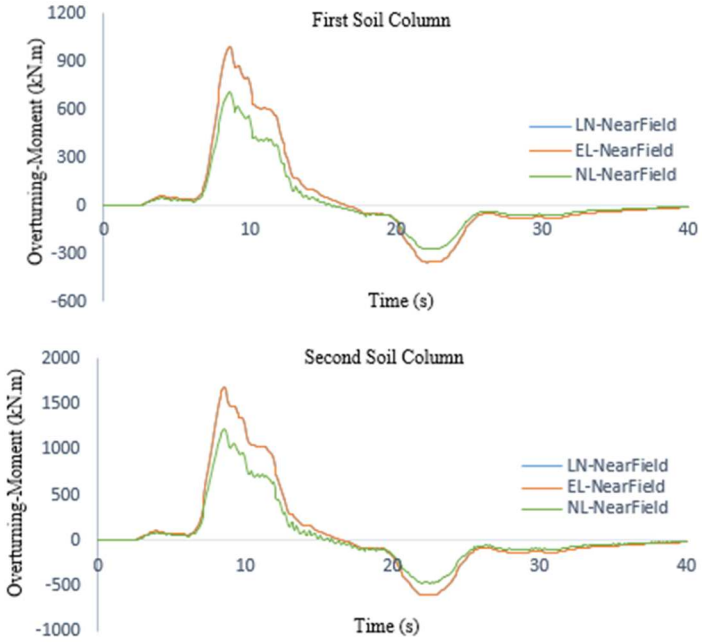

Figure VI.12 Overturning-moment response of structure under near-field soil effect

Based on the results above, it was shown that the overturning-moment response of structure under linear response of near-field soil was larger than the response under nonlinear response analysis of near-field soil. This response result showed about the nonlinear effect of near-field soil on the overturning-moment response of structure subjected to subsequent tsunami force. Thus, the nonlinear effect of near-field soil on the overturning-moment response of structure subjected to subsequent tsunami force should be considered and taken into account.

VI.4.3.3. Story Shear Response of Structure

The story shear responses of structure under both columns of near-field soil subjected to tsunami force are shown in Fig. 6.13 and 6.14, respectively.

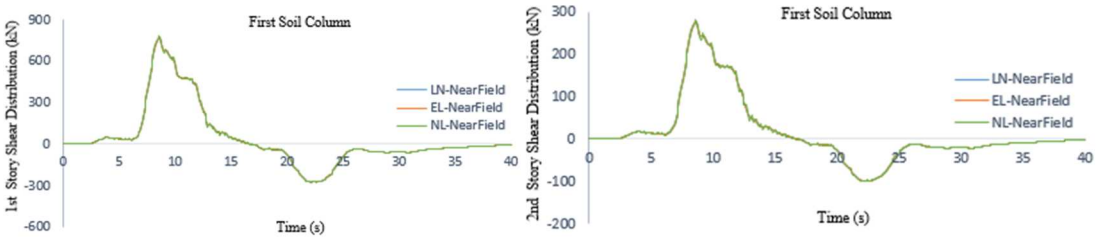

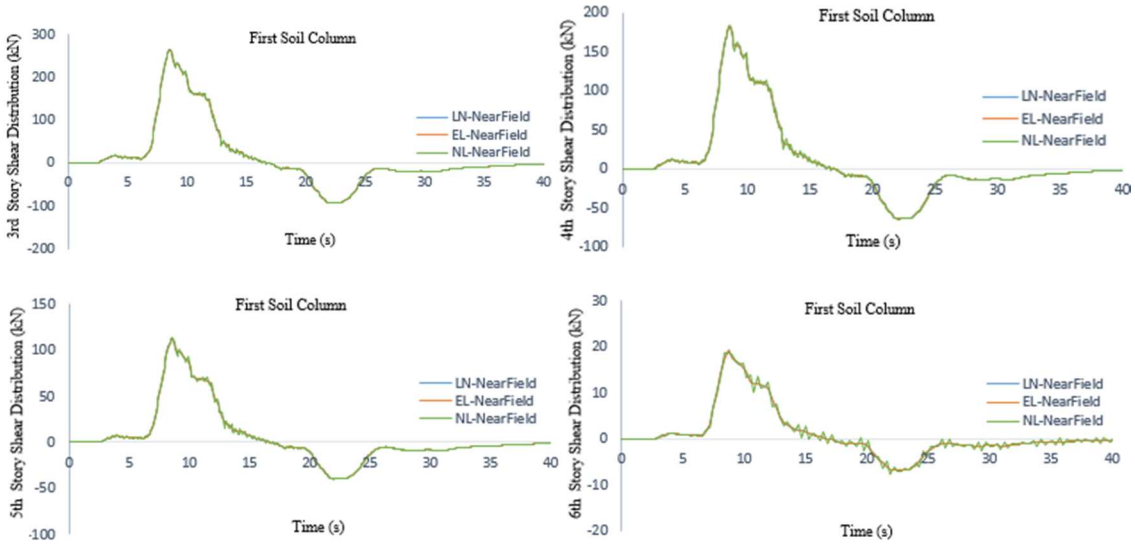

Figure VI.13 Story shear response of structure under first column of near-field soil effect

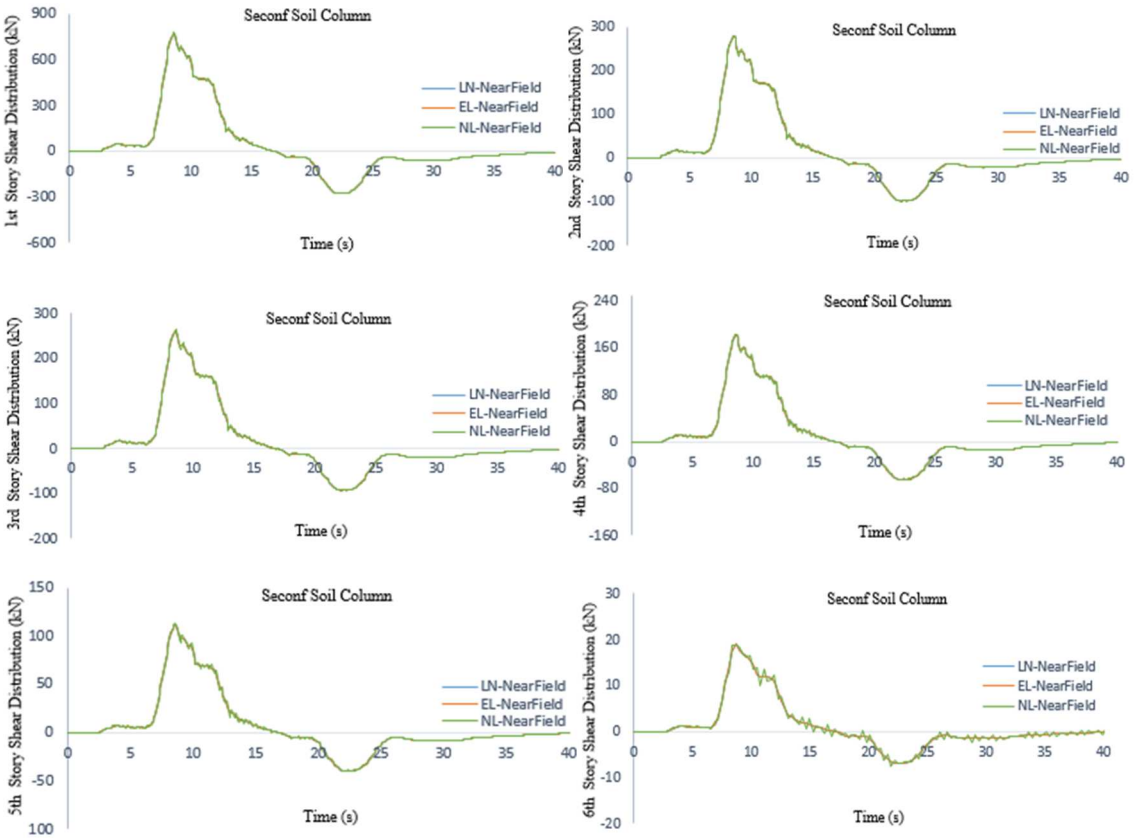

Figure VI.14 Story shear response of structure under second column of near-field

Based on the response results above, it was shown that the story shear responses of structure under linear and nonlinear response of near-field soil effect were slightly different. There was no any significant effect for story shear response under the nonlinear effect of near-field soil subjected to tsunami force. However, further study should be conducted to investigate this effect.

VI.4.4. Response of Structure under Relationship of Earthquake and Subsequent Tsunami Disaster

In this section, the comparison between the responses of structure under tsunami disaster without and after earthquake disaster was conducted. Moreover, the subsequent response of structure was also provided. These comparisons would bring for further understanding about the nonlinear effect of near-field soil on the response of structure under earthquake and subsequent tsunami disaster.

VI.4.4.1. Overturning-Moment Response of Structure

The comparison of overturning-moment response of structure under the effect near-field soil subjected to tsunami and earthquake-tsunami relationship disaster is shown in Fig. 6.15.

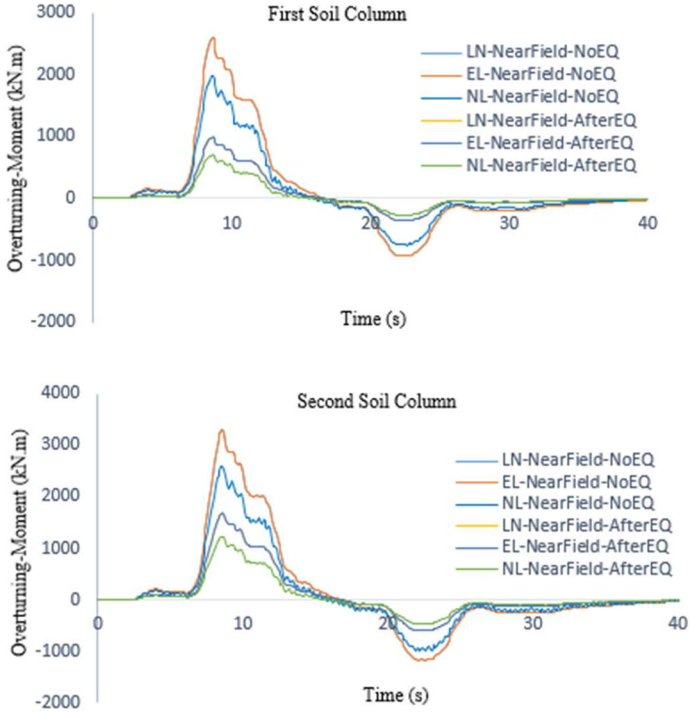

Figure VI.15 Overturning-moment response of structure under near-field soil effect

subjected to tsunami and earthquake-tsunami relationship

As shown in Fig. 6.15, the overturning-moment responses of structure under near-field soil effect subjected to tsunami force was larger than the response under earthquake-tsunami relationship. These response results showed that the near-field soil column was deformed during earthquake disaster and impacted on the overturning-moment response of structure during subsequent tsunami disaster. Thus, the nonlinear effect of near-field soil on the overturning-moment response of structure under earthquake and subsequent tsunami relationship should be considered and taken into account. This condition was applicable for some types of soil condition that required long time to recover as the initial state after earthquake disaster such as clayey soil condition.

VI.4.4.2. Near-Field Soil and Overturning-Moment Response of Structure under Earthquake and Subsequent Tsunami Disaster

The nonlinear response of near-field soil material at surface layer under earthquake and subsequent tsunami disaster is shown in Fig. 6.16 while the overturning-moment response subjected to both disasters is shown in Fig. 6.17 for both near-field soil columns.

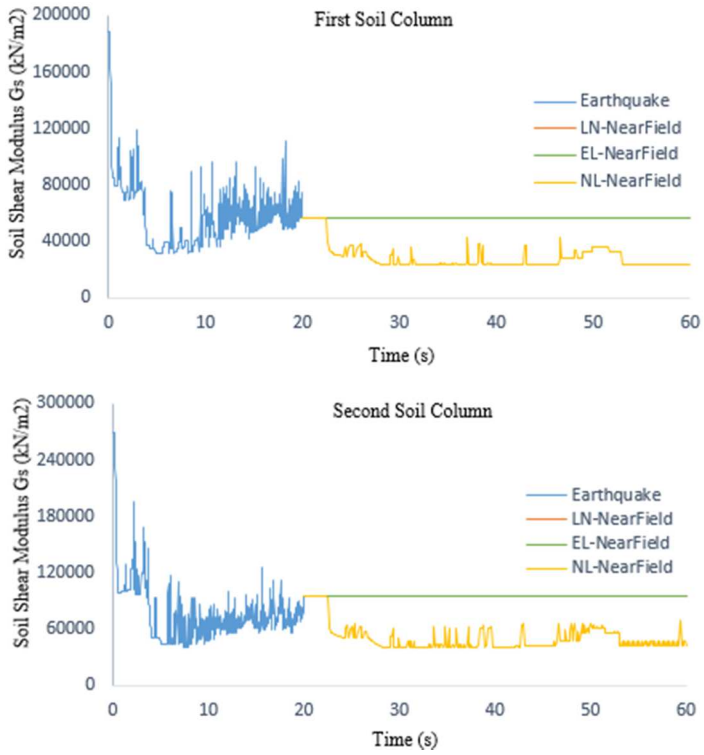

Figure VI.16 Near-field soil stiffness responses under earthquake and subsequent tsunami disaster

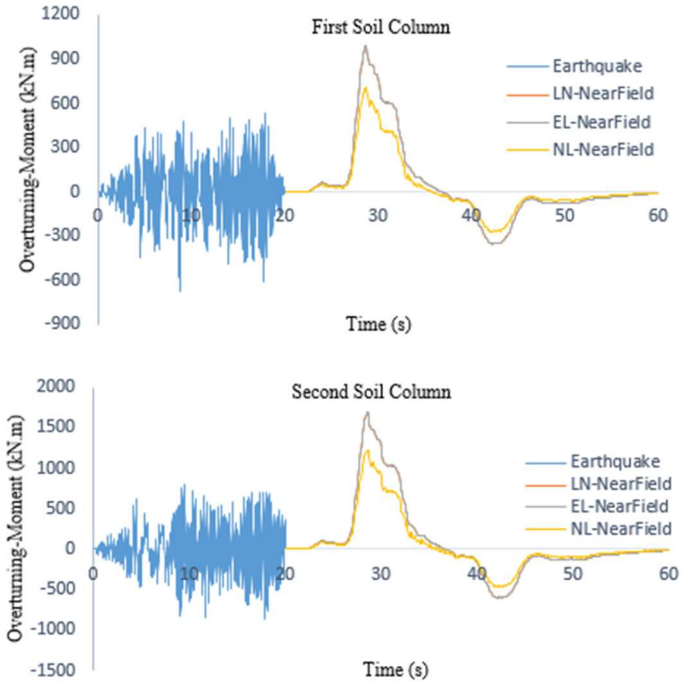

Figure VI.17 Overturning-moment response of structure under earthquake and subsequent tsunami disaster

VI.5. CONCLUSION

The conclusion of this chapter was presented as in the following:

- *Earthquake effect on near-field soil column*: the analytical procedure considering the effect of earthquake on near-field soil column was presented. This analytical procedure was considered for both effects from structural response and FFGM such as FIM, base-shear, overturning-moment, and earthquake motion at the base of near-field soil column, which were the necessary impacts on the near-field soil column.

- *Earthquake and subsequent tsunami effect on near-field soil column*: the analytical procedure considering the effect of both subsequent disasters was presented. The last response of near-field soil material was assigned as the initial material of near-field soil under subsequent tsunami disaster. The condition of soil deposit that was applicable for this analytical model was also presented.

- *Overturning-moment response of structure*: the overturning-moment response of

structure under linear response of near-field soil was larger than the response under nonlinear response of near-field soil. This result showed about the necessity and importance of the nonlinear effect of near-field soil on the overturning-moment response of structure under earthquake and subsequent tsunami disaster. Furthermore, the nonlinear effect of near-field soil on the overturning-moment response of structure subjected to tsunami disaster was larger than the response subjected to earthquake and subsequent tsunami disaster. The response results showed about the effect of earthquake force on the near-field soil response and impacted on the overturning-moment response of structure during tsunami disaster. Thus, the effect of earthquake and subsequent tsunami disaster on the overturning-moment response of structure under the nonlinear effect of near-field soil should be considered and taken into account, especially clayey soil condition that needed long time to recover as initial state after earthquake disaster.

- *Story shear response of structure*: there were very slightly different for the story shear response of structure subjected to earthquake and subsequent tsunami disaster under the linear and nonlinear response of near-field soil. This response result showed about the inefficacy of near-field soil nonlinearity on the story shear response of structure under subsequent tsunami disaster. However, further investigation and discussion should be conducted for deeply comprehension about this effect under tsunami disaster.

In conclusion, the analytical procedure considering the effect of earthquake and subsequent tsunami disaster was presented in this chapter. This proposed analytical procedure was adequate for utilization in practical or research work due to the assumption conditions compared to the reality situation. In this study, the nonlinear effect of near-field soil has showed the significantly effect on the response of structure under earthquake and subsequent tsunami disaster, such as overturning-moment response of structure, which was utilized to evaluate the stability of structure during tsunami disaster. This study would bring for further consideration and discussion about the effect of near-field soil on the response of structure during subsequent tsunami after earthquake disaster.

CHAPTER VII. CONCLUSIONS

The tragedy of the 2011 Great East Earthquake and Tsunami disaster has left unexpected remains of devastation of many buildings and casualties. The structural damages experienced from these disasters are significantly essential for future structural design guideline under earthquake and tsunami disaster. According to the field reports, many RC buildings were damaged and overturned, especially in Onagawa Town. The effect of nonlinear soil-structure interaction was regarded as a significant factor on the structural damage response and the overturning of structure, which has become another impressive issue for structural response under earthquake and tsunami disaster. In order to contribute the solution for these problems, this thesis has proposed some significant analytical models:

- Analytical model considering nonlinear response of soil material and FFGM
- Analytical model considering nonlinear SSI effect under substructure approach
- Analytical model considering the nonlinear effect of near-field soil on the response of structure under earthquake and subsequent tsunami force.

· **Nonlinear Response of Soil Material and FFGM**

◆ *Linear Response Analysis*

In linear response analysis, the target earthquake motion was input at the base of soil column (or surface layer) as an outcrop motion (2E). Then, the FFGM analysis in FD was performed and the within output motion ($E+F$) was extracted at the base of soil column. This motion was applied at the same layer of soil column (as input motion) for FFGM analysis in TD and the target output motion at surface layer was obtained. The within motion ($E+F$) of any location is an actual motion of that location.

◆ *Nonlinear Response Analysis*

In nonlinear response analysis, the procedure is the same as linear analysis but it was required to perform in both linear and equivalent-linear analysis in FD and the within output motion ($E+F$) of both analysis was significant to be the same or almost the same. Then, this motion was applied as the input motion at the same layer for FFGM analysis in TD and the target output motion at the

surface layer was obtained. Some extra layers might be needed in order to obtain the same or similar motion as described above.

In order to verify this analytical model, the nonlinear response of FFGM in TD at the surface layer was compared with the linear and equivalent-linear response motion in FD.

The nonlinear response results showed a good agreement with linear response for a few seconds from starting point and with equivalent-linear response for the last several seconds. The agreement confirmed about the validation of proposed analytical model considering nonlinear response of soil material and motion. Thus, proposed analytical model would be a potential model and adequateness for nonlinear FFGM analysis in TD and facilitated performing the seismic response of structure under nonlinear SSI effect.

- **Nonlinear SSI Analysis**

Due to the simplicity requirement, substructure approach is frequently used in practical work and research field. However, this approach can be performed only with equivalent-linear of soil material in FD. This restriction can cause mismatched response and overestimated results compared to the actual response of structure under earthquake loading. In order to solve this restriction, an analytical model was conducted by taking into account the nonlinear response of soil material and motion.

The seismic response of structure under existing analytical model and proposed analytical model was performed considering linear response of base-shear, overturning-moment, acceleration, and relative displacement in each floor. The response results showed that the structural responses under existing analytical model were larger than the responses under proposed analytical model.

These differences showed the overestimated results of using existing analytical model under substructure approach. Thus, the proposed analytical model considering nonlinear SSI effect would be a potential candidate for SSI problem and showed about the adequateness of this approach compared to the actual response of structure.

- **Nonlinear Effect of Near-Field Soil**

The analytical model considering the effect of near-field soil on the response of structure under earthquake and subsequent tsunami disaster was proposed.

- *Near-Field Soil Column Boundary*

  The analytical procedure considering near-field soil column boundary was proposed based on the effective angle α and depth H. The effective angle α was assumed 45^o.

- *Near-Field Soil Segment Division*

  Based on the variety of near-field soil segment divisions, the segment of 4m was recommended. This segment division value allowed obtaining correctly response of structure under earthquake and tsunami disaster for all typical of soil conditions.

- *Earthquake effect on near-field soil column*: the analytical model considering both effects from structural response and FFGM was presented. These effects were included FIM, base-shear, overturning-moment, and the earthquake motion at the base of near-field soil column.

- *Earthquake and subsequent tsunami effect on near-field soil column*: the analytical procedure considering the effect of both subsequent disasters was presented. The last response of near-field soil material under earthquake disaster was assigned as initial material of near-field soil under subsequent tsunami.

The structural response was performed under two significant effects: tsunami and tsunami-earthquake effect. The response of structure under near-field soil effect showed that:

- *Under Tsunami Effect*

  - *Overturning-moment response of structure*

    The overturning-moment response of fixed-base structure was larger than the response considering the effect of near-field soil column. This result showed about the overestimated result of using fixed-base structure. Thus, the effect of near-field soil should be considered for determining the overturning-moment of structure under tsunami force, especially for soft soil condition.

  - *Story shear response of structure*

    There were very slightly different for the story response of structure under fixed-base and near-field soil effect. This response showed about the inefficacy of near-field soil nonlinearity on the story shear response of

structure during tsunami disaster.

- *Under Earthquake-Tsunami Effect*
  - *Overturning-moment response of structure*

    The overturning-moment of structure considering the effect of near-field soil under tsunami effect was larger than the response under earthquake-tsunami relationship. These results showed about the effect of earthquake on the near-field soil and the overturning-moment response of structure during tsunami disaster. Thus, the effect of earthquake-tsunami on the response of structure should be considered and taken into account, especially clayey soil condition that needs long time to recover after earthquake disaster.
  - *Story shear response of structure*

    There were very slight different for the story shear response of structure under tsunami and earthquake-tsunami relationship. These results showed about the inefficacy of near-field soil nonlinearity on the story shear response of structure during subsequent tsunami disaster.

In conclusion, the proposed analytical model of near-field soil effect was adequate for utilization in practical and research work based on the assumption conditions compared to the reality situation. However, the nonlinear effect of near-field soil on the response of structure should be investigated deeply for further comprehension in order to develop this analytical model for practical utilization and structural design guidelines under tsunami disaster.

· Further Research and Investigation

In this thesis, the effect of nonlinear response of uniform soil on the response of structure has been conducted under earthquake and tsunami disaster. For further research and investigation, there are some aspects that need to consider for the effect nonlinearity of soil on the structural response:

- non-uniform soil medium
- liquefaction effect

These effects would permit for further understanding the response of structure under nonlinear response of soil medium subjected to earthquake and tsunami force.

Moreover, based on the proposed analytical models and assumptions, the city damage simulation considering SSI effect subjected to earthquake and tsunami disaster should be conducted in order to evaluate the damage of city and prepare for the great

further earthquake that can occur any time along Nankai Trough.

Lastly, this thesis has proposed a few analytical models for further consideration and investigation on the nonlinear effect of soil medium on the response of structure, especially under tsunami disaster which is the originality and contribution of this thesis for engineering society and structural design guidelines under earthquake and tsunami disaster.

FURTHER RESEARCH

According to the estimation, the great future earthquake will hit many prefectures along Nankai Trough. In order to mitigate this inevitable disaster, many disaster management plans has been preparing including city damage simulations. The city damage simulation was one of significant management plan that can visualize the response of structures in city during earthquake and tsunami disaster. This visualization can bring for some kinds of disaster mitigation plan:

- The most dangerous zone in the city
- Intervention or preparation for the damage of buildings
- Evacuation zones and directions
- Cost estimation of city damage
- Awareness of city residents preparation

However, in order to simulate the city damage under earthquake and tsunami disaster, the potential and capable program is absolutely significant. Recently, OBASAN, structural analysis program, has been integrated into Integrated Earthquake Simulation (IES) program. This cooperation facilitated performing the city damage simulation, as shown in Fig. 1. However, this simulation can perform only fixed-base structure condition that is unable to represent the actual response of structure considering the interaction of soil and structure during earthquake and tsunami disaster.

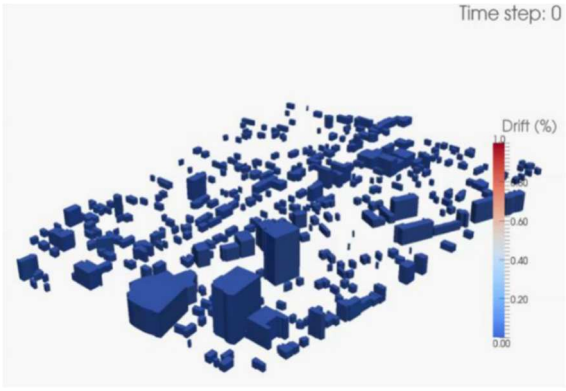

Figure 1 City damage simulation under fixed-base structure condition [47]

· **Advantages of Proposed Analytical Models**

As described above, the city damage simulation considering SSI effect subjected to earthquake and tsunami disaster is very important to represent the actual response of

city damage during disasters.

- *Earthquake disaster*

As mentioned in literature reviews, the seismic response of structure under SSI effect can be performed under two main approaches: direct and substructure approach. Direct approach is a rigorous method for SSI, however, this approach consumed much time and cost, especially for a huge three dimensional analysis such city damage simulation. On the other hand, the substructure approach is a frequently used method in SSI problem due to its simplicity and time consumption, however, this approach can perform only equivalent-linear value of interaction part. Due to this reason, the simulation was unable to perform a fully nonlinear response analysis. However, under the proposed analytical model from this thesis, the substructure approach can perform with the nonlinear response value of interaction part and facilitated performing the nonlinear response city damage simulation under earthquake disaster.

- *Tsunami disaster*

Generally, the interaction effect of soil on the response of structure can be performed only under earthquake force while the proposed analytical model brought for further consideration the effect of near-field soil on the response of structure subjected to tsunami force after or without earthquake disaster. This proposed analytical model facilitated performing the city damage simulation subjected to tsunami force under the effect of near-field soil around the structure.

- *Conclusion*

In conclusion, the proposed analytical models in this thesis have developed not only the analytical models considering the interaction between soil and structure but also facilitated performing the city damage simulation considering soil-structure interaction effect under earthquake and tsunami disaster.

· **City Damage Simulation Input Data**

In order to conduct the city damage simulation, some developments of program and input data are significantly important. These relevant parameters were described in the following sections.

- *Free Field Ground Motion and Dynamic Impedance Integrations*

In order to perform SSI analysis, the FFGM and dynamic impedance analysis

were important factors. These integrations have been done and can perform in OBASAN program.

- *GIS Data of Buildings*

The target of city damage simulation is Kochi City, thus, the GIS data of buildings in this city is very important. From these building data, some important information can be provided:

- Selected and studied area
- Building shape
- Building height
- Construction year.

The GIS data of buildings in Kochi City was shown in Fig.2 while the select area was shown in Fig. 3.

Figure 2 GIS data of buildings in Kochi City

(a) Selected area in GIS data

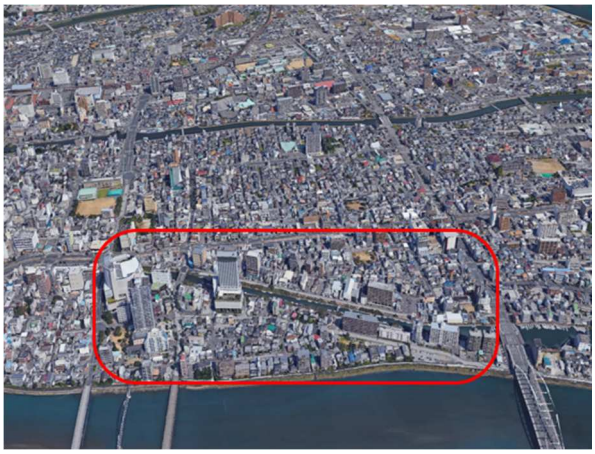

(b) Selected area in Google map

Figure 3 Selected area for city damage simulation

As shown in Fig. 3, the selected area consists many high rise RC buildings that facilitated performing the city damage simulation.

- *Soil Boring Data*

The boring data of selected area was achieved from geotechnical new of Kochi Prefecture [57], as shown in Fig. 4. According to the boring data from selected area, the soil condition is very soft. Due to this condition, the interaction of soil on the response of structure was performed a significant role under earthquake and tsunami disaster.

(a) Boring data location in selected area

ボーリング柱状図

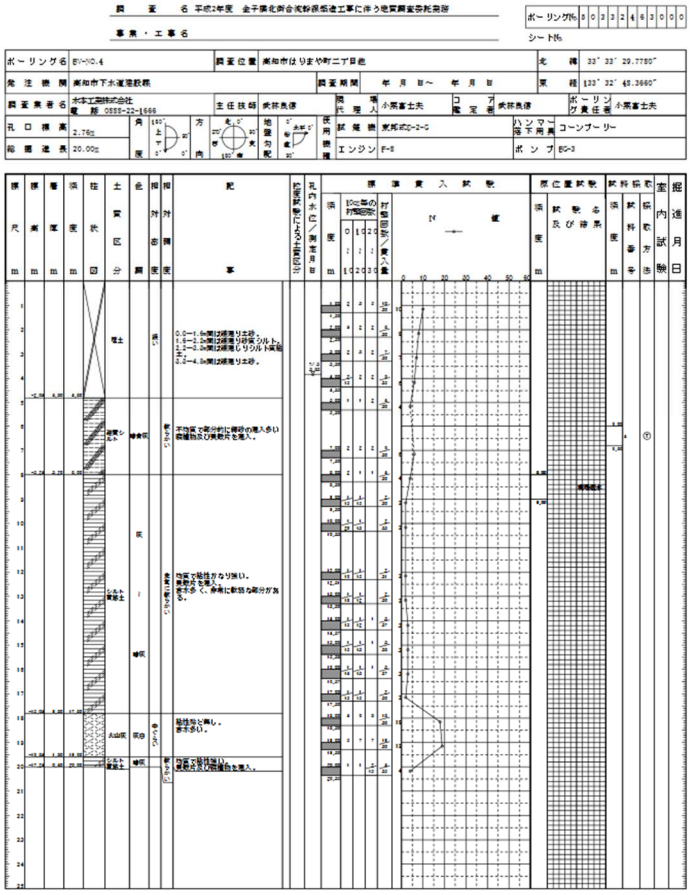

(b) Table of Boring data

Figure 4 Boring data of selected area

- *Earthquake and Tsunami Prediction Data*

The prediction of great future was shown in Fig. 5 while the tsunami inundation height was shown in Fig. 6.

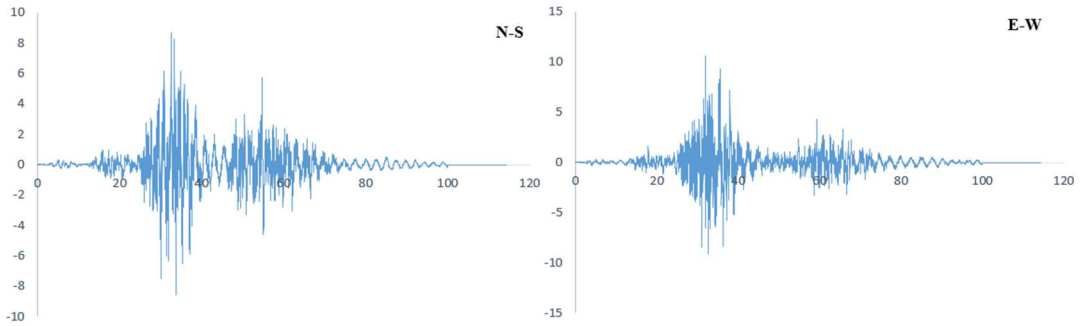

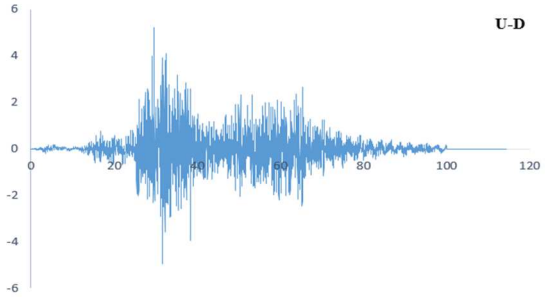

Figure 5 Great future earthquake input motion (m/s2) [47]

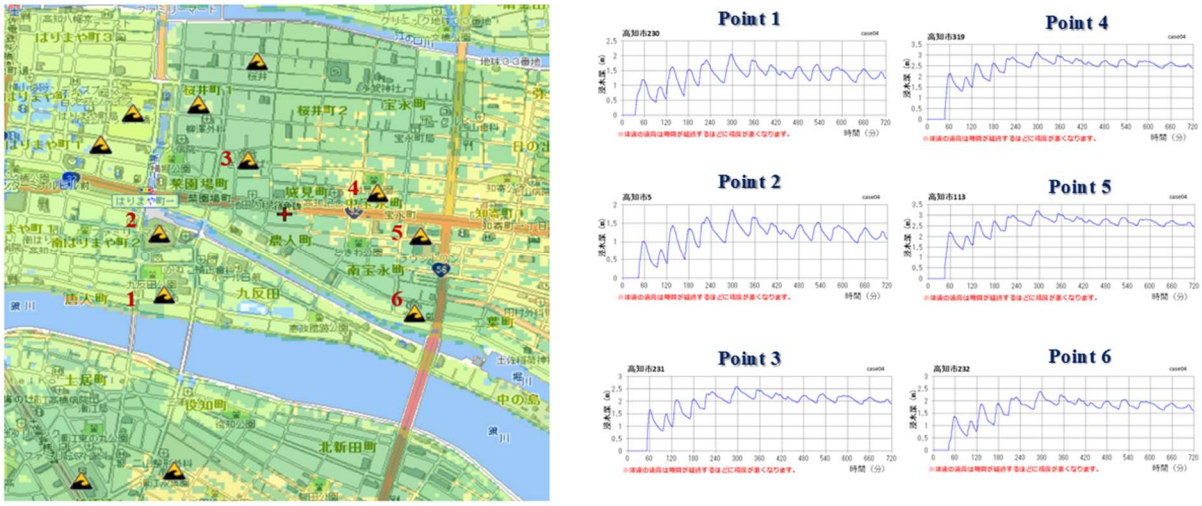

Figure 6 Tsunami inundation around selected area [58]

- **City Damage Simulation Procedure**

  - *Earthquake Disaster*

The city damage simulation procedure under earthquake disaster was described briefly as in the following:

- The FFGM of selected area was achieved by OBASAN
- The FIM can be achieved by FFGM, soil condition, and wave motion type
- The dynamic impedance was obtained by OBASAN according to soil condition and building foundation shape.

- The seismic response of buildings and visualization of selected area can be obtained by integration of OBASAN and IES.

- *Tsunami Disaster*

The city damage simulation procedure under tsunami disaster was described briefly as in the following:

- The near-field soil was modeled according soil condition
- The near-field soil response under earthquake disaster can be obtained by OBASAN.
- The response of structure under near-field soil effect subjected tsunami force and visualization can be achieved by integration of OBASAN and IES.

According to description above, the city damage simulation under earthquake and subsequent tsunami disaster considering soil interaction effect can be obtained and visualized.

REFERENCES

[1] Japan Agency for Marine-Earthquake Science and Technology, (2015). “Study on the interrelation between the Tokai, Tonankai and Nankai earthquakes”, //www.jamstec.go.jp/donet/rendou/en/about/

[2] Kabeyasawa T., (2012). “Damage survey on buildings and the lessons from the 2011 East Japan Earthquake”, *Proceedings of the International Symposium on Engineering Lessons Learned from the 2011 Great East Japan Earthquake*, Tokyo, Japan.

[3] Masanori I., Isao N., I. O., Hiroshi F., Yasuo O., (2012). “Brief review of building damage by the 2011 Tohoku Japan Earthquake and following activities for disaster mitigation”, Proceedings of the 44th Joint Panel on Wind and Seismic Effects, Japan.

[4] Kabeyasawa T., Okuda Y., Fukai A., (2012). “Evaluation of lateral and buoyant forces on reinforced concrete buildings by the tsunami of the 2011 East Japan Earthquake”, *Proceedings of 15th World Conference on Earthquake Engineering*, Lisbon, Portugal.

[5] Harry Y., Andre R. B., Harrison K., Jessica C., (2014). “Tsunami loadings on structures review and analysis”, *Proceedings of the 34th International Conference on Coastal Engineering*, Seoul, Korea.

[6] Carlo G. L., Mario M., (2013). “Soil-structure interaction under earthquake loading: Theoretical frame work”, *Alert Doctoral School 2013*.

[7] Japan Cabinet Office, (2005). “Design guideline for tsunami evacuation buildings”, Japan.

[8] FEMA, (2009). “NEHRP recommended seismic provisions for new buildings and other structures”, FEMA P-750/2009 Edition, Building Science for the Federal Emergency Management Agency, Washington D.C.

[9] Ottaviani M., (1975). “Three-dimensional finite element analysis of vertically loaded pile groups”, *Journal of Geotechnical Engineering*, Vol. 25, pp. 159-174.

[10] Randolph M. F., (1981). “The response of flexible piles to lateral loading”, *Journal of Geotechnical Engineering*, Vol. 31, pp. 247-259.

[11] Lin H. T., Roesset J. M., Tassoulas J. L., (1987). “Dynamic interaction between adjacent foundations”, *Journal of Earthquake Engineering and Structural Dynamics*, Vol. 15, pp. 323-343.

[12] Karabalis D. L., Beskos D. E., (1986). “Dynamic response of 3-D embedded foundations by the boundary element method”, *Journal of Computer Methods in Applied Mechanics and Engineering*, Vol. 56, pp. 91-119.

[13] Estorff O. V., Stamos A. A., Beskos D. E., (1991). “Dynamic interaction effects in underground traffic systems”, *Journal of Engineering Analysis with Boundary Elements*, Vol. 8, pp. 167-175.

[14] Karabalis D. L., Mohsen M., (1998). “3-D dynamic foundation interaction on layered soil”, *Journal of Soil Dynamics and Earthquake Engineering*, Vol. 17, pp. 139-152.

[15] Padron L. A., Aznarez J. J., MaesoO., (2007). “BEM-FEM coupling model for the dynamic analysis of piles and pile groups”, Journal of Engineering Analysis with Boundary Elements, Vol. 31, pp. 473-484.

[16] Padron L. A, Aznarez J. J., Maeso O., (2009). “Dynamic structure-soil-structure interaction between nearby piled buildings under seismic excitation by BEM-FEM model”, *Journal of Soil Dynamics and Earthquake Engineering*, Vol. 29, pp. 1084-1096.

[17] Lehmann L., Heinz A., (2001). “Dynamic structure-soil-structure interaction applying the Symmetric Galerkin Boundary Element Method (SGBEM)”, *Journal of Mechanics Research Communications*, Vol. 28, pp.297-304.

[18] Wolf J. P., (1985). “Dynamic soil-structure interaction”, Prentice Hall.

[19] Javier A., Luis E. P. R., (1998). “Effects of foundation embedment during building-soil interaction”, *Journal of Earthquake Engineering and Structural Dynamics*, Vol. 27, pp. 1523-1540.

[20] Javier A., Martha S., Francisco J. S. S., (2002). “Effects of wave passage on the relevant dynamic properties of structures with flexible foundation”, *Journal of Earthquake Engineering and Structural Dynamics*, Vol. 31, pp. 139-159.

[21] Cristina M., Juan J. A., Luis A. P, Orlando M., (2013). “Effects of soil-structure interaction on the dynamic properties and seismic response of piled structures”, *Journal of Soil Dynamic and Earthquake Engineering*, Vol. 53, pp. 160-175.

[22] Mejia L. H., Arulnathan, Murugaigah S., Thomann T., (2014). “Soil-structure interaction analysis of the Manhattan bridge foundations”, *Proceeding of 10th U.S. National Conference on Earthquake Engineering Frontiers of Earthquake Engineering*, Anchorage, Alaska.

[23] Mylonakis G., Sissy N., Gazatas G., (2006). “Footings under seismic loading: Analysis and design issued with emphasis on bridge foundations”, *Journal of Soil Dynamic and Earthquake Engineering*, Vol. 26, pp. 824-853.

[24] National Institute of Standards and Technology, (2012). “Soil-structure interaction for building structures, U.S. Department of Commerce, Engineering Laboratory, Gaithersburg, MD 20899, U.S.

[25] Idriss I. M., Joseph I. S., (1992). User’s manual for SHAKE91: A computer program for conducting equivalent-linear seismic response analyses for horizontally layered soil deposits, University of California, Davis, California, U.S.

[26] Bardet J. P., Ichi K., Lin C. H., (2000). A computer program for equivalent linear earthquake site response analyses of layered soil deposits, University of Southern California, California, U.S.

[27] Nikolaou S., Mylonakis G., Gazatas G., Tazoh T., (2001). “Kinematic pile bending during earthquakes: Analysis and field measurements”, Journal of Geotechnique, Vol. 51, pp. 425-440.

[28] Gazatas G., (1983). “Analysis of machine foundation vibration: State of the art”, *Journal of Soil Dynamic and Earthquake Engineering*, Vol. 2, 2-42.

[29] Gazatas G., (1991). Foundation vibration, Foundation Engineering Handbook Chapter 15, 2nd edition, Chapman and Hall, New York, U.S.

[30] Pais A., Kausel E., (1988). “Approximate formulas for dynamic stiffness of rigid foundations”, *Journal of Soil Dynamics and Earthquake Engineering*, Vol. 7, pp. 213-227.

[31] Nakai S. et al., (2006). “Seismic response analysis and design of buildings considering dynamic soil-structure interaction”, Handbook, Japanese Version.

[32] Archiectural Institute of Japan, (1998). “Recommendations for design of building foundations”, Japan.

[33] Camilo P., Youssef M. A. H., (2009). “Damping formulation for nonlinear 1D site response analyses”, *Journal of Soil Dynamics and Engineering*, Vol. 29, pp. 1143-1158.

[34] Kramer, S. L., (1996). “Geotechnical Earthquake Engineering”, Prentice Hall, New Jersey, U.S.

[35] Youssef M. A. H., (2012). “User manual and tutorial of DEEPSOIL”, Department of Civil and Environmental Engineering, University of Illinois at Urbana-Champaigan, U.S.

[36] Newmark N. M., (1959). “A method of computation for structural dynamics”, *Journal of Engineering Mechanics Division*, pp. 67-94.

[37] Rayleigh J. W. S., Lindsay R. B. (1945). “The theory of sound”, Vol. 2(1), New York, U.S.

[38] Chopra A. K., (1995). “Dynamics of structures: Theory and application to earthquake engineering”, Prentice-Hall International Series in Civil Engineering and Engineering Mechanics, Englewood Cliffs, NJ: Prentice Hall.

[39] Youssef M. A. H., Duhee P., (2002). “Viscous damping formulation and high frequency motion propagation in nonlinear site response analysis”, *Journal of Soil Dynamics and Earthquake Engineering*, Vol. 22, pp. 611-624.

[40] Tatsuoka F., Fukushima S., (1978). “Stress-strain relation of sand for irregular cyclic excitation”, *Research Bulletin*, Vol. 30, pp. 26-29.

[41] Idriss I. M., Dobry R., Singh R. D., (1978). “Nonlinear behavior of soft clays during cyclic loading”, Journal of Geotechnical Engineering Division, Vol. 104, pp. 1427-1447.

[42] Ishihara K., (1996). “Soil behavior in earthquake geotechnics”, Oxford Science Publications.

[43] International Building Code, (2006). International Code Council, U.S.

[44] Kabeyasawa T., Matsumori T., Katsumata H., Shirai K., (2005). “Design of the full-scale six story reinforced concrete wall-frame building for testing at E-defense”, *Proceedings of the first NEES/E-Defense workshop on collapse simulation of reinforced concrete structures*, Berkeley, California, U.S, 23-45.

[45] Kim Y., Kabeyasawa T., Matsumori T., (2007). “Dynamic collapse analysis of the six-story full scale wall-frame tested at E-Defense”, *Proceedings of 8th Conference on Earthquake Engineering*, Singapore, Singapore.

[46] Adriano B., Mas E., Koshimura S., (2014). “Tsunami inundation features verification through numerical modeling and video analysis: Case study of Onagawa town on the 2011 Tohoku earthquake”, *Proceedings of Asia Oceania Geosciences Society 11th Annual Meeting*, Japan.

[47] Panon L. (2015). “Development of nonlinear analysis method to simulated nonlinear behavior of RC walls in RC wall-frame buildings suffering damage from earthquake and subsequent tsunami”, Doctoral thesis, Department of Infrastructure System Engineering, Kochi University of Technology, Japan.

[48] Chock G., Carden L., Robertson I., Olsen M., Yu G., (2013). “Tohoku tsunami-induced building failure analysis with implications for U.S. tsunami and seismic design codes”, *Journal of Earthquake Spectra*, Vol. 29, pp. 99-126.

[49] Narith P., Yoshiro K., (2016). “Seismic response of structure under nonlinear

soil-structure interaction effect", Proceeding 7th International Conference on Computational Methods (ICCM2016), Berkeley, California, U.S.

[50] Narith P., Yoshiro K., (2015). "Soil-structure interaction analysis integration in an advanced application tool for disaster mitigation", *Proceedings of the 3rdPlanoCosmo and 10th Society for Social Management Systems International Conference*, Bandung, Indonesia.

[51] Latcharote P., KAI Y., (2013). "High performance computing of dynamic structural response analysis for the Integrated Earthquake Simulation", *Proceedings of the 13th East Asia Pacific Conference on Structural Engineering and Construction (EASEC-13)*, H-1-1, Hokkaido, Japan.

[52] International Building Code, International CodeConcile, U.S, 2006.

[53] Gazatas G., Yegian M., (1979). "Shear and Rayleigh waves in soil dynamics", Journal of Soil Dynamic and Earthquake Engineering, Vol. 105, pp. 1455-1470.

[54] Gazatas G. (1982). "Vibrational characteristics of soil deposits with variable wave velocity", *International Journal for Numerical and Analytical Methods in Geomechanics*, Vol. 6, pp. 1-20.

[55] Rourk M. J., Bloom M., Dobry R., (1982). "Apparent propagation velocity of body waves", *Journal of Earthquake Engineering Structural Dynamics*, Vol. 10, pp. 283-294.

[56] Rourk M. J., Castro G., Hossain I., (1984). "Horizontal soil strain due to seismic waves", *Journal of Geotechnical Engineering*, Vol. 110, pp. 1173-1187.

[57] http://geonews.zenchiren.or.jp/kochi/webgis/

[58] http://bousaimap.pref.kochi.lg.jp/kochi/top/agreement.asp?dtp=6&dtpold=&npg=/kochi/search/landmarkplist.asp&npr=dtp=6/kc1=1/pl=3

[59] Guidebook on Excavation Works Considering Neighboring Structures, Japanese version, 2015.

LIST OF PUBLICATIONS

- **Journal Papers**
  - Narith Prok and Yoshiro Kai (2015). “Soil-Structure Interaction Analysis Integration in an Advance Application Tool for Disaster Mitigation”, *Internet Journal of Social Management Systems Sciences.*

  - Narith Prok and Yoshiro Kai (2016). “Seismic Response of Structure under Nonlinear Soil-Structure Interaction Effect”, *International Journal of Computational Methods.*

  - Narith Prok and Yoshiro Kai (2016). “Effect of Near-Field Soil on Overturning-Moment of Structure under Earthquake and Tsunami Force”, *Journal of Japan Association for Earthquake Engineering.*

- **Conferences Papers**
  - Narith Prok and Yoshiro Kai (2016). “Overturning-Moment of Structure under Near-Field Soil Effect Subjected to Tsunami Force”, *Japan Association Earthquake Annual Meeting 2016 Conference,* Japan.

  - Narith Prok and Yoshiro Kai (2016). “Seismic Response of Structure under Nonlinear Soil-Structure Interaction Effect”, *7th International Conference on Computational Methods*, U.S.

  - Narith Prok and Yoshiro Kai (2015). “Soil-Structure Interaction Analysis Integration in an Advanced Application Tool for Disaster Mitigation”, *3rd PC and 10th SSMS International Conference,* Indonesia.

  - Narith Prok and Yoshiro Kai (2014). “Damage Prediction of Buildings Suffering from Earthquake and Tsunami Considering Soil-Structure Interaction”, *China-Japan Innovation Forum on New Energy Utilization and Sustainable Development Conference,* China.

  - Narith Prok and Yoshiro Kai (2014). “Attempting New Parameters for Pile Damage Response due to Earthquake and Subsequent Tsunami”, Proceeding of AIJ Shikoku Chapter Architectural Research Meeting, Japan.

APPENDIX:
OBJECT-BASED STRUCTURAL ANALYSIS PROGRAM (OBASAN)

A.1. INTRODUCTION

OBASAN, stands for Object-Based Structural Analysis, is a structural analysis program based on C/C++ language. OBASAN is originally constituted by Prof. Yoshiro Kai and being developed by several researchers in order to enhance OBASAN capacity. In OBASAN, one building can be performed as a single degree of freedom (SDOF), multi-degree of freedom (MDOF), or frame structure model represented by mass and beam components. OBASAN can perform well for reinforced concrete and steel structure which can be analyzed in static and dynamic loading such as earthquake loading. OBASAN consists several types of structural components such as beam, column, wall, spring, etc. These elements can be performed with six degrees of freedom, which means three directions in translation (dx, dy, dz) and three directions in rotation (tyz, txz, txy). OBASAN demands four steps for analysis process such as input data, computation and analysis, output data, and system control. The architecture of OBASAN and analysis step are presented in the following sections.

A.2. ARCHITECTURE OF OBASAN

As mentioned above, OBASAN has been constructed in C/C++ language and composed more than 300 classes to perform different types of structural analysis. These classes are divided under eight main classes as shown in Fig. 1. These classes are CUnitValue, TransElement, NastranData, ObjectData, CFemObject, OutPutData, OutTypeData, and SystemController.

A.2.1. OBASAN Input Data

In order to analyze structural response under static or dynamic loading, OBASAN requires input data elements to model structural type and other settings as described in Table 1. These requirements include node data, element data, element type, material, damping type, dof, load type, hysteretic role, and analysis type. However, another type of input data for ground motion analysis has been made as the objective of this thesis. This new input data will be provided in the following section for OBASAN capacity enhancement.

Table 1 OBASAN input data

Node data	Node ID, DOF, node coordinate, mass, mass moment inertia.
Element data	Element ID, element type, node number, material name.
Element type	Spring, beam, column, macro-shell.
Material	Depth, width, young modulus, shear modulus, strength, etc.
Damping type	Rayleigh, Caughey, local viscous, stiffness proportional, etc.
DOF	Translation: dx,dy,dz and Rotation: tyz, tzx, txy.
Load type	Nodal load, surface load, etc.
Hysteretic type	Bilinear, Tri-linear, Inada, Takeda, Kabeyazawa, etc.
Analysis type	Newmark, Static, Differential, Frequency, etc.

A.2.2. OBASAN Output Data

After analyzing structural model, OBASAN can generate output data in various forms including node output, element output, modal output, and hysteretic output as described in Table 2. In OBASAN, output data can be generated in the same file or different file according to user.

Table 2 OBASAN output data

Node output	Displacement, velocity, acceleration, reaction force.
Element output	Stress, strain, deformation, internal force.
Modal output	Eigenvalue, eigenvector, period, frequency.
Hysteresis output	Ductility, stiffness degrading factor.

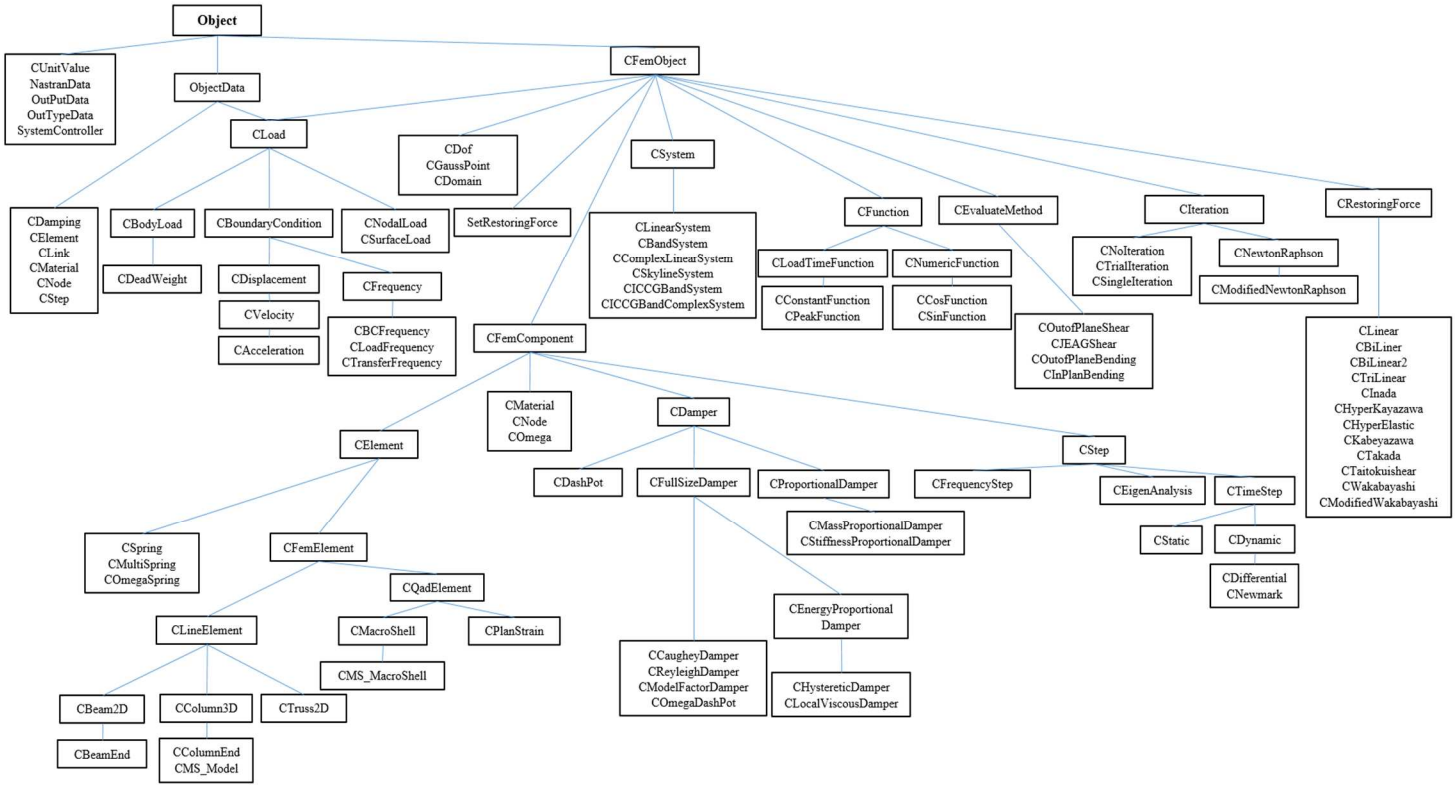

Figure 1 Original OBASAN architecture

A.3. ENHANCEMENT OF OBASAN CAPACITY

As described above, OBASAN capacity has been enhanced according to the requirement of each researcher. However, the objective of this thesis is to integrate FFGM analysis into OBASAN and can be performed for both FD and TD. The theory of wave propagation for both FD and TD has been presented already in chapter 3. In this section, the new architecture of OBASAN and example for input data of ground analysis are provided for both domains.

A.3.1. New Architecture of OBASAN

As shown in Fig. 2, new classes for performing ground motion analysis are shown in green colors. This extension includes CShake and CShakeTime (soil-element), CSoilDashot (damping), CWavePropogationStep (analysis step), and CModifiedRambergOsgood (hysteretic rule).

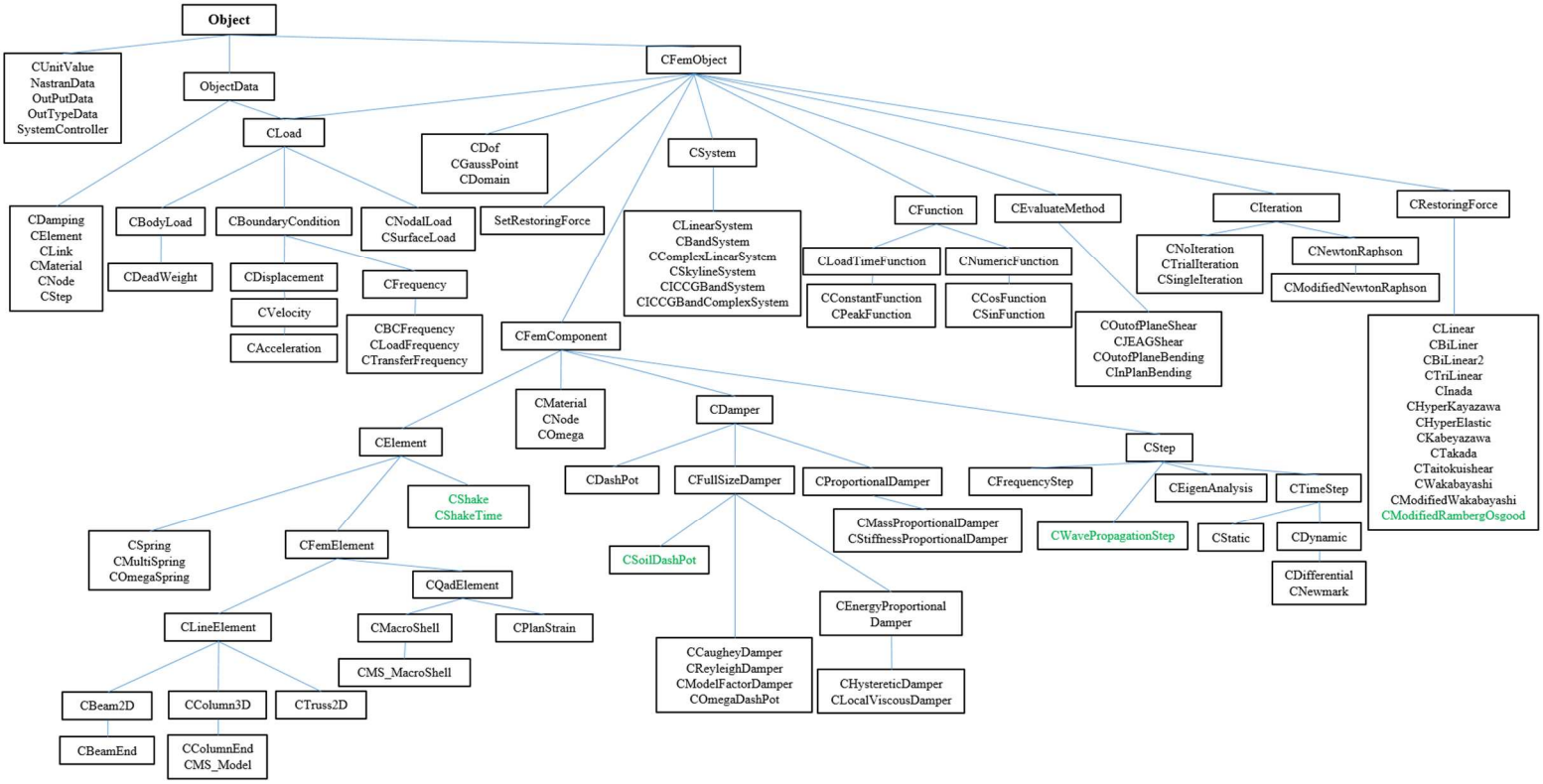

Figure 2 New architecture of OBASAN

A.3.2. Input Data Model for Ground Motion Analysis

· ***Frequency Domain***

The input data for ground motion analysis in FD is shown in the following description:

#Ouput
Output, object, “Output.txt”
ElementOption, acceleration;
ElementID, 1;
manual;

#System
System, Type, Gauss;

#Component classification
ElementType, Soil, Shake;
ElementType, Bedrock, Shake;

#Object direct input type
FromHere, Object

#Component
Layer, ID, 1, Type, Soil, Depth, 3.5[m], Material, Layer1, include1, “GG0-Sand.txt”, include2, “D-Sand.txt”;
Layer, ID, 2, Type, Soil, Depth, 3.5[m], Material, Layer2, include1, “GG0-Sand.txt”, include2, “D-Sand.txt”;
Layer, ID, 3, Type, Soil, Depth, 3.5[m], Material, Layer3, include1, “GG0-Sand.txt”, include2, “D-Sand.txt”;
Layer, ID, 4, Type, Soil, Depth, 4.5[m], Material, Layer4, include1, “GG0-Sand.txt”, include2, “D-Sand.txt”;
Layer, ID, 5, Type, Soil, Depth, 5.0[m], Material, Layer5, include1, “GG0-Sand.txt”, include2, “D-Sand.txt”;
Layer, ID, 6, Type, Bedrock, Material, BedRock, include1, “GG0-Rock.txt”, include2, “D-Rock.txt”;

#Material
Material, Layer1, Rho, 18.1[kN/m3];

```
Material,    Layer1,    Vs,                 180[m/s];
Material,    Layer1,    OutputMotionType,     0;
Material,    Layer1,    InputMotionType,      0;
Material,    Layer1,    Ds,                 0.05;
Material,    Layer1,    InputMotionLayer,     6;
Material,    Layer1,    Iteration,           10;
Material,    Layer1,    InitialStrain,        0;

Material,    Layer2,    Rho,          18.1[kN/m3];
Material,    Layer2,    Vs,                 180[m/s];
Material,    Layer2,    OutputMotionType,     1;
Material,    Layer2,    InputMotionType,      0;
Material,    Layer2,    Ds,                 0.05;
Material,    Layer2,    InputMotionLayer,     6;
Material,    Layer2,    Iteration,           10;
Material,    Layer2,    InitialStrain,        0;

Material,    Layer3,    Rho,          18.1[kN/m3];
Material,    Layer3,    Vs,                 180[m/s];
Material,    Layer3,    OutputMotionType,     1;
Material,    Layer3,    InputMotionType,      0;
Material,    Layer3,    Ds,                 0.05;
Material,    Layer3,    InputMotionLayer,     6;
Material,    Layer3,    Iteration,           10;
Material,    Layer3,    InitialStrain,        0;

Material,    Layer4,    Rho,          18.1[kN/m3];
Material,    Layer4,    Vs,                 180[m/s];
Material,    Layer4,    OutputMotionType,     1;
Material,    Layer4,    InputMotionType,      0;
Material,    Layer4,    Ds,                 0.05;
Material,    Layer4,    InputMotionLayer,     6;
Material,    Layer4,    Iteration,           10;
Material,    Layer4,    InitialStrain,        0;

Material,    Layer5,    Rho,          18.1[kN/m3];
```

```
Material,    Layer5,    Vs,                180[m/s];
Material,    Layer5,    OutputMotionType,    1;
Material,    Layer5,    InputMotionType,     0;
Material,    Layer5,    Ds,                  0.05;
Material,    Layer5,    InputMotionLayer,    6;
Material,    Layer5,    Iteration,           10;
Material,    Layer5,    InitialStrain,       0;

Material,    BedRock,   Rho,                 19.3[kN/m3];
Material,    BedRock,   Vs,                  550[m/s];
Material,    BedRock,   OutputMotionType,    1;
Material,    BedRock,   InputMotionType,     0;
Material,    BedRock,   Ds,                  0.02;
Material,    BedRock,   InputMotionLayer,    6;
Material,    BedRock,   Iteration,           10;
Material,    BedRock,   InitialStrain,       0;

#Wave
Acceleration, ID, 0, Dof, dx, Type, peak, include, “Kobe.txt”;

#Analysis Frequency Setting
Analysis, Type, Wavepropagation, Numebr, 1000, step, 0.02;

#end of object type input
enddata

#end of all data input
enddata
```

- ***Time Domain***

The input data for ground motion analysis in TD is shown in the following description:

```
#output
output, object, “Output.txt”
NodeOption, acceleration;
```

NodeID, 1;
manual;

#System
System, Type, Gauss;

#Component Classification
ElementType, soil, ShakeTime;
ElementType, rock, ShakeTime;

#Object direct input type
FromHere, Object

#Damping
Damp, ID, 0, Type, SoilDashPot, h, 5%, ElementID, All;

#Node
Node, ID, 1, Dof, 1, 0, 0, 0, 0, 0, xyz, 0.0[m], 0.0[m], 0.0[m];
Node, ID, 2, Dof, 1, 0, 0, 0, 0, 0, xyz, 0.0[m], 0.0[m], -5.0[m];
Node, ID, 3, Dof, 1, 0, 0, 0, 0, 0, xyz, 0.0[m], 0.0[m], -9.0[m];
Node, ID, 4, Dof, 1, 0, 0, 0, 0, 0, xyz, 0.0[m], 0.0[m], -13.0[m];
Node, ID, 5, Dof, 0, 0, 0, 0, 0, 0, xyz, 0.0[m], 0.0[m], -17.0[m];

#Component
Layer, ID, 1, Type, Soil, Node, 1, 2, Material, Layer1, include1, “GG0-Sand.txt”, include2, “D-Sand.txt”;
Layer, ID, 2, Type, Soil, Node, 2, 3, Material, Layer2, include1, “GG0-Sand.txt”, include2, “D-Sand.txt”;
Layer, ID, 3, Type, Soil, Node, 3, 4, Material, Layer3, include1, “GG0-Sand.txt”, include2, “D-Sand.txt”;
Layer, ID, 4, Type, Soil, Node, 4, 5, Material, Layer4, include1, “GG0-Sand.txt”, include2, “D-Sand.txt”;

Material
Material, Layer1, Rho, 19.0[kN/m3];
Material, Layer1, Vs, 350[m/s];

```
Material,	Layer1,	dof,	dx;
Material,	Layer1,	FirstFrequencyMode,	1;
Material,	Layer1,	HighFrequencyMode,	0;
Material,	Layer1,	HalfStrain,	0.000694;
Material,	Layer1,	restoringforce,	ModifiedRambergOsgood;
Material,	Layer1,	MaxDamping,	0.28;

Material,	Layer2,	Rho,	19.0[kN/m3];
Material,	Layer2,	Vs,	350[m/s];
Material,	Layer2,	dof,	dx;
Material,	Layer2,	FirstFrequencyMode,	1;
Material,	Layer2,	HighFrequencyMode,	0;
Material,	Layer2,	HalfStrain,	0.000694;
Material,	Layer2,	restoringforce,	ModifiedRambergOsgood;
Material,	Layer2,	MaxDamping,	0.28;

Material,	Layer3,	Rho,	19.0[kN/m3];
Material,	Layer3,	Vs,	350[m/s];
Material,	Layer3,	dof,	dx;
Material,	Layer3,	FirstFrequencyMode,	1;
Material,	Layer3,	HighFrequencyMode,	0;
Material,	Layer3,	HalfStrain,	0.000694;
Material,	Layer3,	restoringforce,	ModifiedRambergOsgood;
Material,	Layer3,	MaxDamping,	0.28;

Material,	Layer4,	Rho,	19.0[kN/m3];
Material,	Layer4,	Vs,	350[m/s];
Material,	Layer4,	dof,	dx;
Material,	Layer4,	FirstFrequencyMode,	1;
Material,	Layer4,	HighFrequencyMode,	0;
Material,	Layer4,	HalfStrain,	0.000694;
Material,	Layer4,	restoringforce,	ModifiedRambergOsgood;
Material,	Layer4,	MaxDamping,	0.28;

#wave
acceleration,	ID,	0,	Dof,	dx,	NodeID,	5,	Type,	peak,	include,
```

“Kobe.txt”;
#Analysis Setting
Analysis, Type, Newmark, start, 0, end, 20, step, 0.02;

#end of object type input
enddata

#end of all data input
enddata

A.3.3. Example of Free Field Ground Motion Analysis in FD

In this study, an example, uniform soil deposit was assumed in the depth 20m rested on the bedrock. The properties of both soil and bedrock are shown the table 3. The record motion of Kobe earthquake was assumed as input motion at bedrock in this example, as shown in Fig. 3. In this example, linear and equivalent analysis are performed under OBASAN and verified by a widely used program, for FD analysis, SHAKE91. The results show a good agreement for both analysis as illustrated in Fig. 4 and 5.

Table 3 Soil and bedrock property

Layer	Unit Weight (kN/m^3)	Shear Velocity (m/s)	ξ(%)
0.00-3.50	18.10	180	5
3.50-7.00	18.10	180	5
7.00-10.5	18.10	180	5
10.5-15.0	18.10	180	5
15.0-20.0	18.10	180	5
BedRock (Soft)	19.30	550	2

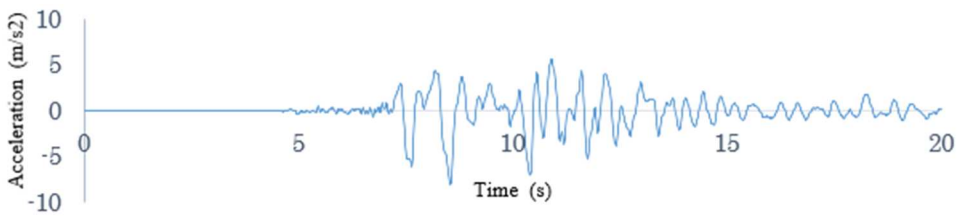

Figure 3 Kobe earthquake input motion

Frequency Domain (FD)

Linear Analysis

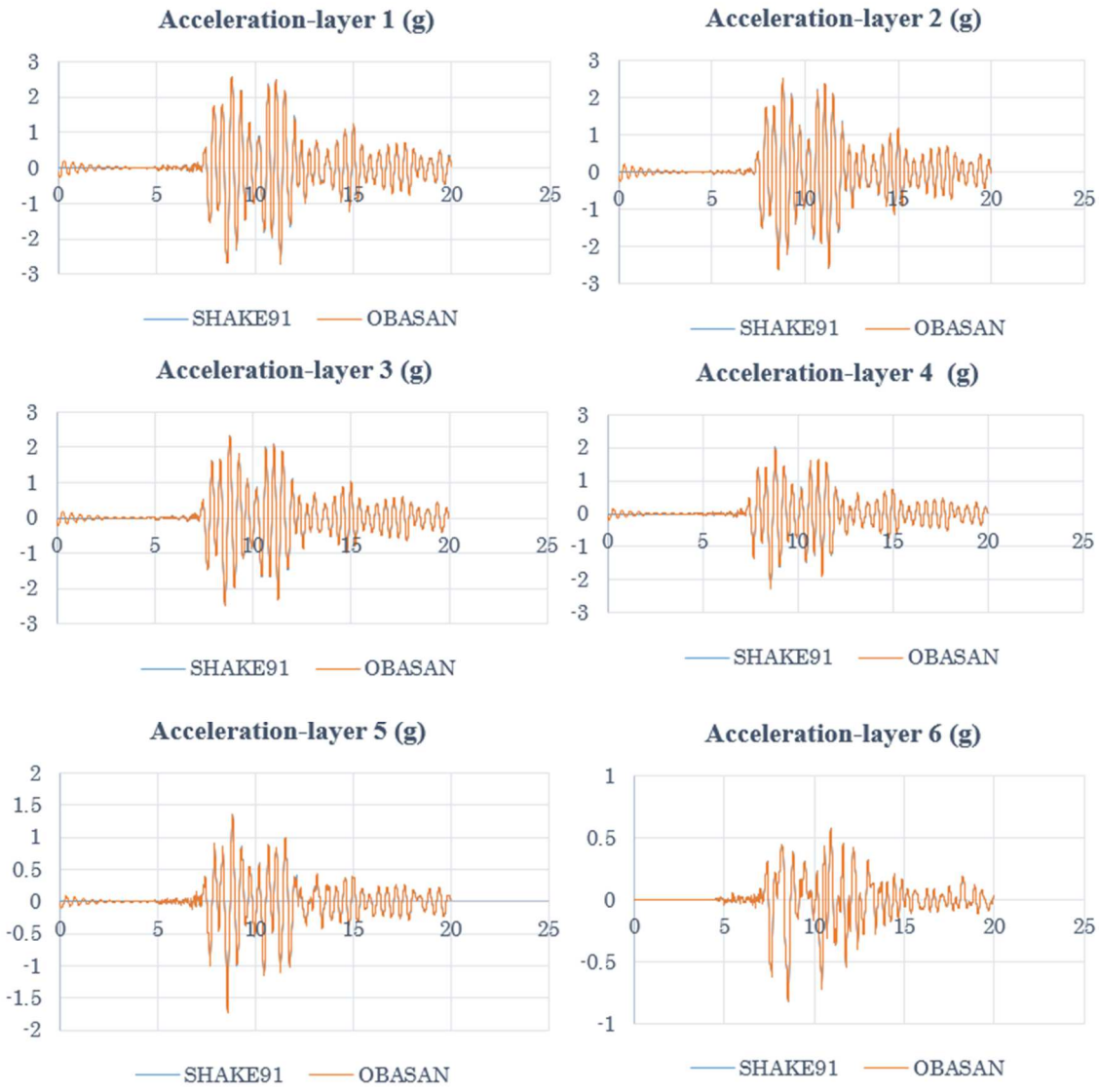

Figure 4 Linear response analysis of FFGM

Equivalent Linear Analysis

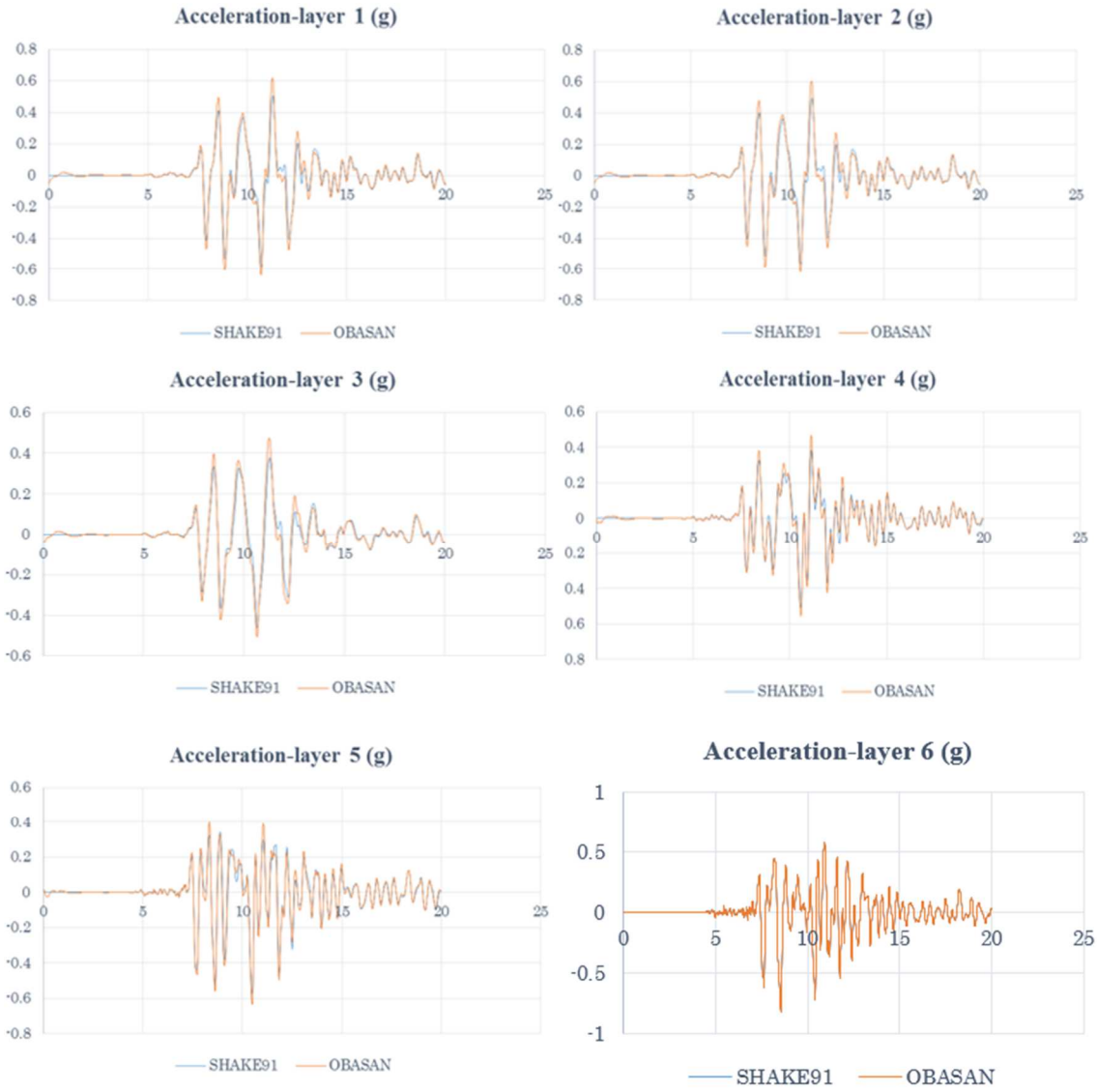

Figure 5 Equivalent-linear response analysis of FFGM

A.3.4. Example of Free Field Ground Motion Analysis in TD

For FFGM analysis in TD, an example, soil deposits was assumed in the depth 17m rested on the bedrock. The properties of both soil and bedrock are shown the table 4. The same Kobe earthquake motion is used in this example. In this analysis, linear and equivalent analysis is performed under TD analysis and verified by FD analysis. As shown in Fig. 6 and 7, the results show a good agreement between both analyses. Furthermore, the nonlinear response analysis in TD is also presented in Fig. 8.

Table 4 Soil and bedrock property

Depth (m)	$V_s(m/s)$	$\gamma(kN/m3)$	ξ (%)
0.00-5.00	180	18.0	5
5.00-9.00	340	18.0	5
9.00-13.0	600	19.0	5
13.0-17.0	600	19.0	5
Bedrock	900	21.0	1

Time Domain

Linear Analysis

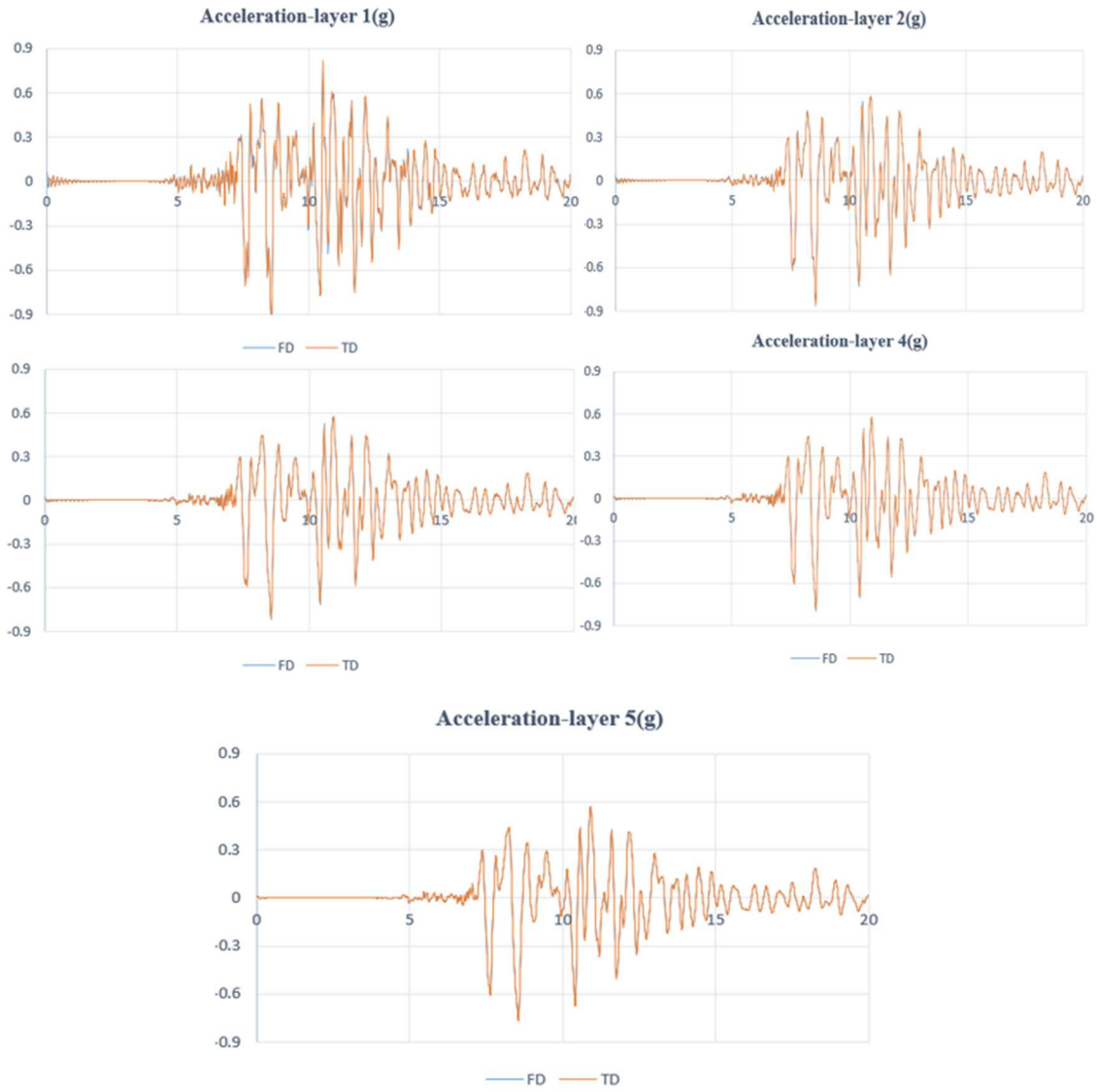

Figure 6 Linear response analysis of FFGM in FD and TD

Equivalent Linear Analysis

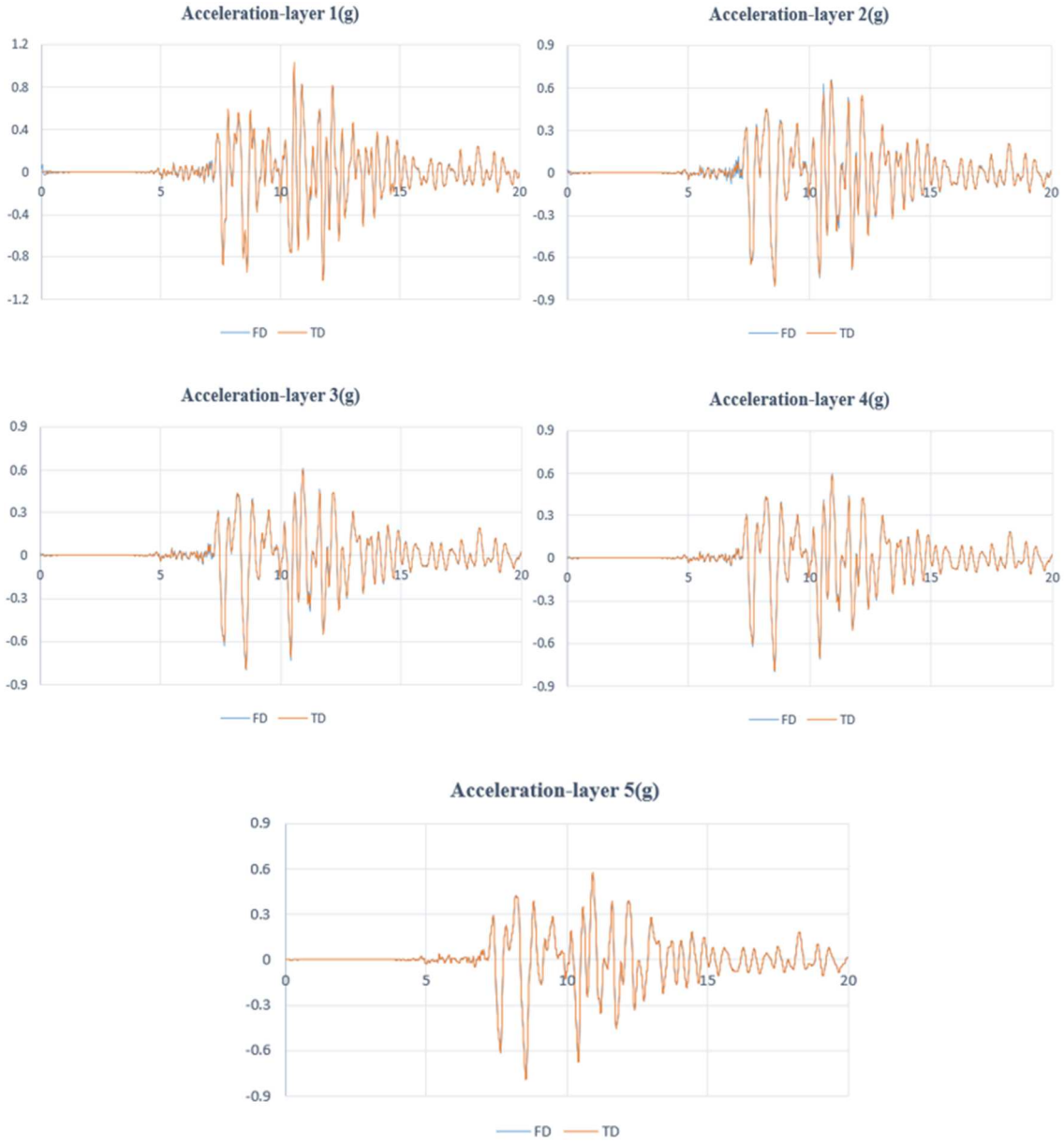

Figure 7 Equivalent-linear response analysis of FFGM in FD and TD

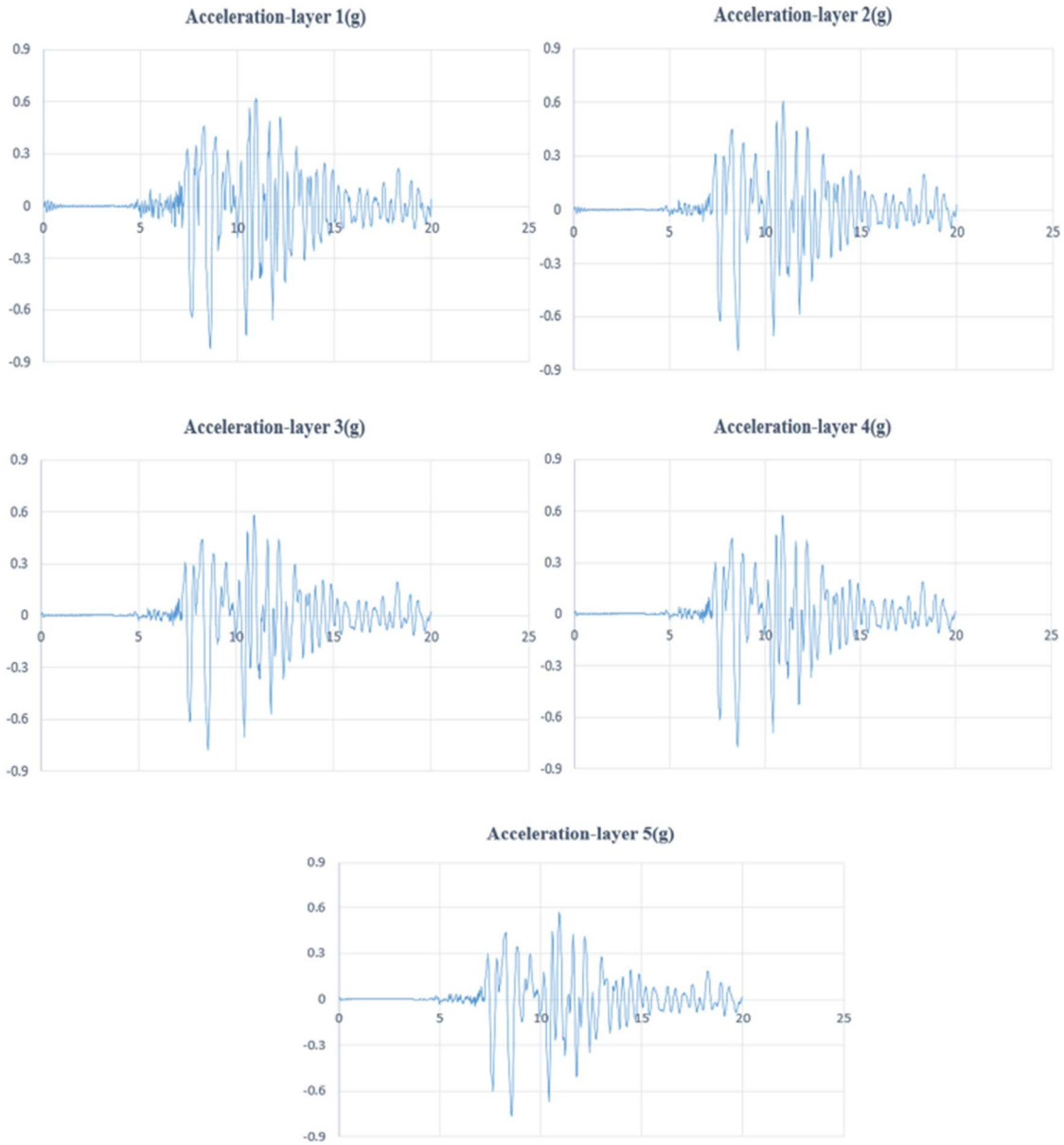

Figure 8 Nonlinear response analysis of FFGM in TD